Circuit mechanisms for learning in the rodent Prefrontal cortex and their dysfunction in Schizophrenia

Inauguraldissertation

zur
Erlangung der Würde eines Doktors der Philosophie
vorgelegt der
Philosophisch-Naturwissenschaftlichen Fakultät
der Universität Basel

von

Arghya Mukherjee

von Asansol, Indien

Basel, 2018

Genehmigt von der Philosophisch-Naturwissenschaftlichen Fakultät
auf Antrag von

Prof. Dr. Pico Caroni
(Fakultatsverantwortlicher und Dissertationsleiter)

Prof. Dr. Andreas Luethi
(Koreferent)

Basel, 19.09.17

Prof. Dr. Martin Spiess
(Dekan)

Table of Contents

Preface

Humans and other higher mammals do more than just learn associations between sensory cues and outcomes. We engage in complex top down control of behavior where our internal states and intentions drive us to choose actions that are distant from our goals. Our ability to make such choices not only helps in predicting the outcome of current behavioral contexts and direct our responses as per our needs, but also shapes our future behavioral strategies. One of the most enduring mysteries of the brain is this process of decision-making. What neural mechanisms helps us choose a course of action between several different possibilities? How do we decide to stick with a response and how do we decide to switch to an alternative response? Ultimately, this seemingly willful but complex behavior emerges from interactions between neurons.

One important feature of the neural mechanisms behind decision-making is that they are shaped by experience. Thus, they depend on areas of the brain, which can learn the 'rules of the game' – what outcomes are desirable and what responses can be directed towards achieving these outcomes? The structure, most frequently, implicated in such top down control is the Prefrontal cortex (PFC). Indeed the complexity of the PFC structure and functions is greatest in humans and much simpler in mammals such as rodents, which parallels the ability of higher order primates to make complex decisions. Moreover, the effects of PFC dysfunction in humans are most apparent where cognitive control is needed.

In this thesis, I explore the mouse prefrontal cortex, primarily the Prelimbic and Infralimbic cortices, which are known to play antagonistic roles in goal-oriented behavior. Using recently developed chemogenetic tools, I will show how these two areas are connected with each other and the functional significance of these connections in learning competing associations. In a second part, I will show how local neuronal networks within the PFC and the hippocampus are affected in a mouse model of schizophrenia and propose a clinically relevant therapeutic strategy for long-term amelioration of the cognitive symptoms of this disorder.

Rationale and Goals

Flexible behavior, as shown by most mammals, requires continuous decision making where appropriate actions must be chosen from an array of available actions based on our current goals and prior experience. The medial prefrontal cortex (mPFC) is essential for selecting such appropriate actions and inhibiting inappropriate ones. The prefrontal cortex is not a homogenous structure but rather an agglomeration of sub-areas, which sub serve different functions. For example, the anterior cingulate is required for effort-based decision-making (Walton et al., 2003; Rushworth et al., 2004) while the orbitofrontal cortex is essential for value based decision-making (Niv and Schoenbaum, 2008). However, the outcome of a decision making process is selection of a singular behavioral action or learning a new association. Hence, it would be reasonable to hypothesize that this selection would be a product of the combined output of the various prefrontal areas and the interactions among them. Thus, to understand the neurobiological substrates of decision making one needs to explore the prefrontal cortex at two different levels: 1. The internal microcircuit and neuronal networks within individual prefrontal areas, and 2. Functional interactions among the prefrontal areas. The broad goal of my thesis was to use both of these approaches to study the prefrontal cortex of a well-established model organism (mouse) which has a relatively simple behavioral repertoire yet is evolutionarily complex enough to generalize my findings to higher order animals.

First, I focused my attention on the Prelimbic (PreL) and Infralimbic (IL) regions of the mouse medial prefrontal cortex (mPFC). These two areas have been studied most extensively among the rodent prefrontal areas. In several behavioral domains, the PreL and IL exert distinct and opposing, influences over behavior; in a PreL-Go/IL-NoGo manner. The most common examples of this complementary function are the expression and extinction of conditioned fear responses or drug seeking behavior (Peters et al., 2009). Furthermore, neuronal tuning studies have shown that the PreL neurons are tuned to the representation of goals in goal directed learning while the IL neurons appear to tune to alternative choices. I investigated how the PreL and IL cortices interact among each other to influence learning and selection of behavioral strategies. Such, interactions between IL and PreL or other prefrontal areas have not

been studied in detail in the past with one notable exception. Research done by Ji and Neugebauer (2012) have shown that optogenetic activation of IL inhibits PreL pyramidal cells in vivo, implying an existence of feed-forward inhibition from the IL to PreL. I carried out selective chemogenetic silencing of PreL or IL during different sub phases of the Intra-dimension/ extra-dimension set shifting task (IEST) or trace learning and extinction to evaluate their individual contributions. My findings suggest that PreL promotes application of behavioral strategies or new learning corresponding to previously learnt associations while IL is required to learn alternative associations across different learning paradigms. Next, using viral mediated tracing techniques I show the existence of reciprocal layer5/6 derived IL↔PreL projections. Using selective unidirectional silencing/activation of these projections, I have shown that the IL→PreL and PreL→IL projections are required at different phases of learning. Unidirectional IL→PreL projections are specifically required during IL mediated alternative learning (eg: extinction) and bi-directional PreL↔IL projections are required +12-14h post learning to setup the role of IL in subsequent learning of alternative choices.

Prefrontal cortex dysfunction has been identified as a key neurobiological correlate of cognitive deficits associated with many neuropsychiatric disorders like Schizophrenia, Attention deficit/Hyperactivity disorder etc. Exploring the dysfunction of defined prefrontal neuronal networks and circuits in rodent models of neuropsychiatric disorders can be also be a rewarding approach towards understanding decision making. In the second part of the thesis, I explored the dysfunction in the Parvalbumin (PV) interneuron network in a mouse model of Schizophrenia.

Parvalbumin interneurons have been shown to synchronize network activity, supporting different types of neuronal network oscillations, such as gamma and theta oscillation, ripple and spindle activity (Amilhon et al., 2015; Stark et al., 2014; Lapray et al., 2012). Thereby, they play a significant role in the formation and consolidation of memories to support learning and behavior (Karunakaran et al., 2016; Donato et al., 2013). Finally, dysfunction of the Parvalbumin interneuron system, in the prefrontal cortex of human schizophrenia patients, has emerged as a core substrate underlying the cognitive deficits in the disease (Lewis, 2014). Thus, studying the dysfunction of

the PV network in Schizophrenia not only provides a way to understand its role in prefrontal function but also raise the possibility of developing therapeutic strategies to ameliorate the associated cognitive deficits. I first showed that the PV network in LgDel+/- animals fail to mature with respect to those of their wild type counterparts and remain stuck in an immature state, which is also associated with altered neural synchrony in the gamma band and behavioral deficits. I further show that stimulation of the PreL PV neuron network within a specific window of treatment during early adulthood can rescue the dysfunctional PV network synchrony as well as behavioral deficits. In recent years, interactions between the hippocampus and prefrontal cortex (PFC) have emerged as key players in various cognitive and behavioral domains (Harris and Gordon, 2015). Disruptions in hippocampal-prefrontal interactions have also been observed in psychiatric disease, most notably schizophrenia (Godsil et al., 2013). I found that long-term rescue of the PreL PV state and associated behavioral deficits in LgDel+/- mice can also be mediated through direct stimulation of the ventral hippocampal (vH) PV network. However if the rescue is targeted to PreL while preventing it in vH or vice versa, it fails to mediate any behavioral rescue in LgDel+/- mice. Thus suggesting that long-term rescue of the PV pathology and cognitive deficits in LgDel+/- animals requires a rescue of the entire hippocampal-prefrontal axis.

1. Introduction

1.1. The Prefrontal cortex

Located in the anterior end of the mammalian brain the Prefrontal cortex is a collection of anatomically and functionally distinct brain regions, which play different roles in cognitive control. The prefrontal areas have a unique connectivity pattern with almost all neocortical and some subcortical structures (Bedwell et al., 2014, Kondo and Witter, 2014, Hoover and Vertes, 2011, Vertes, 2004). This provides a perfect framework to integrate a diverse range of information needed for top down control of behavior. Such behavior is largely driven by rule learning, where new information is incorporated and processed in the context of previous experience to result in 'rules' for guiding future behavior. Thus, traditionally, the PFC has been studied in the context of decision-making processes like working memory, error detection (Holroyd et. al., 2002), reinforced learning and its extinction (Rushworth et al., 2011)

The PFC has also been in recent focus due to a growing recognition that dysfunction in its development and circuitry may underlie cognitive symptoms associated with disorders such as Schizophrenia (Volk and Lewis, 2010), Bipolar disorder and Attention-deficit/Hyperactivity disorder (Schubert et al., 2015). Although the extent to which cognitive processes are functionally homologous across humans, non-human primates and rodents remain controversial, rodent models of such disorders have proven to be an invaluable tool for studying these processes. Taking a reductionist approach, neurobiologists working with rodents have been able to allocate behavioral endo-phenotypes to anatomical subdivisions within the prefrontal cortex with increasing specificity. This process is aided by recently developed microscopic techniques, which allow us to observe neuronal activity in prefrontal cortical areas at single neuron resolution in freely behaving mice/rats. Moreover, chemogenetic and optogenetic manipulations of well-defined assemblies of neurons with high temporal and spatial resolution offers a possibility to map the dysfunctions at the level of microcircuits, cell assemblies and molecular processes. This in turn offers newer targets for drug development and novel therapeutic strategies. In the following sections, I will describe the structure and function of different rodent prefrontal areas. I will also describe mnemonic functions of the medial PFC in a broader context of its role in goal directed behavior and decision-making. Finally, I will explore the

dysfunction of the medial PFC (mPFC) in the context of psychiatric and cognitive disorders.

1.2. Structural organization of the rodent Prefrontal Cortex

Comparison of neuroanatomy across multiple species show that the evolution of the Prefrontal cortex parallels the evolution of cognition. Thus, higher order mammals such as humans and non-human primates have a highly elaborated PFC. The areas that comprise the monkey PFC are often grouped into anatomically different subfields, namely, the orbital and medial (Brodmann area 10, 11, 13, 14), the lateral (Brodmann areas 46, 12, 45), and the mid-dorsal (Brodmann area 9) regions. The earliest descriptions of the prefrontal cortex were based on anatomical criterion like cortical projection areas of the mediodorsal thalamic nuclei or having a granular layer IV and a location rostral to the agranular premotor areas (Barbas and Pandya, 1989). Yet such cytoarchitectonic criterions for defining the prefrontal cortex are not enough when comparing distantly related species such as monkeys and mice. For example, unlike in primates, the rodent PFC is agranular and lacks a discernable layer IV. On the other hand, primate and rodent PFC share similar patterns of projections from the mediodorsal thalamus. Thus, the rodent PFC is defined based on multiple levels of comparison with the primate PFC, beyond just cytoarchitectonics (Ongur and Price, 2000).

The criteria taken into consideration for defining a rodent PFC homologous to the primate PFC are: 1) similarities in input-output connectivity, 2) functional homologies at the level of single cells, network activity and behavioral roles, 3) distribution of receptors and neuro-modulatory projections and 4) development and maturation criterion (Uylings et al., 2003). Based on these criterions the rodent prefrontal cortex comprises of a medial prefrontal cortex (mPFC), a lateral PFC (lPFC) and a ventral region (vPFC). The medial PFC can be further subdivided into a dorsal part (dmPFC) consisting of the Anterior Cingulate cortex (ACC) and the Prelimbic cortex (PreL), and a ventral part (vmPFC) consisting of the Infralimbic cortex (IL) and medial Orbital cortex (MO). The lateral subdivision of the rodent PFC includes the dorsal and ventral Insular areas (AID, AIV) and the lateral Orbital cortex (LO). Lastly, the ventral PFC encompasses the ventral Orbital and the ventrolateral Orbital cortex (VLO). However,

most functional and anatomical studies of the rodent PFC have focused on a broader subdivision of the PFC, namely mPFC (ACC, PreL, IL) and the Orbitofrontal PFC (MO, LO, VO, VLO). Hence, in the subsequent sections I will focus my discussion on these regions.

1.2.1 Anterior Cingulate cortex

The rat anterior cingulate cortex (ACC) is an integral part of the prefrontal cortex and lies on its medial surface rostral and caudal to the genu of the corpus callosum. It consists of Layers I, II/III, V and VI and lacks a layer IV (Devinsky et al., 1995). Based on neuroanatomy the ACC can be further subdivided into a dorsal (ACCd) and a ventral (ACCv) subpart. In ACCd the cells are arranged in a columnar fashion in comparison to the ACCv (Van de Werd, 2010). Furthermore, in LVI the cells in ACCd are columnar in arrangement while those of ACCv are arranged in horizontal rows. Like other cortical areas, Layer I of ACC mainly contains interneurons and fibres projecting from other parts of the brain. Some of these incoming fibers also form connections in the deeper layers of the ACC. Layers II-III mainly consists of pyramidal neurons while layers V-VI contain both pyramidal neurons and interneurons. The dendrites of deep-layer pyramidal cells spread into the superficial layers of the ACC (Wu et. al., 2009), and so it is likely that neurons between different layers of ACC also form synaptic connections. However, such intra layers connections and their functional relevance in the ACC has remained largely unexplored.

The projections into the ACC can be broadly classified into three systems. The first set of projections originate from the medial thalamus, which in turn receive projections from the spinothalamic tract (Yang et al., 2006; Shyu et al., 2009). These thalamic projections were recently shown to directly excite Parvalbumin interneurons in the ACC to mediate feed forward inhibition onto Layer II-III neurons (Delevich et. al, 2015). A second set of inputs originate from the Amygdala, specifically from the central nucleus while a final set of inputs originate from other sensory cortical areas like the somatosensory cortex (S1) and the Insular cortex (Han et al., 2015). In turn, the ACC sends out projection to subcortical structures like the hypothalamus, periacquedectal grey and dorsal horn of the spinal cord via layer V pyramidal neurons (Bragin et al., 1984). ACC neurons also send reciprocal projections to the amygdala, specifically the

BLA, and to the main norepinephrine producing brain sites – locus coeruleus (LeDoux, 2000; Tovote et al., 2015). The ACC also has bi-directional connectivity to the neighboring mPFC areas such as PreL and IL (Medalla and Barbas, 2012) as well as the Retrosplenial cortex (RSC). Importantly the ACC is part of the Papez circuit where it receives inputs from the anterior thalamic tracts and sends outputs to the hippocampal formation via the entorhinal cortex (Jankowski et al., 2013). Thus, the ACC has a significant role to play in the control of emotional expressions. Recent studies have also shown a direct projection from the ACC to the dorsal hippocampus (dH) which is required for the expression of learnt fear (Rajasethupathy et. al., 2015). The overall connectivity of the ACC show an anterior posterior gradient where connections to and from the limbic and emotion processing regions are more segregated to the anterior side while the posterior side mostly communicates with dorsal and lateral frontal areas and is thought to be involved in top-down regulation (Bliss et al, 2016; Etkin et al, 2011).

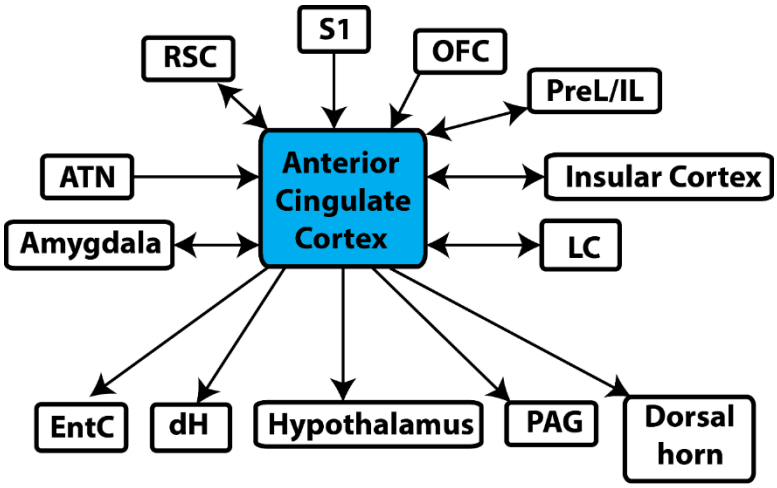

Figure 1.1: Input/output connectivity of ACC: The ACC receives various inputs from nociceptive centres like the thalamus as well as from emotive centres such as the amygdala. In turn the ACC sends direct projections to the dorsal horn of the spinal cord. This loop has been predicted to be important for central sensitization. ATN: Anterior thalamic nuclei; LC: Locus coeruleus; dH: dorsal Hippocampus; EntC: Entorhinal cortex; S1: primary Somatosensory area.

1.2.2. Orbitofrontal cortex

The Orbitofrontal cortex is so called due to its location around the eye socket in primates. In rodents, the OFC is determined as those areas of the frontal lobe that have strong anatomical and functional parallels with the primate OFC. Thus, the rodent

OFC encompasses the dorsal bank of the rhinal sulcus including the lateral orbital regions – MO, LO, VO and VLO (Groenewegen 1988; Ray and Price, 1992). Like other PFC areas the OFC is also comprised of Layers I, II, III, V and VI and a missing LIV. The border between layers II and III are indistinguishable in VO and VLO while MO and LO have a clear border between these two layers (Van de Werd, 2010). The various OFC areas can also be distinguished based on the distribution of Parvalbumin positive interneurons (PV), which are the primary source of perisomatic inhibition in the cortex. The LO and VLO have a high density of these interneurons spread across all layers while the MO has a sparse distribution of these interneurons. The OFC can also be distinguished by the absence of dopaminergic afferents. Specifically, the MO, VLO and LO are largely bereft of dopaminergic projections while the VO has dopaminergic fibers in its caudal part. Finally, like the ACC, intra layer connectivity and its functional significance has not been explored in the OFC (Van de Werd, 2010).

With respect to its input/output connectivity, the OFC is positioned at the intersection of multimodal sensory networks and circuits involved in emotion and memory. A chief characteristic of the orbital network is that it receives inputs from all sensory cortical systems, including olfaction, taste/visceral afferents, vision, and somatic sensation (Rolls, 1996; Groenewegen and Uylings, 2000; Ongur and Price, 2000; Hoover and Vertes, 2007). However, although the OFC has extensive sensory inputs, it only weakly connects with the motor system. It also has strong connections with the limbic system, including the hypothalamus, amygdala, and hippocampus and nucleus accumbens (Rempel-Cowler, 2007b; Floyd et al., 2001). Of the limbic areas, the OFC connects strongest with the amygdala. All parts of the orbitofrontal cortex receive input from the amygdala, primarily originating from the basolateral, basomedial, and lateral nuclei. The medially situated VO and VLO areas issue projections to the anterior portion of the amygdala, with sparse termination distributed across the basomedial nucleus, medial nucleus, central nucleus and intercalated nuclei. Notably, the VO and VLO sends projections to autonomic output areas, including the medial and central nuclei of the amygdala, and issue only weak projections to the basolateral amygdala. Taken together these OFC projections to sensory emotion and reward-related regions suggest that the OFC is likely to be important in encoding the value of incoming stimuli. (Hoover and Vertes, 2011; Rempel-Cowler, 2007a)

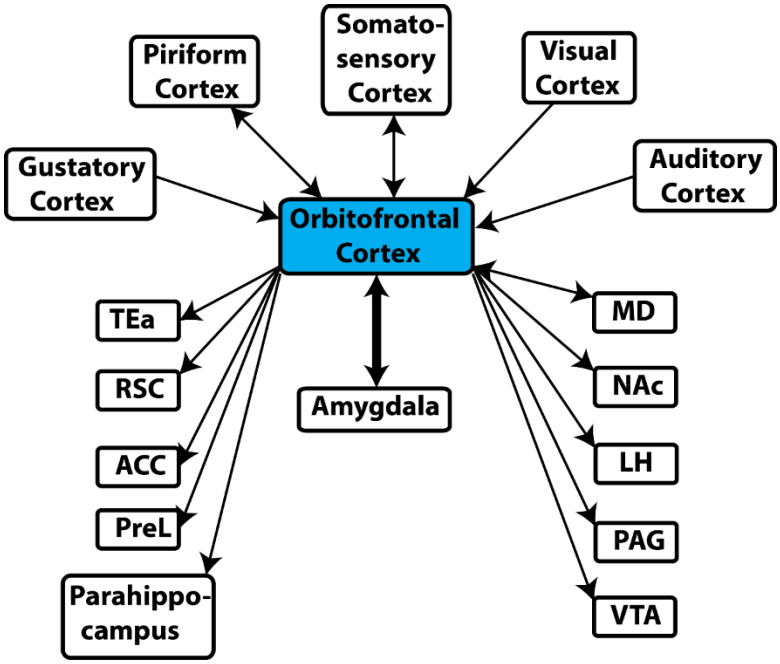

Figure 1.2: Input/output connectivity of OFC: The OFC receives inputs from all sensory modalities. It also sends outputs to higher order cortical areas like PreL, ACC and RSC as well as to subcortical areas, which regulate actions, such as accumbens, lateral hypothalamus, PAG etc. Of all cortical areas the OFC has the densest reciprocal connections across the amygdalar complex. This pattern of connectivity puts the OFC in a unique position to integrate sensorimotor inputs with action selection based on emotive states. TEa: Temporal association area; RSC: Retrosplenial cortex; MD: Medio-dorsal thalamus; LH: Lateral hypothalamus.

1.2.3 Ventromedial PFC: Prelimbic and Infralimbic cortex

Lying next to each other in the dorso-ventral axis, the Prelimbic (PreL) and Infralimbic (IL) cortices form the ventral subdivision (vmPFC) of the medial PFC of rodents. The rodent vmPFC exhibits laminar organization with deep and superficial layers and lack a discernable layer IV like the rest of the rodent PFC (Caviness, 1975; Yang et al., 1996; Uylings et al., 2003; Van de Werd et al., 2010), Anatomically the PreL cortex is easily distinguished from the IL by the structure of cortical layers. For example, layer V of PL is less well organized compared to more dorsal regions (i.e., ACC), whereas layer VI cells are arranged in a horizontal fashion. Moreover, in the PreL layers II, III and V are clearly distinguishable, where a densely packed layer II is separated from layer V by a sparsely packed layer III. On the other hand, a unique feature of IL is that cells of layer II spread far into layer I, while in PreL only few cells of layer II are seen in layer I. Therefore, layer II appears wider in IL than in PreL. In general, IL layers II-

VI have a relatively homogenous layout in terms of cell size and density, with smaller cell bodies compared to PreL (Uylings and van Eden, 1990; van de Werd et al., 2010). Another discerning feature of the PreL and IL is a relative sparse distribution of Parvalbumin interneurons compared to other PFC areas. Moreover, these interneurons are restricted mostly to layer V and VI. A further distinction between PreL and IL can be made with respect to dopaminergic projections, where the PreL receives substantially more DA afferents than the IL (van de Werd et al., 2010).

Apart from the thalamus and parts of the cortex, PreL and IL areas have functionally and anatomically segregated outputs. One such area of differential projection is the Nucleus accumbens (NAcc), an area involved in reward signal processing. PreL fibers distribute extensively throughout the core and shell regions of NAcc. By contrast, IL fibers project selectively to the medial shell of the accumbens (Vertes, 2004). IL and PreL also project very differently to the amygdala. IL fibers distribute widely throughout the anterior part of the amygdala, mainly to rostral and medial Amygdala (MEA), the capsular and medial subdivisions of the central Amygdala (CEA), and to the baso-medial nucleus. By contrast, the PreL fibers selectively target the central nucleus (capsular portion) and the BLA. IL and PreL also project differentially to the hypothalamus. IL projects significantly to the dorsomedial hypothalamic nucleus/area, the lateral hypothalamus and supramammillary nuclei (McDonald et al., 1996; Vertes, 2004). On the other hand, PreL fibers mainly pass through the hypothalamus and terminate in the brain stem. The IL and PreL also send differential projections to the brain stem. The IL efferents mainly target SN, a primary site for dopamine production and the ventrolateral regions of the pontomesencephalic PAG. By contrast, PreL efferents project mainly to the VTA and to a lesser extent to the SNc as well as to the ventrolateral pontine PAG (Floyd et al., 2000; Vianna and Brandão, 2003; Hoover and Vertes,2007). Within the cortices the PreL and IL have primarily ipsilateral and largely overlapping connections. For example, IL and the PreL both project to the ACC, entorhinal cortex, piriform cortex and insular cortex (Vertes, 2004). The input connectivity into the mPFC is less segregated between the PreL and IL with notable exceptions. A recent study (Senn et al., 2014) showed that the IL and PreL receive reciprocal connections from distinct, non-overlapping population of neurons in the basal amygdala. In addition, BLA projections also synapse a small percentage of PV interneurons in the PreL and IL (Gabbott et al., 2006). Thus, BLA projections can

functionally modulate mPFC output via feed-forward inhibitory mechanisms. Furthermore, a population of ventral CA1 neurons synapses onto layers I and V of the IL and these same hippocampal neurons also synapse on entorhinal neurons, which may be important for integrating contextual and spatial information (Swanson, 1981). With the above exceptions, the PreL and IL receive inputs from most sensory association cortices in the temporal and parietal lobes as well as the other prefrontal areas like OFC and ACC. This suggests that the PreL and IL might integrate incoming information from multiple sources to drive appropriate behavioral responses. However, the cortico-cortical interactions between IL and PreL have not been studied in detail. A study in slice cultures has shown that the IL has higher frequency local field potentials (LFP) than PreL, and these differ when the two regions are disconnected—implying some level of functional connectivity between them (van Aerde et al., 2008). In addition, optogenetic activation of IL inhibits PreL pyramidal cells in vivo (Ji and Neugebauer, 2012) – implying an existence of feed-forward inhibition from the IL to PreL.

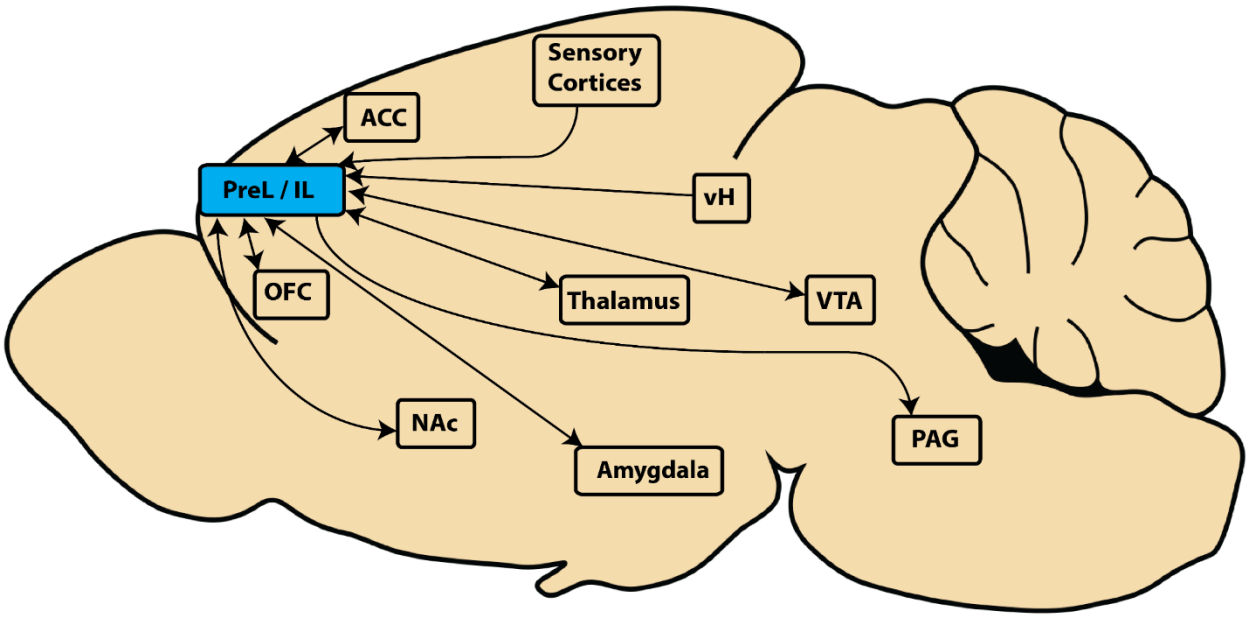

Figure 1.3: Input/output connectivity of PreL and IL: The PreL and IL are reciprocally connected to all cortical and sub-cortical areas involved in goal-directed behavior. They also receive direct inputs from the ventral hippocampus. ACC: Anterior cingulate cortex; OFC: Orbitofrontal cortex; NAc: Nucleus Accumbens; vH: ventral Hippocampus; VTA: Ventral tegmental area; PAG: Periacquadectal grey.

1.2.4 The cortico-basal ganglia-thalamo-cortical loop

Other than the region-specific connections of the prefrontal areas, the PFC is part of an important neuronal network in the brain whose dysfunction has been implicated in a number of disorders such as Schizophrenia: the cortico-basal ganglia-thalamo-cortical loop. Within the prefrontal cortex three such loops have been described, each originating from a different prefrontal area. Cortico-striatal terminals are primarily from the LV and LIII pyramidal neurons and are distributed in patches in the basal ganglia. Unlike the temporal and posterior regions of the cortex, the PFC has highly organized connections with the basal ganglia via the striato-palladial and striato-nigral circuits. Projections from PFC and ACC cortical areas terminate primarily in the rostral striatum, including the ventral striatum (VS), caudate, and putamen. The vmPFC projection field to the striatum is very limited and is concentrated within the shell and a narrow column along the medial border of the caudate nucleus adjacent to the ventricle (Bonelli and Cummings, 2007). In contrast to the mPFC, the OFC projects to the central and lateral parts of the VS and extend more centrally than the mPFC projections. OFC projections also continue dorsally along the medial regions of the caudate nucleus and ventromedial putamen. However, their location is lateral to the vmPFC projections. Within the OFC projections, there also is some topography such that medial OFC regions terminate medial to those from more lateral OFC areas. The projections from ACC to the striatum are extensive and stretch from its rostral end to the anterior commissure. Terminals are located in both the central caudate nucleus and putamen. Overall, the ACC fibers terminate somewhat lateral to those from the OFC. Thus, the OFC terminal fields are positioned between the vmPFC and ACC, reflecting a topographic arrangement of cortico-striatal projections originating from the PFC. In turn these striatal areas projects to globus pallidus interna (GPi), globus pallidus externa (GPe), and caudolateral SN (Bronstein et al., 2001; Houk, 2001). The globus pallidus (GP) connects to the ventrolateral, ventral anterior, and centromedian nuclei of the thalamus, whose outputs are to supplementary motor area, premotor cortex, and motor cortex. Finally, the thalamic nuclei have reciprocal connections to the putamen and to the frontal cortex thus completing the circuit. Taken together the components of the prefrontal cortex that mediate behaviors are reflected in the

organization and connections between areas of PFC and in their projections to the striatum and thalamus (Bonelli and Cummings, 2007; Haber, 2016).

1.3. Functional roles of the rodent PFC

1.3.1 Anterior Cingulate Cortex

The Anterior cingulate cortex has a role in a variety of cognitive functions. Recent studies have concluded that the ACC plays an important role in mediating instrumental behaviors that require discrimination of multiple relatively similar stimuli. In particular, the ACC could be a structure enhancing stimulus discrimination, if stimuli share common elements, i.e., are in the same sensory modality and are similar (Cardinal et. al., 2003). Additionally the ACC has also been implicated in effort-based decision-making, where animals prefer high-effort actions, which lead to a larger reward than an alternative low effort action, which leads to a smaller reward while animals with an ACC lesion preferred the low effort reward. Although when the same degree of effort was required to obtain a large or small reward ACC lesioned animals showed preference for the larger reward like sham controls (Walton et al., 2003). This shows that the ACC is important in decision-making processes where an association has to be made between the effort required to obtain a reward and the magnitude of the reward itself (Rushworth et al., 2004).

The ACC has also been the focus of recent studies to understand how nociceptive signals are used to accomplish behavioral goals such as avoiding noxious stimuli and in turn to better understand the cognitive effects of chronic and acute pain. Specifically the anatomical connection of the ACC with areas involved in emotional responses like the amygdala suggest a role for the ACC in processing anxiety and fear in relation to painful stimuli or experiences (Gabbot et al., 2005; Cassel and Wright, 1986; Buchanan et al., 1994). In all animals, pain can result in expression of conditioned behavior triggered by the context in which the painful event occurred to prevent aggravating the pain. Using classical fear conditioning paradigms recent studies have shown that activation of ACC neurons results in freezing behavior and a conditioned fear memory for the place where the activation occurred (Tang et al., 2005). Conversely, bilateral inactivation of the ACC inhibits formation of conditioned fear

memory induced by foot-shocks. In rodents trace fear conditioning induces AMPA receptor mediated responses in the ACC and rodent models of chronic pain show consistently impaired trace fear memory as well as increased anxiety like behavior. Other experiments have shown that high levels of baseline anxiety in rodents contribute to an increase in acute visceral pain responses (Robbins et al., 2007). A recent study also found that selective optogenetic activation of pyramidal neurons of the ACC in mice induced anxiety- and depression-like behavior (Barthas et al., 2015). These findings, taken together, support the idea that activity in ACC neurons influences anxiety and fear behavior in response to nociceptive events. (Bliss et al., 2016)

1.3.2 Orbitofrontal cortex

Recent studies in rodents and primates indicate that the OFC is crucial for signaling information about expected outcomes and for using these signals to guide flexible behaviour i.e. value based decision-making (Gallagher et al., 1999; Pickens et al., 2003, 2005). Specifically, OFC signals predict characteristics, such as sensory properties (size, shape, texture and flavor) and unique value of specific outcomes that an animal expects given particular circumstances and cues in the environment. Evidence for such a role comes from behavioral as well as neuronal recording studies. Neuronal activity studies show that the OFC neurons demonstrate anticipatory firing, which are especially strong before the animal receives a reward or a punishment. For example, in discrimination learning, neurons in the rat OFC demonstrate selective firing in anticipation of sucrose (reward) or quinine (punishment) (Schoenbaum et al., 1998). Initially these neurons fire to one of the two outcomes, with further training they fire in anticipation of the outcome and finally fire in response to the cues predicting the outcome. However, unlike reward-responsive neurons, which also show a transfer of activity from outcomes to cues with training, the OFC neurons do not modulate their firing with respect to unexpected changes in the reward (omission or unexpected delivery) (Schoenbaum et al., 2003; Takahashi et al., 2009). Although such anticipatory firing has been seen in other areas, it first appears in the OFC and persists across all trial events, rather than being triggered by them. Thus suggesting that signaling expected outcomes, be they rewarding or punitive, is a major function of

OFC neurons. Such a hypothesis for OFC function is also backed up by behavioral studies.

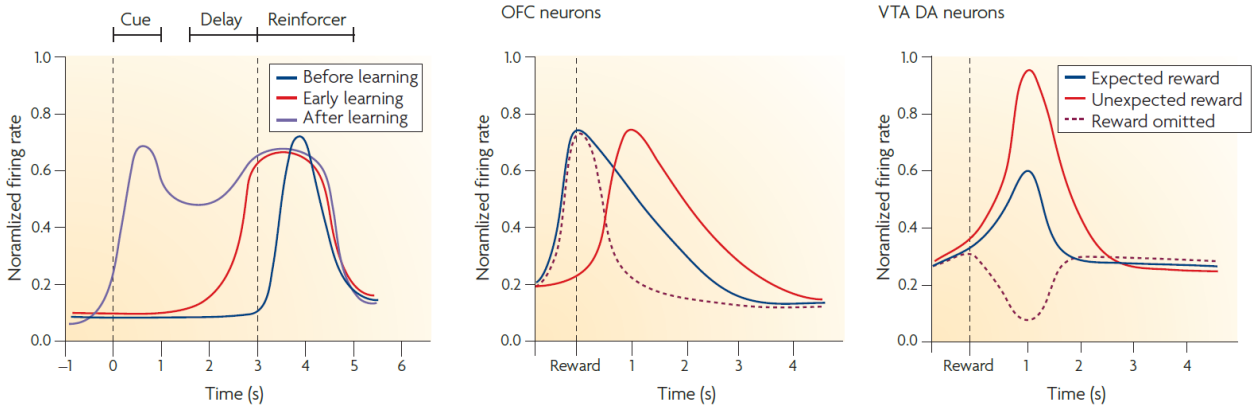

Figure 1.4: OFC neurons fire to expected outcomes across all phases of learning: The OFC neurons initially fire after reinforcement in the early phases of a task and with learning, they also fire to the cue itself. These OFC neurons do not stop firing in response to the reward even in later phases of learning, unlike reward responsive VTA neurons fire more strongly in response to unexpected rewards and decrease firing when an expected reward is not delivered. (Schoenbaum et. al., 2009)

A conclusive example of the role of the OFC in signaling expected outcomes is seen in Pavlovian reinforcer devaluation experiments. Here, an animal, which has been trained to associate a cue with a particular reward, is exposed to a protocol where the value of the reward is reduced by pairing it with illness or by feeding it to satiety. Subsequently the animals' ability to use that new value to guide its learnt response is assessed by presenting the cue alone. Animals normally show a reduced response to the predictive cue, reflecting their ability to access current lower value of the reward. However, rats with OFC lesions fail to show this effect of devaluation (Machado and Bachevalier, 2007). The role of OFC is fundamentally different from amygdala, which also shows anticipatory signaling but is only necessary during earlier phases of the devaluation protocol. Several other value guided behavioral paradigms like Pavlovian to instrumental transfer; delayed discounting, reversal learning and other second order behaviors show a similar role for OFC (Chudasama and Robbins, 2003; Hutcheson and Everitt, 2003; Mobini et al., 2002). It is to be noted that in rodents the OFC neurons also encode for the action response that leads to a favored outcome unlike the primate OFC that only codes for the value of the outcome. Interestingly disruption of the above behaviors is also seen when lesions to the OFC are made after the animals have

learned the underlying cue–reward and response–reward associations. This suggests that the OFC signals are crucial for updating associative representations in other brain areas in the face of unexpected outcomes by contributing necessary information to calculate the teaching signals required to drive such learning (Niv and Schoenbaum, 2008; Wallis, 2011).

1.3.3 Ventromedial PFC: PreL and IL

The PreL and the IL are known to exert distinct opposing influences across several behavioral domains. Most studies on the role of these two areas have been conducted using fear learning and its extinction. For example, PreL lesions or genetic inactivation interferes with conditioned fear expression (Corcoran and Quirk, 2007; Laurent and Westbrook, 2009; Sierra-Mercado et al., 2011; Sangha et al., 2014). In parallel, inhibiting PreL interneurons disinhibit its output to BLA and in turn enhances fear expression. On the other hand, IL inactivation or lesions impair initial acquisition of fear extinction learning as well as its retention (Laurent and Westbrook, 2009). Conversely, optogenetic stimulation of IL during extinction training accelerates the extinction learning and enhances its retention in subsequent retrieval tests (Do-Monte at al., 2015). Also, retention of extinction memory is dependent on gene transcription and protein synthesis in the IL (Santini et al., 2004; Mueller et al., 2008). Taken together this suggests that the PreL is required for fear expression while the IL is required for its extinction. Interestingly, recent experiments done with trace fear conditioning show that optogenetic silencing of PreL during the trace periods of the training protocol disrupts fear expression on retrieval (Gilmartin et al., 2013). It has also been reported that IL inactivation immediately following extinction training failed to prevent extinction retention (Sierra-Mercado et al., 2011). This suggests that the PreL and the IL need to be ‘online’ during fear learning and extinction respectively to mitigate their roles in flexible expression of fear memories. This is further supported by counter-conditioning paradigms where conditioned fear can be reduced by co presentation of a separate conditioned stimulus (CS) not paired with an aversive unconditioned stimulus (US) but instead paired with a positive reinforcement like a reward. In such cases inactivation of the IL (and not PreL) blocks the ability of the reward related CS to reduce conditioned freezing during retrieval.

The opposing roles of PreL and IL can also be extended to reward reinforced behavior. In conditioned place preference tasks (CPP) a reward like food or cocaine is paired continuously with a spatial location in a context. Upon retrieval and in absence of the reward animals chose to spend more time in the rewarded space. In such tasks, inactivation of the PreL can attenuate CPP while stimulating the PreL enhances CPP (Moorman et al., 2014). Moreover, direct electrical stimulation of the PreL alone during training (without reward) can induce CPP while inactivation of the PreL prevents reinstatement of cocaine CPP after its extinction. Conversely, activating IL after cocaine CPP enhances its extinction while silencing it interferes with extinction (van den Oever et al., 2013). Furthermore, IL stimulation post extinction attenuates the reinstatement of cocaine CPP while its inactivation exaggerates CPP reinstatement (LaLumiere et al., 2012). Simultaneous blocking of the PreL during reinstatement can also prevent this exaggerated reinstatement of cocaine CPP. This also suggests that behavioral flexibility as shown in these tasks is dependent on the concerted action of the PreL and IL. The PreL-Go and IL-stop operational logic have also been extended to goal directed behavior where the PreL and IL are key regulators in switching between goal-directed actions and habit based responses, where the PreL is (Barker et al., 2014; Baleine and O'Doherty, 2010) required for goal-directed behavior and the IL for habit learning. This PreL-go/IL-stop property of the vmPFC creates an optimal framework to encode behavioral flexibility, which allows an animal to choose between multiple alternative response strategies based on evidence, contingencies and internal goals.

1.4. Structural plasticity in the mPFC

The development and maturation of a cortical area reflects more than a simple temporal unfolding of a genetic blueprint. Rather, it represents a complex interplay of experiential and genetic factors that mold an emerging brain area. Owing to the complexity of building a brain, which has to adapt to a specific ecological niche post birth, there is an early life overproduction of neurons and their connections. These are later sculpted by experience dependent neural activity. Thus, it is possible to use a minimum of genetic instructions to build brains that are appropriate for the specific ecological niche of an animal. In humans, the peak synaptic density in the sensory cortices is reached by the first-year post birth while the prefrontal areas reach their

peak by 5 years of age (Petanjek et al., 2011). Interestingly this overproduction of synapses is the highest in in the PFC among all cortical areas. Starting from early childhood these synapses undergo extensive pruning and it continues in the PFC up to the third decade of life. Rodents also share a similar trajectory of maturation of the PFC as seen in human beings (Petanjek et al., 2011). In rats, the PFC cytoarchitectonics characteristics stabilizes last at 30 days post birth when compared to sensorimotor areas, which stabilize at 24 days (van Eden et al., 1990). Thus, among all cortical areas the PFC has the strongest potential to be shaped as a consequence of childhood and adolescent experiences like social and psychological stress, sensorimotor stimulation/deprivation and hormonal changes. This in turn can radically alter the functional circuitry of the PFC and resulting cognitive functions.

1.4.1 Sensorimotor stimulation

One of the most prevalent method of studying structural plasticity is by measuring changes in dendritic arborization, spine densities, cortical thickness and expression of neurotransmitters as a consequence of housing animals in complex environments with toys, tunnels, nests, etc. over prolonged periods. In adult animals, this type of environmental complexity, also known as environmental enrichment, leads to an increase in dendritic complexity and spine densities across most cortical and subcortical structures. Surprisingly a prolonged exposure to environmental enrichment leads to no change in PFC structural plasticity in adult rats and instead a decrease in dendritic complexity in male rats (Kolb et al., 2003, Comeau et al., 2010). In a different set of experiments, early life sensory stimulation in rats improved motor and cognitive functions as well as increased dendritic complexity and spine densities in both mPFC and OFC (Richards et al., 2012). Taken together these experiments show that the maturing prefrontal is more plastic than in adulthood unlike other neocortical regions, the hippocampus (HPC), and striatum.

1.4.2 Psychoactive drugs

Some of the largest and most robust changes in prefrontal cortex structural plasticity are caused by repeated administration of psychoactive drugs. When animals are given repeated doses of psychomotor stimulants, there is strong behavioral effect

(hyperactivity) that is accompanied with dendritic changes in prefrontal cortex and NAc (Robinson and Kolb, 1999a,b, 2004). For example, when animals got repeated low doses of amphetamine there was an increase in dendritic length and spine density in mPFC and NAc but a corresponding decrease in these measures in OFC (Crombag et al., 2005). Interestingly the differential effect of psychoactive drugs on the mPFC vs OFC also hold true for other psychoactive substances such as cocaine, and tetrahydrocannabinol. These changes are not restricted to pyramidal neurons alone, as one study found that a single injection of methamphetamine in adulthood led to a 20% increase in the density of GABAergic synapses in the PFC (Dawirs et al., 1997). The above mentioned anatomical changes are also accompanied by changes in gene expression in the PFC. Specifically amphetamine injections increased the expression of Fibroblast growth factor-2 (FGF-2) in the PFC (Cuppini et al., 2009). This factor is proposed to reduce neuronal excitability by inhibiting voltage gated sodium and potassium currents. Thus, the PFC shows rapid and persistent changes in their ultrastructure and gene expression in response to psychomotor stimulants.

1.4.3 Stress

Stressful experiences have been a second focus of recent studies in structural plasticity in the PFC. For example, in male rats chronic stress dramatically reduces synapses in layer III pyramidal neurons throughout the mPFC (Cook and Wellman, 2004; Radley et al., 2006, 2008; Bloss et al., 2010, 2011). Interestingly the synaptic loss in young animals can recover within 3 weeks post the stressful experience but older animals fail to show this recovery (Goldwater et al., 2009). Along with chronic stress, short-term mild stress can also result in structural changes in the PFC like retraction of dendrites. It is interesting note that the PFC ultrastructure is inherently different in males and females due to sexual dimorphism. Accordingly, the effect of stress on structural plasticity in the PFC is different across the genders (Muhammad et al., 2012). A recent study on the epigenetic effects of adult stress in mPFC, OFC, and the hippocampus showed increase in global methylation in both sexes in prefrontal areas but a decrease in the hippocampus. When examining the RNA from the above brain regions, chronic stress exposure led to mostly non-overlapping changes in gene expression across the different sexes and brain regions. These epigenetic data are consistent with the morphological data in showing both regional

and sex differences in the effect of stress on the prefrontal cortex plasticity (Kolb et al., 2014). From these two critical points emerge about the prefrontal cortex. First, unlike other cortical areas, the PFC shows age dependent changes in structural plasticity in response to sensorimotor stimulation, where young and adolescent animals have a more plastic PFC. Second, owing to the prolonged maturation timeline of the PFC post birth, experience dependent plasticity can strongly change their neurodevelopmental trajectory and subsequent function in adult hood.

1.5. Memory processes within the mPFC

1.5.1 Synaptic rearrangements in memory formation

The neural mechanisms for memory formation and storage can be classified into two related theories: the 'synaptic plasticity theory' postulated by Donald Hebb and 'the cellular engram theory' proposed by Richard Semon (Semon 1904, 1909). The very first proponent of the synaptic theory of memory formation was Santiago Ramon y Cajal, who suggested that contacts between neurons as site of memory storage (Ramon y Cajal, 1893). Subsequent work by Donald Hebb suggested a theoretical mechanism where synapses between neurons are strengthened by co-ordinated activity by the participating neurons (Hebb, 1949), now referred to as spike-time-dependent plasticity. Seminal work done by Eric Kandel using the Aplysia siphon-withdrawal reflex provided the first evidence for the synaptic theory of learning (Kandel et al., 2014). Subsequent discovery of long-term synaptic potentiation in the 1970s elucidated the molecular events that lead to synaptic strengthening on coordinated activity (Bliss and Lomo, 1973). The most commonly studied form of LTP is NMDA receptor dependent LTP where a large influx of calcium ions into the post synapse through the NMDA receptor leads to clustering of AMPA receptors and a resulting enhancement of synaptic transmission. Disrupting part of this process, for example by blocking AMPA receptor trafficking, leads to disruption of memory formation (Nabavi et al, 2014; Kessels et al., 2009). In addition to synaptic strengthening learning also leads to structural changes such as increased spine turnover and synaptic rearrangements (Caroni et al., 2012, 2014).

1.5.2 Cellular basis of memory allocation

The idea for a 'connected complex of excitations that exist as a unified engram complex', as the basis for a memory trace, was first proposed by Richard Semon in the early 1900s (Semon 1904, 1909). This theory envisions a system whereby a part of the original learning condition (Eg: a cue) can reactivate the engram complex and thus provide a framework for memory storage and retrieval (Schacter et al., 1978).

Studies over the last 40 years have provided us with strong evidences towards a cellular basis for memory engrams, where subpopulations of neurons in a brain area or multiple brain areas store individual episodic memories. A notable work from the 1980s used single cell activity in the inferotemporal cortex of monkeys performing a visual delayed matching-to-sample task. The authors demonstrated that groups of neurons differentially responded to color depending on attentional processes and this activity was correlated to retention and retrieval of the visual memory (Fuster and Jervey, 1981). Further evidence for a cellular basis of memory formation came from examining the expression of immediate early genes (IEGs) like c-fos and Zif268 where populations of cells active during the initial learning paradigm were selectively reactivated during memory retrieval (Reijmers et al., 2007, Tayler et al., 2013, Zelikowsky et al., 2014). These observational studies have been recently corroborated by gain of function and loss of function studies. By overexpressing the transcription factor CREB in a random population of amygdalar neurons immediately prior to learning a group of researchers could bias the storage of the corresponding memory to these neurons. Subsequent ablation of these neurons led to a loss of the encoded memory as seen by failure to retrieve the memory (Han et al, 2007, Han et al., 2009, Zhou et. al., 2009). Finally, gain of function studies have further strengthened the cellular theory of memory storage. In a recent study, researchers were able to genetically tag a population of neurons active during learning and subsequently reactivate them in the absence of any original learning cues to result in behavioral retrieval of the memory (Liu et al., 2012, Kim et al., 2014; Yiu et al., 2014). Thus, the synaptic plasticity theory and the cellular engram theory together provide a conceptual framework for encoding, storage and retrieval of memories.

1.5.3. Memory consolidation

A newly formed memory might exist for minutes or days or years before it is retrieved. To support such a varied degree of persistence, several neurological processes have evolved which operate at all levels, namely, neuronal networks, structural plasticity and molecular levels to form a stable memory. Memory consolidation is an umbrella term describing these processes.

Memories can be broadly divided into short-term (minutes,) and long-term (days, years) memories. Short-term memories do not depend on transcription and synthesis of new proteins, while *de novo* protein synthesis is required for long-term memories (Bekinschtein et al., 2007). The process of long term consolidation of memories is triggered by the initial learning itself and involves early (minutes) and late (hours) events to form stable memories by strengthening and formation of synapses (Caroni et al., 2014; De Roo et al., 2008; Holtmaat & Svoboda, 2009; Ruediger et al., 2011; Takeuchi et. al., 2013). In the early stages of memory consolidation, a learning event triggers neuronal depolarization and an influx of Ca2+, which initiates a downstream molecular cascade that results in transcription and translation of plasticity-related proteins (PRPs). In turn, these PRPs induce structural and functional changes in local neuronal networks, resulting in new, remodeled, or strengthened synaptic connections among an assembly of neurons, which forms the memory engram.

Among the PRPs, the immediate early genes (IEGs) are of special note. IEGs such as c-Fos, Arc, Zif268 have been linked to long-term consolidation (Katche et al., 2010 and 2013; Nakayama et. al., 2015). As shown for c-Fos, the IEG transcripts are expressed within minutes after learning while the protein products can be detected forty-five minutes after the initial learning event and remain upregulated for up to 4h (Karunakaran et. al., 2016). Since most IEGs are transcription factors (c-Fos, Zif268) or actin cytoskeleton remodelers (Arc), they likely play a role in formation and strengthening of new synapses through epigenetic mechanisms, differential gene expression and de novo synthesis of synaptic proteins e.g. scaffolding proteins of the post synaptic density (Holtmaat & Caroni, 2016). Currently it remains unclear whether the entire cell population active (by IEG expression) during the original memory acquisition event are reactivated on memory retrieval.

Interestingly a second wave of IEG and other signaling factor expression is seen hours post-acquisition in a late window of memory consolidation. For example, phosphorylated MAP kinase levels, which peak around 15 minutes post memory acquisition also shows a second peak at 9h post-acquisition (Trifilieff et al., 2006). Similarly, c-fos is also detected in a second wave of IEG expression 12-15h post memory acquisition. (Katche et. al., 2010). While the precise role of this second delayed window of consolidation remains unclear it is functionally essential for long-term persistence of memories. Recent work has shown that interfering with local dopaminergic signaling or de novo protein synthesis in this window in the mPFC or the hippocampus can disrupt later retrieval of aversive memories (Rossato et. al., 2009; Gonzales, 2014). Interestingly this deficit in memory retrieval can be reverted by BDNF administered in this same window (Bekinschtein et. al., 2007). Recent work has also shown that learning induced plastic changes in Parvalbumin interneurons are crucial in this window for long-term persistence of memories (Girardeau et al., 2009; Karunakaran et al., 2016). Other cellular and synaptic proteins are also upregulated in this delayed window albeit with different temporal scales. For example, a second protracted peak of Arc expression is seen in the hippocampus CA1 area 8-24h after spatial exploration (Ramirez-Amaya et. al., 2005). In conclusion, this second late and protracted window of memory consolidation involves a variety of transcriptional, translational, signaling and structural changes, which are essential for persistence of memories and have been suggested to support flexible learning. (Katche et al., 2013)

1.5.4. mPFC in short-term memory

Numerous studies have implicated the mPFC, like the primate dorsolateral PFC (dlPFC) in a form of short-term memory, which spans over minutes and is referred to as working memory. Similar to primates with damage to dlPFC, rodents with mPFC damage also show deficits in tasks requiring a delayed response (Horst and Laubach, 2009). The role in working memory is further supported by observations that both, rodent mPFC and primate dlPFC, exhibit persistent cellular activity during delay periods that is selective for a prior or upcoming target location (Baeg et al., 2003; Funahashi, 2006). Another study showed that when rats were required to hold down a lever until cued; a third of mPFC cells significantly altered their activity during the delay (Narayanan and Laubach, 2006). However, in general the mPFC is not required

to form short-term memory for locations, odors, or objects (Birrell and Brown, 2000; Seamans et al., 1995). It is interesting to note that short-term memory for rewarded odors do depend on mPFC when either a large number of odors must be remembered or odor associations must be learnt through social interaction (Boix-Trelis et al., 2007). Thus, the mPFC is only required for a very specific form of short-term memory called working memory or if the demand for short-term memory storage is very high.

1.5.5. mPFC in long-term memory

Early imaging studies first indicated a specific role for mPFC in long-term memory. A study examining metabolic activity in multiple mouse brain regions during retrieval of rewards on an eight-arm maze, either 5 or 25 days after learning, showed that the mPFC had significantly more activity during remote retrieval compared with recent. This selective activation of mPFC in remote memory has also been replicated in tests of both spatial and fear memory (Frankland et al., 2004; Teixeira et al., 2006). Consistent with these imaging results, inactivating mPFC also leads to deficits in retrieval of remote memories while leaving recent memory intact (Frankland et al., 2004; Ding et. al, 2008). However, several lines of evidence support the involvement of mPFC in recent memory. Of note is a recent study where optogenetic silencing of the PreL during the trace period of trace fear condition led to disruption of memory retrieval the next day (Gilmartin et al., 2013). Other studies have also directly demonstrated the requirement of mPFC for retrieval of recent navigational (Churchwell et al., 2010), object-place (Lee and Solivan, 2008) and fear memories (Corcoran and Quirk, 2007), learned a day or two prior to testing. It is not clearly understood why in some experiments the mPFC is not required for recent retrieval. However, an explanation for this could be that mPFC serves for both storage and representation of a memory on different time scales. During retrieval of recent memories, the role of mPFC is to represent context, events and responses while the mapping between them is stored within the hippocampus. On the other hand, during remote retrieval, the mPFC does both, i.e. represents as well as stores context-event-response mappings. Thus, the brain may be less able to compensate for its loss during remote retrieval than during recent. (Euston et al., 2012)

1.6. Oscillations and mPFC function

The brain uses electromagnetic oscillations as a way of linking ongoing processing across multiple brain areas. To this end, a wide variety of frequencies are involved, from the slow oscillations seen during sleep (starting at a fraction of a Hertz) to high frequency gamma oscillations reaching 80–100 Hz. By transiently increasing and decreasing the degree by which oscillations in the two structures keep a constant phase relationship, different areas can regulate the extent to which their computations interact. This allows for a dynamic functional network whose participating members can change rapidly along with task demands. For example, by shifting the phase relationship between gamma oscillations, a higher visual area like V4 can tune itself on a V1 column whose receptive field contains a preferred stimulus, thereby steering visual attention (Womelsdorf et al., 2007) to that stimuli. Furthermore, oscillations at different frequencies may coordinate incoming information from different sources. For example, the hippocampal subfield CA1, can selectively tune in to signals from the CA3 subfield or the entorhinal cortex by oscillating at characteristically different gamma frequencies inherent to these structures (Colgin et al., 2009).

Among the different types of oscillations, gamma oscillations have been strongly linked to the working memory function of mPFC. Specifically, gamma oscillations reflect rhythmic firing of inhibitory interneurons, particularly parvalbumin (PV)-expressing fast-spiking interneurons. The synchronized rhythmic patterns of spiking and synaptic inhibition of these PV neurons give rise to the electrical signatures identified as gamma oscillations. Interestingly, the intrinsic and synaptic properties of fast-spiking PV interneurons seem to be tuned to produce gamma oscillations at specific frequencies (Galarreta and Hestrin, 1999; Gibson et. al., 1999; Bartos et al., 2002). Mechanisms through which gamma oscillations contribute to circuit function can be classified based on locus of their action. Gamma oscillations can act on local excitatory neurons to regulate their responses to incoming stimuli, to modulate the patterns of local circuit activity or to enhance the efficacy of their output. In parallel, gamma oscillations can act as a clock relative to which the precise timing of spikes of distributed neurons can carry information and indicate their participation in a common neural representation (Fries et. al, 2007; Singer 1993).

In the PFC gamma oscillations increase during tasks that involve attention (Kim et al., 2016), cognitive control and social interaction (Cho et al., 2015). Moreover, the power of these oscillations also scale up with task demand. For example, the power of gamma oscillations in the PFC increases with the number of items being stored (Roux et al., 2012). Furthermore, a recent study showed that optogenetic stimulation of mPFC PV interneurons at 30–40 Hz improved performance, whereas stimulation at 1–10 Hz produced a much larger decrement in performance in an attention task. Although these oscillations are generated locally, they can be synchronized across long distances and correlate well with behavior. For example, synchronization between spiking activity in PFC neurons and hippocampal gamma oscillations is necessary for successful encoding of spatial information in a working memory task (Spellman et al., 2015; Tamura et al., 2016; Sohal, 2016).

1.7. The Hippocampal-Prefrontal axis

Several direct and indirect pathways link the hippocampus and the PFC. In both rodents and primates, the PFC receives monosynaptic glutamatergic connections from the hippocampus (Condé et al., 1995; Hoover and Vertes, 2007, Thierry, 2010). These originate only in the ventral hippocampus (vH) and target the mPFC, with stronger projections to ventral sub regions (Condé et al., 1995; Hoover and Vertes, 2007). Recently a monosynaptic connection originating from the anterior cingulate cortex and terminating in CA1 and CA3 of dorsal hippocampus (dH) has also been identified (Rajasethupathy et. al., 2015). Additionally the hippocampus and PFC can also interact via indirect routes, like through the thalamic nucleus reuniens (NR) which reciprocally connects to vH and mPFC (Vertes, 2006; Cassel et al., 2013). A second indirect rout of communication could be through the lateral entorhinal cortex, which also connects reciprocally to both the structures (Moser et. al., 2010).

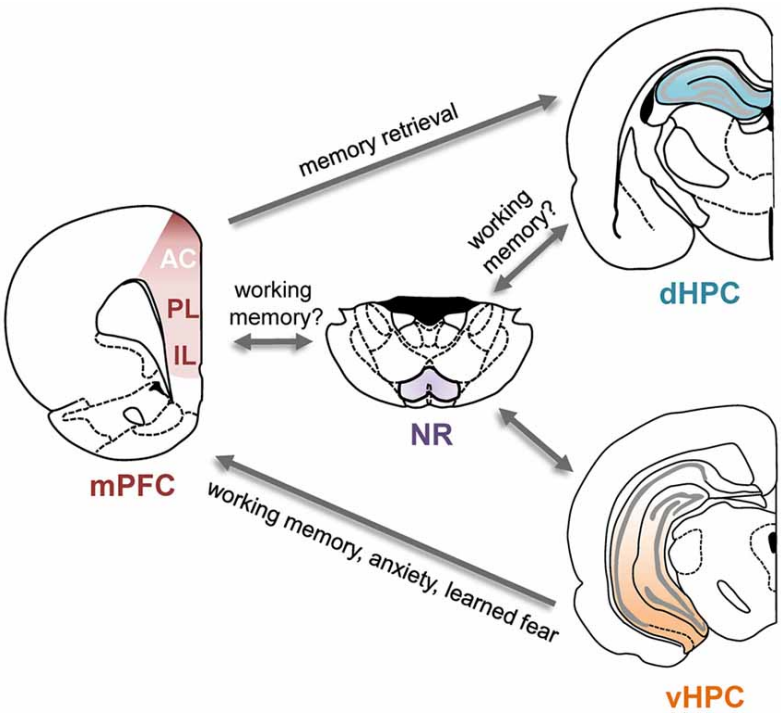

Figure 1.5: The hippocampal-prefrontal axis: The vH sends monosynaptic projections to the vmPFC while the ACC projects to the dH directly. The vH-vmPFC connection has been implicated in expression of learnt fear and working memory while the ACC-dH projection is involved in fear memory retrieval. The hippocampus and prefrontal cortex can also communicate via the reuniens and lateral entorhinal cortex. (Sigurdsson and Duvarci, 2016)

Hippocampal and prefrontal neurons often spike within a short time (~100 ms) of each other (Siapas et al., 2005). Furthermore, these spikes in prefrontal neurons can lead or lag behind spikes in the hippocampus, showing a directionality of influence (Siapas et al., 2005; Wierzynski et al., 2009). Prefrontal neurons are also modulated by the phase of hippocampal theta oscillations (4-12Hz) (Buzsáki, 2002). Prefrontal neurons tend to fire more at certain phases of the theta oscillation, a phenomenon referred to as “phase locking” (Siapas et al., 2005; Sigurdsson et al., 2010). Such phase-locked PFC neurons also show cross-correlations with hippocampal neurons, suggesting they reflect the same phenomenon (Siapas et al., 2005). Interestingly, prefrontal neurons can be phase-locked more strongly to either past or future phases of hippocampal theta oscillations although on average phase-locking to the past is stronger (Siapas et al., 2005; Sigurdsson et al., 2010). Lastly, hippocampal-prefrontal synchrony can be observed in the “coherence” of LFPs recorded in the two structures (Adhikari et al., 2010).

Functionally, Hippocampal-Prefrontal interactions are important during behaviors in which both areas are involved and their different functions need to be coordinated. One such example is spatial working memory (SWM), which measures animals' ability to remember spatial locations for short durations. In a typical version of the task, animals must choose which arm of a maze to enter during a "choice phase based on their memory of a previously visited arm (Dudchenko, 2004). Lesion studies have shown that SWM tasks require both the hippocampus and the PFC in rodents (Yoon et al., 2008; Churchwell and Kesner, 2011). Simultaneous recording from the two structures in rats showed increased hippocampal-prefrontal synchrony in the choice phase (from phase-locking, LFP coherence and cell pair cross-correlations) compared to a task phase in which the behavior was the same but no working memory was required (Jones and Wilson, 2005). Moreover, this synchrony increases gradually as the mice learn indicating that structural plasticity in this circuit underlies learning (Sigurdsson et. al., 2010). Interestingly and in contrast to the theta frequency, gamma synchrony increased only in the sample phase of the task where animals need to encode spatial locations into memory. Thus, the synchrony across different frequency spectra reflect different functional processes. Disconnection lesion studies where the hippocampus-PFC connections are severed also result in impairments in the SWM task (Wang and Cai, 2006; Churchwell et al., 2010) and have been corroborated by recent studies with optogenetic silencing of these projections (Spellman et. al., 2015).

Hippocampal-prefrontal interactions also likely play an important role in long-term memory and its consolidation. Synchrony in the hippocampal-prefrontal axis is observed in sleeping rats, with hippocampal activity leading activity in the PFC (Wierzynski et al., 2009) suggesting that these interactions support system consolidation of memories. Moreover, patterns of neural activity that occurred in the PFC during wakeful experience are also "replayed" during subsequent sleep simultaneously with "sharp-wave ripple" events in the hippocampus (Peyrache et al., 2009). In addition to these, a recent study has shown that optogenetic manipulation of projections from ACC to dH are both necessary and sufficient for retrieval of contextual memory, as measured by contextual fear responses (Rajasethupathy et al., 2015). Finally, long-term synaptic plasticity at ventral hippocampal inputs to the PFC has been shown to be involved in the extinction of fear responses (Hugues et al., 2006;

Peters et al., 2010). Thus, hippocampal-prefrontal interactions underlie many a cognitive function and learning paradigms.

1.8. Remodeling of mPFC circuitry in adolescence

Since the PFC has a protracted window of maturation, extending beyond adolescence into adulthood, it is important to look at the changes in prefrontal circuitry during this period. Recent studies have shown that in rodents adolescence is a critical period for the maturation of both glutamatergic and GABAergic transmission in the PFC, particularly due to changes in the weight of neuromodulatory projections such as monoamines and cannabinoids.

It has been proposed that dopamine might facilitate the maturation of PFC by a D1 receptor-dependent enhancement of prefrontal NMDA trans-mission (O'Donnell, 2010; Tseng et al., 2009). In the adult PFC D1 receptor stimulation leads to long lasting plateau depolarizations in pyramidal neurons but these plateaus are only seen post the age of P45. This suggests that dendritic sodium and calcium transients are able to effectively couple distal apical activity with the somatic activity only beyond this age (Tseng and O'Donnell, 2005; Zhu, 2000). This finding is corroborated by the increase in density of DA innervation in the PreL from adolescence until P60 (Kalsbeek et al., 1988). Recordings from GABAergic neurons in the juvenile PFC (P15-35) reveal that D1 and not D2 receptors increase the excitability of fast spiking neurons of which Parvalbumin neurons are a major class (Gorelova et al., 2002; Tseng et al., 2006). However, it is only after adolescence, around P50, that a powerful excitatory effect through D2 receptor mediated signaling onto GABAergic activity emerges in the PFC (Tseng et al., 2006; Tseng and O'Donnell, 2007). Thus, DA modulation of GABAergic activity in the PFC undergoes developmental regulation such that D1 and D2 receptor-mediated facilitation of interneuronal excitability becomes markedly enhanced after P50 (Tseng and O'Donnell, 2007). It is interesting to note that PFC PV neurons also upregulate the expression of PV across adolescent to reach a steady state level in adulthood (Caballero et. al., 2014a) along with a 30% increase in the frequency of spontaneously generated IPSCs (Cass et. al., 2014). Also, there is a selective increase in excitatory inputs onto PV positive fast-spiking basket cells during adolescence.

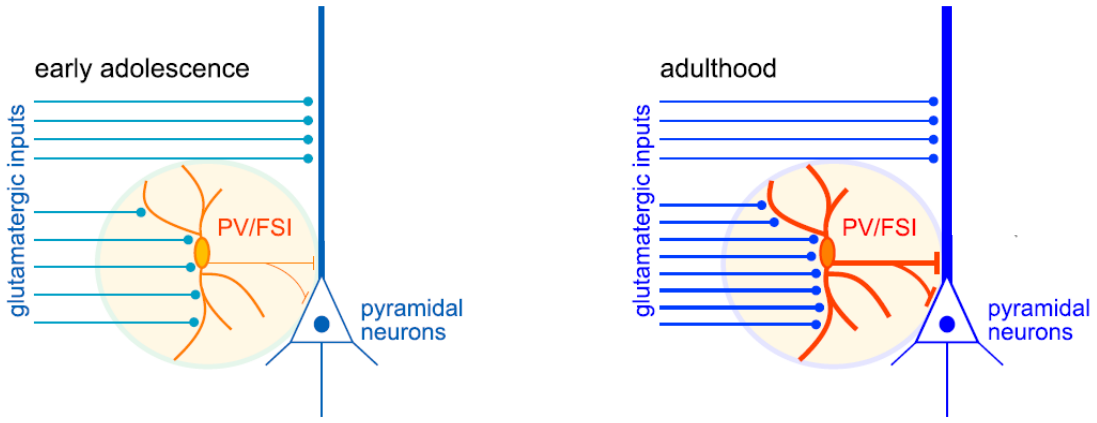

Figure 1.6: Periadolescent changes in Prefrontal microcircuitry: Adolescent rodents express increasing levels of Parvalbumin from adolescence, which stabilizes in an adult steady state at P60. There is an associated increase in glutamatergic synaptic activity onto PV interneurons as animals transition from adolescence to adulthood. (Cabarello et al., 2016)

Similarly, glutamatergic connectivity into the PFC also changes through adolescence. Of particular interest are the glutamatergic inputs carrying contextual and emotional information from the vH and amygdala respectively. One recent study showed that LTP in the PFC, following hippocampal stimulation, doesn't emerge until P50 although the amygdala can trigger prefrontal LTP from P30 itself, suggesting a delayed strengthening of the hippocampus-PFC projections (Caballero et. al., 2014b; Flores-Barrera et. al., 2014). Surprisingly, unlike other cortical areas where there is a developmental switch from GluN2B to GluN2A transmission, in the PFC, GluN2B transmission emerges specifically in the hippocampus to PFC glutamatergic synapses at P50. The slow kinetics of GluN2B-containing NMDA receptors (Vicini et al., 1998) might provide a functional advantage by selective amplification of the information originating from the ventral hippocampus.

1.9. mPFC dysfunctions in neuropsychiatric disorders

Since the 1930s, frontal lobe dysfunction has been implicated in psychiatric illnesses such as mood disorders and schizophrenia. This hypothesis primarily originated from studies in chimpanzees where prefrontal cortex removal resulted in massive reduction in aggression and an inability to experimentally induce neuroses in the animals

(Jacobsen, 1936). This led to the infamous and failed psychosurgical technique of lobotomy whereby the prefrontal cortex or its thalamic connections were severed in an effort to make mentally disturbed patients more manageable. Since then however neuroscience has come a long way in understanding prefrontal cortical dysfunction and its role in multiple cognitive and psychiatric disorders.

1.9.1. Post-Traumatic Stress Disorder (PTSD)

Short-lived fear is an instinctual response that is adaptive and critical for survival in the face of danger but can lead to anxiety and detrimental generalizations when it is chronic. Post-traumatic stress disorder (PTSD) is a neuropsychiatric disorder where fear related memories of a traumatic experience are over generalized and become resistant extinction. Symptoms include high level of anxiety, nightmares, flashback and changes in physiology such as increased heart rate and perspiration. Almost 10% of all trauma victims end up suffering from PTSD.

In rodents, the PreL and IL regions of the vmPFC and their projections to the amygdala have been implicated in appropriate expression of fear and its extinction. Specifically inactivating the PreL reduces fear expression while inactivation of the IL prevents extinction learning and retention (Sierra-Mercado et. al, 2011). Similarly, in human beings the dorsal anterior cingulate (dACC) and the ventromedial PFC (vmPFC) has been implicated in expression and extinction of fear respectively. Extinction of fear is the foundation of behavioral therapies for PTSD, in which patients are repeatedly exposed to trauma-related stimuli in a safe environment. Functional neuroimaging studies have shown that individuals with PTSD often display decreased blood flow to the mPFC upon recalling a traumatic experience, which might disrupt extinction learning (Semple et. al., 1996; Bremner et al., 1999). Similar to rodents, human vmPFC has an inhibitory control over the amygdala (Delgado et al., 2008). Studies have shown that the vmPFC-amygdala pathway may be dysregulated in some cases of PTSD (Gilboa et al., 2004; Garfinkel et al., 2014) while patients with bilateral vmPFC damage show increased amygdala activation to aversive images (Motzkin et al., 2015). Thus, vmPFC regulation of the output of amygdala may be a common circuit underlying fear extinction. On the other hand, the dACC has received considerable attention for regulating fear expression as in healthy subjects this brain region is

activated by conditioned stimuli (Milad et al., 2007). Thus, dACC signaling may correspond to ongoing fear responses and it has been shown that PTSD patients display a greater activation of dACC during extinction recall (Milad et al., 2009). Thus, a better understanding of mPFC dependent fear expression and extinction in rodents can provide useful therapeutic strategies for the treatment of PTSD in human patients (Giustino and Maren, 2015).

1.9.2 Schizophrenia

Schizophrenia is a debilitating psychiatric illness that affects roughly one percent of the population and typically emerges between the ages of 18 and 25 years of age. The disease manifests itself in numerous symptoms that are classified as either ‘‘positive’’ (hallucinations, delusions, disorganized speech and behaviour), or ‘‘negative’’ (flattened affect, social withdrawal, avolition and anhedonia). While psychosis is frequently the most striking clinical feature of schizophrenia, disturbances in cognitive processes are now regarded as a core feature of the illness (Elvevåg and Goldberg 2000). The cognitive impairments are the most disabling and persistent feature of the disease and the magnitude of these impairments are the best predictors of long-term prognosis of the disorder. Moreover, the cognitive symptoms manifest earlier in life in the ‘prodromal’ phase itself before the first episode of psychosis (FEP) and clinical diagnosis of the disease. Thus, the cognitive symptoms can be a predictor for high-risk patients and their therapeutic amelioration has become a strong focus of recent research.

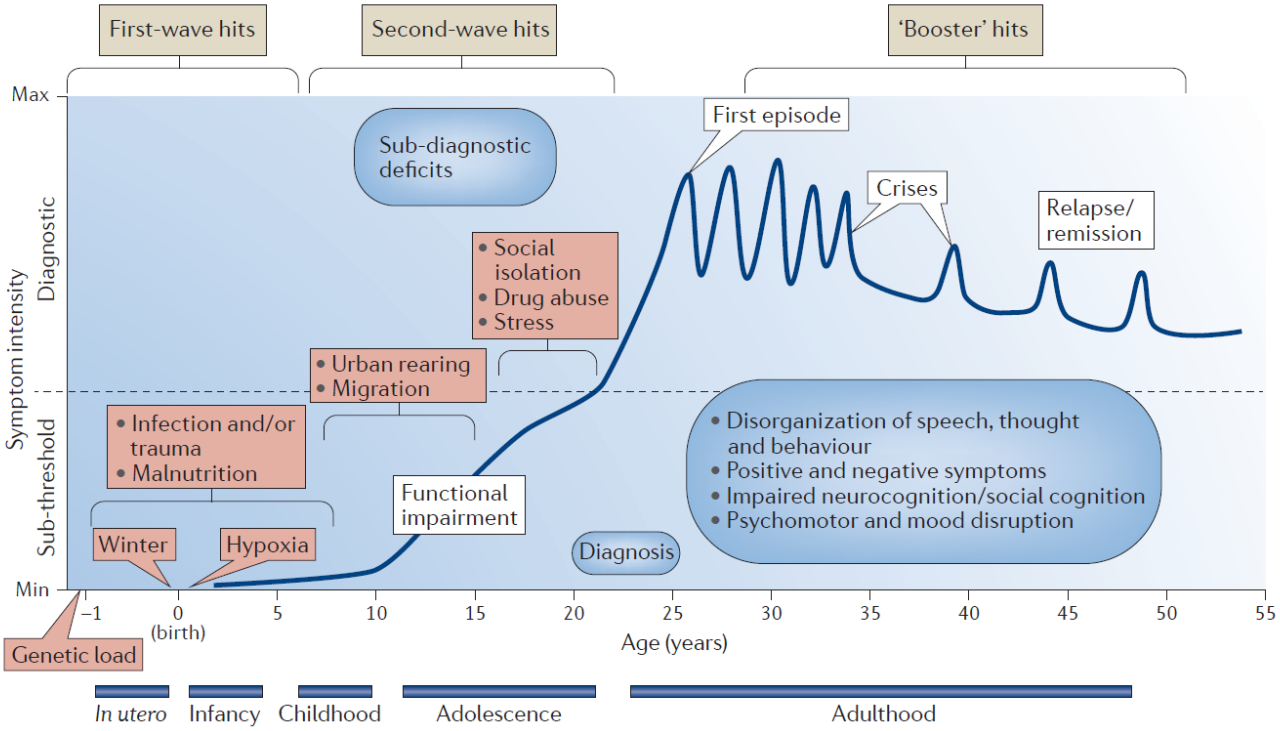

Figure 1.7: Onset and progression of Schizophrenia in relation to risk factors: Schizophrenia is first diagnosed in young adults by the first episode of psychosis. Preceding the FEP there is a prodromal at-risk phase around adolescence where sub-threshold psychosis and cognitive deficits are present. Various environmental insults or hits can trigger psychosis in the at-risk population and result in clinically diagnosed schizophrenia. Once diagnosed the disease follows a fluctuating course of acute psychotic episodes interspaced by periods of recovery (Millan et. al., 2016)

The range of cognitive deficits in schizophrenia suggests an overarching alteration in top-down cognitive control, which is a key function of the dlPFC in humans. Gamma frequency (30–80 Hz) oscillations in dlPFC neural networks are thought to be a key neural substrate for cognition (Howard et al., 2003). Consistent with these observations, individuals with schizophrenia exhibit altered activation of the dlPFC (Minzenberg et al., 2009) and lower power of frontal lobe gamma oscillations (Cho et al., 2006; Minzenberg et al., 2010) during tasks that require cognitive control. Since Parvalbumin interneurons are central to the generation of local gamma oscillations, deficient GABAergic neurotransmission in the dlPFC has been hypothesized to be a key feature of the disease. Indeed, in individuals with schizophrenia, negative modulation of GABAergic neurotransmission worsened symptoms (Ahn et al., 2011), whereas positive modulation was associated with increased task evoked frontal lobe gamma oscillations (Lewis et al., 2008). Furthermore, deficits in dlPFC PV

interneurons and its circuitry is a conserved feature in post-mortem analysis of the brains of patients (Guidotti et al., 2000; Curley et al., 2011). Specifically, in patient sample, 50% of dlPFC PV neurons express no detectable levels of GAD67 mRNA. Moreover, these same neurons also show a marked reduction in PV mRNA although the density of the PV neurons is comparable to unaffected individuals (Hashimoto et al., 2003). Post-synaptic $GABA_A\alpha1$receptors are also reduced in the dlPFC of patients. Taken together this suggest an overall dysfunction of PV neurons and their local inhibitory signalling in the dlPFC of schizophrenics.

GABAergic dysfunctions in the mPFC is often found in rodent models of Schizophrenia. Moreover, animal models with targeted disruption of PV neurons often show cognitive deficits similar to human schizophrenic patients. A hemizygous chromosomal microdeletion at the 22q11.2 locus is associated with extensive cognitive impairments and schizophrenia in humans (Green et al, 2009; Gothelf et al., 2004). It is the strongest known genetic risk factor for schizophrenia with 40% of carriers developing the disorder (Schneider et al., 2014). A mouse model, called LgDel, of this deletion targeting a homologous mouse chromosome also show behavioural deficits like deficit in pre-pulse inhibition, impaired spatial alternation learning in the T-maze and impaired reversal and discrimination learning, which indicate towards impaired cognitive functions (Stark et al. 2008, Sigurdsson et al. 2010; Meechan et al., 2015). Thus studying the neurodevelopmental phenotype of Parvalbumin interneurons in the mPFC of this mouse model can provide us with new therapeutic approaches towards Schizophrenia.

2. Results

2.1

Infralimbic cortex required for learning alternatives to Prelimbic promoted associations through reciprocal connectivity

Arghya Mukherjee and Pico Caroni

Nature Communications (2018) 9(1):2727

Introduction

Top-down control through prefrontal cortex (PFC) is believed to link internal goals to perception, thought and action in order to promote flexible behavior and guide learning (Miller and Cohen, 2001). Studies in humans, monkeys and rodents have revealed how pyramidal neurons in different prefrontal areas are tuned to distinct aspects of goal-oriented behavior, including the detection of expected and unexpected information, of the value of rewards, information and actions, and of options selected and not selected (Rushworth et al., 2011; Kolling et al., 2012; Gourley and Taylor, 2016; Hamilton and Brigman, 2015). From these studies, the view has emerged that prefrontal areas might, together, inform circuitry involved in learning outside these areas about the changing value of information and possible actions, e.g. by keeping this information into working memory to direct attention and goal-oriented behavior (Miller, 2000; Miller and Cohen, 2001; Gilmartin et al., 2005, 2013). Testing these predictions and understanding the roles of different subdivisions of prefrontal cortex in learning and memory, as well as understanding the underlying circuit mechanisms, might be achieved through area- and circuit-specific loss and gain-of-function experiments during learning.

PreL and IL are two major medial PFC areas in rodents thought to mediate control of goal-oriented behavior (Hok et al., 2005; Ito et al., 2015; Tanji and Hishi, 2008). Both PreL and IL neurons exhibit dense connectivity with brain areas such as striatum, nucleus accumbens, amygdala (Knapska et al., 2012; Little and Carter, 2013) and hippocampus, consistent with roles in top-down control of learning and memory (Groenewegen and Uylings, 2000; Vertes et. al., 2004; Hoover and Vertes, 2007). Neuronal activity in human dorsolateral PFC (a prefrontal area related by some studies to rodent medial PFC) was correlated to the reward value of action choices (Tanji and Hoshi, 2008; Kim and Shadlen, 1999; Morris et al., 2014). Furthermore, PreL neurons were tuned to the value of goals, e.g. in goal-directed spatial navigation (Hok et al., 2005; Ito et al., 2015), whereas IL neurons appear to be tuned to alternative choices (Suto et al., 2016). In rodents, lesion studies have suggested that medial PFC (including PreL and IL) is critically important for flexible behavior (Rich and Shapiro, 2007, 2009; Qualian and Gisquet-Verrier, 2010; Brady and Floresco, 2015). IL was shown to be critically important in extinction of Pavlovian fear conditioning and in

controlling addiction (Peters et al., 2009; Sierra-Mercado et al., 2011; Laurent and Westbrook, 2009; Courtin et al., 2013, 2014; Sangha et al., 2014; Barker et al., 2014; Giustino and Maren, 2015). Furthermore, IL has been implicated in the development of habits (Killcross and Coutureau, 2003; Smith et al., 2012; Smith and Graybiel, 2013), and in the control of pain, impulsivity and depression (David-Perreira et al., 2016; Tsutsui-Kimura et al., 2016; Fuchikami et al., 2015). Taken together, neuronal tuning and lesion studies have suggested that PreL and IL might have complementary and possibly opposite roles in goal-oriented flexible learning (e.g. Sotres-Bayou and Quirk, 2010; Sierra-Mercado et al., 2011; Giustino and Maren, 2015). Comparable important roles for flexible behavior as those assigned to rodent PreL and IL, have been assigned to primate PFC. These findings have raised the question of how PreL and IL might interact to influence learning, and what might be the possible underlying circuit mechanisms. Elucidation of these questions might provide insights into how distinct but functionally related prefrontal cortical areas might together support flexible learning and memory.

To investigate whether and how PreL and IL might exert complementary and possibly opposite roles in learning, we carried out local PreL or IL silencing experiments during learning, and traced and functionally targeted connectivity between these two prefrontal areas using specific viral vector mediated tracing and pharmacogenetic silencing. We provide evidence for direct reciprocal layer5/6-derived PreL-IL connectivity. Using intra- and extra-dimensional set-shifting tasks, as well as fear conditioning and extinction protocols, we provide evidence that PreL supports new learning by promoting application of previously learned associations, whereas IL is required to learn alternative associations. Neither PreL nor IL was required to recall learned associations when no new learning was involved. We then show that the role of IL to promote alternative learning specifically depends on unidirectional IL->PreL connectivity during learning, whereas reciprocal PreL<->IL connectivity is specifically required during a time window 12-14h after learning of a particular association to set up the role of IL to learn alternative associations. Taken together, our results define distinct and opposite roles of PreL and IL specifically to support new learning, and provide circuit-level evidence that IL mediates learning of associations alternative to those supported by PreL through direct reciprocal PreL-IL connectivity.

Results

Reciprocal PreL/IL layer5/6 connectivity

As a first step towards investigating circuit mechanisms underlying possible interactions between PreL and IL in learning, we determined whether these adjacent prefrontal areas were directly connected with each other. We delivered a Cre-expressing retrograde CAV2 (Kremer et al., 2000) to PreL (or IL) and AAV8 expressing Cre-dependent DREADDs (Sternson and Roth, 2014) and mCherry for visualization of dual-infected neurons. Twelve to fourteen days after these viral deliveries, we analyzed brain sections for marked projection neurons. We detected prominent reciprocal layer 5/6-derived connectivity between PreL and IL (**Fig. 1A**). Specifically, neurons projecting from IL to PreL were mainly located in layer6 (59.1± 3.6% of total, n= 5 animals), followed by layer5 (33.2 ± 7.3 %) (11.1 ± 1.7% of total GABAergic; Saffari et al., 2016), and neurons projecting reciprocally from PreL to IL were located to comparable extents in layer6 (48.1 ± 5.5% of total) and layer5 (45.3 ± 3.7%) (4.7 ± 3.2% of total GABAergic) (**Fig. 1B**).

To determine the cortical layer(s) in which IL→ PreL (or PreL→IL) terminate within the respective other cortical area, we applied combinatorial infection of CAV2-Cre and AAV9-flex-Synaptophysin-Myc to infect these neurons, visualizing their synaptic terminals (**Fig. 1C**). We found that axons of IL→PreL or of PreL→IL projection neurons mainly terminate in layer 6, layer 5 and layer 2 of PreL (respectively IL) (**Fig. 1C**). In addition, collaterals of these same axons targeted basolateral amygdala (BLA) (**Fig. 1C**), but not a number of additional potentially relevant target regions, including nucleus accumbens (**Fig. 1C**; we detected numerous GFP+ axons, but failed to detect Synaptophysin-Myc+ presynaptic terminals in this area), hippocampus or primary motor cortex M1 (Fig. 1c). For nucleus accumbens, it is possible that weak or spatially highly restricted presynaptic terminals by IL->PreL and/or PreL->IL projection neurons went undetected in our experiments. Alternatively, different neurons might account for functional projections between PreL/IL and nucleus accumbens.

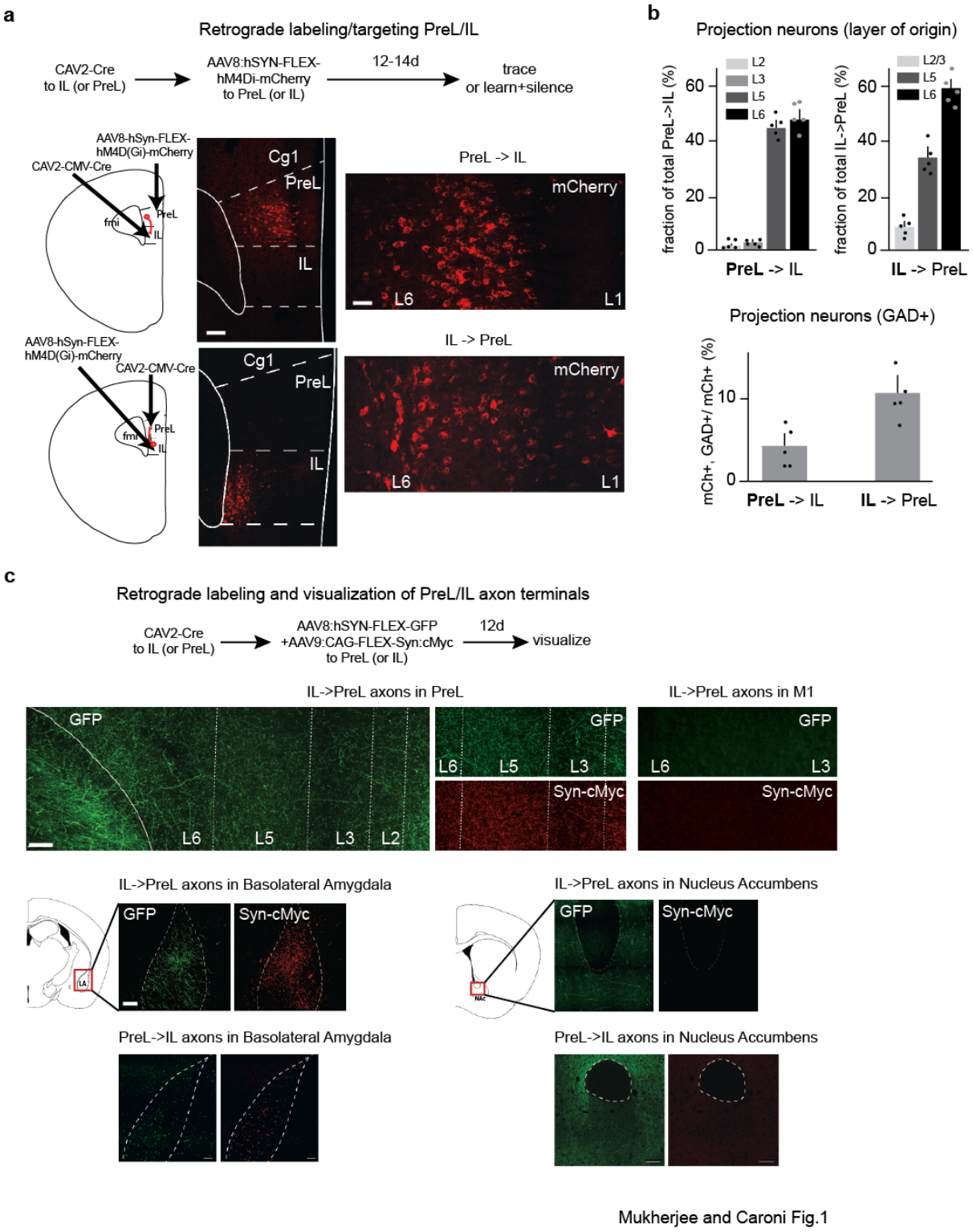

Figure 1. Reciprocal PreL/IL layer5/6 connectivity.

a: Retrograde labeling of PreL->IL and IL->PreL connectivity. Schematic of experimental procedure, and examples of PreL->IL and IL->PreL labeling experiments. Bars: 150um(left), 35um(right) um.
b: Cortical layers from which IL neurons project to PreL or PreL neurons project to IL (in % of total projecting neurons; top), and fraction of GAD+ neurons among PreL->IL and IL->PreL projecting neurons (bottom). n= 5 for both PL→IL and IL→PL groups.

c: Analysis of IL->PreL and PreL->IL projecting axon collaterals. Top: schematic of labeling experiments with GFP and Synaptophysin-cMyc fusion protein. Panels: examples of IL->PreL and PreL->IL projecting axon (GFP) collateral terminals (Syn-cMyc) in PreL and BLA, but not in M1 and Nucleus Accumbens. Bar: 300 um.

Shift-learning: PreL to apply rules and IL to learn alternatives

We then investigated specific roles of PreL and IL in learning and memory by transiently and bilaterally silencing PreL or IL at acquisition or recall of different forms of learning. To achieve local silencing of PreL or IL, we pharmacogenetically activated local parvalbumin (PV) interneurons, thereby effectively silencing local principal neurons (Magnus et al., 2011; Sparta et al., 2014; Karunakaran et al., 2016). To this end, we injected an AAV expressing a Cre dependent activating ligand-gated ion channel construct (PSAM-5HT3; this engineered hybrid channel construct does not respond to the endogenous neurotransmitters ACh or 5HT, and the artificial ligand PSEM308 (short PSEM) does not displace 5HT from endogenous 5HT3 receptor) in a PV-Cre mouse line (Magnus et al., 2011). The neurons expressing the channel could be detected by labeling with α-Bungarotoxin-Alexa488, and activated by i.p. delivery of the corresponding ligand PSEM. Specific targeting of IL was achieved under stereotactic guidance through slightly oblique orientation delivery angles. This was done in order to reach IL without contacting PreL, thereby minimizing drug and virus spread to PreL (**Fig. 2A, Fig. S1**; Methods). Silencing specificity and effectiveness were verified through analysis of cFos induction in layer2/3 neurons of PreL and IL 90min after acquisition of fear conditioning (**Fig. S2**; see also **Fig. 6**). In control experiments, silencing through local delivery of the GABA-A agonist muscimol had closely comparable impacts on learning to silencing through local PV neuron activation (**Fig. S3**). Therefore, throughout this study, we consistently silenced PreL or IL through pharmacogenetic PV activation since the silenced region could be verified in every mouse through visualization of confined viral expression with α-Bungarotoxin. Only mice with verified specific targeting of PreL or IL were included in the analysis (Methods).

We first carried out selective silencing experiments as mice performed subtasks of an intra/extra-dimensional set-shifting protocol (IEST) (Bissonette et al., 2008; Garner et al., 2006; Brady and Floresco, 2015) (**Fig. 2B**). In this sequential learning protocol

closely comparable to the Wisconsin card-sorting task applied in humans to test prefrontal executive functions, mice learn a defined sequence of changing cue/goal associations during five consecutive days. General features of the task (e.g. two adjacent compartments at one end of a box, with cups holding a food pellet hidden by bedding material; daily experimental procedure) were kept constant throughout IEST, and only cue/reward associations changed on consecutive days (**Fig. 2B**). Criterion was defined as the number of trials required to produce a series of eight out of ten correct decisions (digging for a hidden food pellet in the correct cup). Accordingly, the minimal number of trials to reach criterion was eight. We further set an upper threshold at 50 trials, beyond which increasing numbers of trials appeared to be progressively less related to learning, possibly due to decreased attention. For each of the subtasks, we carried out separate silencing experiments in either PreL or IL by delivering ligand PSEM 20min before the learning protocol (silencing within 1-2min, and up to 45-60min). Corresponding controls locally expressed the pharmacogenetic activator channel in PV neurons, but were treated with saline instead of ligand.

On the first of day of IEST, mice learned to dig for reward at the cup associated with a particular odor (yellow O(A); simple discrimination, SD; which cup was associated with the rewarded odor changed randomly between the two possible positions), and took about 20 trials to reach criterion (**Fig. 2C**). On the next day, the odors (O(A) and O(B)) and the particular odor-reward association (yellow O(A)) were left unchanged, but an additional set of (distracting) cues (texture around the cups; T(1) and T(2)) was introduced in the task (complex discrimination, CD). In a first set of experimental mice, PreL or IL was silenced specifically during CD (**Fig. 2C**). Under the modestly changed circumstances involved in CD, vehicle-treated mice efficiently applied the previous odor-reward association, now reaching criterion in 9-10 trials (instead of 20 trials on the previous day). In striking contrast, mice with silenced PreL took again about 20 trials to reach criterion (**Fig. 2C**). Silencing IL did not affect CD performance (**Fig. 2C**). In a separate set of mice, silencing PreL (or IL) did not affect recall of SD (no distracting textures; **Fig. 2C**). We therefore conclude that mice with silenced PreL failed to apply the previously learned odor-reward association to rapidly learn CD in the presence of potential distractors.

In the next group of experimental mice, PreL or IL was silenced specifically during the next IEST sub-task, i.e. intra-dimensional shift (IDS) (**Fig. 2D**). In this subtask, new pairs of odors (O(C) and O(D)) and textures (T(3) and T(4)) were introduced, but reward was again associated with one particular odor (blue-violet O(C); **Fig. 2B**). Vehicle-treated mice rapidly focused on the newly rewarded odor as the correct cue/reward association, and reached criterion in 12-14 trials (**Fig. 2D**). By contrast, mice with silenced PreL took again 20-22 trials to reach criterion, apparently failing to apply the previously learned association between the odor dimension and reward to rapidly learn in IDS (**Fig. 2D**). Mice with silenced IL only needed 9-10 trials to reach criterion in IDS, possibly suggesting an IL-promoted tendency to consider focusing on the alternative (distracting) dimension when none of the two new odors was identical to the previous odor-reward association, thereby slowing IDS learning (**Fig. 2D**). In a separate group of mice, silencing of PreL or IL did not affect recall of the cue/reward associations at IDS (**Fig. 2D**), further supporting the notion that PreL and IL are specifically required to promote learning of new cue/reward associations within a given task, but not to retrieve those associations in the absence of variations requiring further learning.

In the next set of experimental mice, PreL or IL was silenced specifically during the subsequent IEST subtask, i.e. intra-dimensional reversal (IDSRe; **Fig. 2E**). In this subtask, none of the cues were changed, but mice now had to associate the opposite odor (magenta O(D)) with reward, i.e. they had to learn an alternative to the most recent cue-reward association under conditions identical to those previously associated with the opposite association (**Fig. 2B**). Strikingly, vehicle-treated mice strongly resisted learning the alternative odor-reward association and required about 30 trials (instead of 20 trials for SD, and 20 trials for CD or IDS with silenced PreL) to reach criterion. Notably, mice with silenced PreL only took 10-11 trials to reach criterion, suggesting that PreL accounted for perseverance with the most recent (now un-rewarded) odor-reward association, interfering with learning of the alternative (odor) association (**Fig. 2E**). In striking contrast, mice with silenced IL mostly failed to reach criterion before 50 trials, suggesting a failure to learn the alternative odor-reward association (**Fig. 2E**).

To investigate whether IL might be important to learn alternatives to the most recent association, as opposed to being important to learn new associations within the same set of cues, an additional group of mice was presented again with the original IDS cue-reward associations after undergoing IDSRe (reversal of IDSRe; **Fig. 2E**). Vehicle-treated mice took again about 30 trials to reach criterion, suggesting that in the continued presence of identical cues, and in spite of the fact that they had already learned the cue-reward association in IDS before, they resisted overcoming the most recent IDSRe association to learn reversal of IDSRe (**Fig. 2E**). Mice with silenced IL took again nearly 50 trials to reach criterion, consistent with the notion that IL is important to learn alternatives to the most recent association, regardless of whether these were identical to a previously learned association (**Fig. 2E**). By contrast, and unlike IDSRe, silencing PreL did not improve performance in reversal of IDSRe (**Fig. 2E**). That might reflect the fact that the previous IDSRe specifically involved learning an alternative association within the same setting promoted by IL, and not an association learned with the support of PreL.

In a final group of experimental mice, PreL or IL was silenced specifically during the final IEST subtask, i.e. extra-dimensional shift (EDS; **Fig. 2F**). Mice were now presented with two new sets of cues (O(E), O(F), T(5), T(6)), and reward was now associated with a texture (green, T(5)), not an odor. In this case, mice had to learn an alternative dimensional association, and learn to associate a particular texture with reward (**Fig. 2B**). Vehicle-treated mice apparently resisted shifting from odors to textures as the dimension associated with reward, and took again about 30 trials to reach criterion (**Fig. 2F**). Notably, and in contrast to the previous IEST subtasks, mice with either silenced PreL or silenced IL both failed to learn EDS within 50 trials (**Fig. 2F**). These results were consistent with the interpretation that IL is required to learn the alternative dimensional association in EDS (textures instead of odors), whereas PreL promotes learning of the new association between a texture and reward.

Taken together, these results suggest that when, within the same task, cue-reward associations change and require further learning, PreL promotes application of the previous association rule, thereby supporting (CD, IDS) or interfering (IDSRe) with new learning (**Fig. 2G**). By contrast, IL promotes learning alternatives to the most recent association, thereby supporting (IDSRe, EDS) or interfering (IDS) with new

learning. Finally, PreL is important to again learn a cue-reward association within the new dimension and the same task (EDS, **Fig. 2G**).

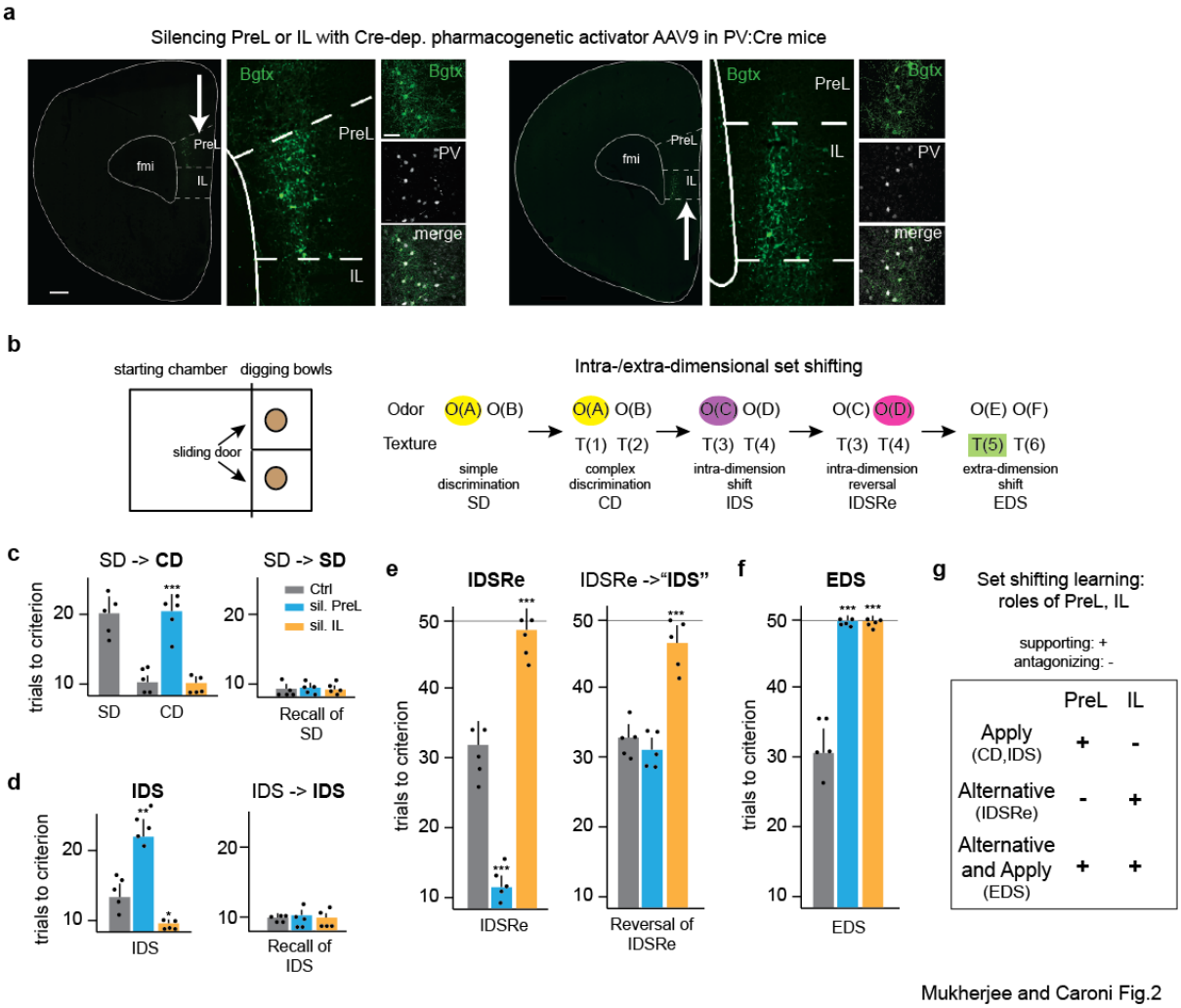

Figure 2. Shift-learning: PreL to apply rules and IL to learn alternatives.

a: Representative images for delivery to PreL or IL of Cre-dependent AAV9-pharmacogenetic activator in PV-Cre mice. Bgtx: visualization of (Bungarotoxin+) virus; PV: PV immunocytochemistry. Bar: 100 um.
b: Schematic of set shifting protocol (background color: rewarded association).
c-f: Requirements for activity in PreL or IL during IEST subtask learning. **c**: CD (n=5 each; (F (2, 12) = 17.1, ***P) or recall of SD (n=5 each; F (2, 12) = 1.9, P = 0.1916 *ns*); **d**: IDS (n=5 each; F (2, 12) = 24.62, ***P) or recall of IDS (n=5 each; F (2, 12) = 0.78, P = 0.4722, *ns*); **e**: IDSRe (n=5 each; F (2, 12) = 233.5, ***P) or reversal of IDSRe (n=5 each; F (2, 12) = 127.9, ***P) ; **f**: EDS (n=5 each; F (2, 12) = 43.01, ***P). Bar diagrams: trials to criterion for virus-expressing mice treated with vehicle (Ctrl) or mice in which PreL (blue) or IL (yellow) was silenced (PV neuron activation; PSEM ligand 20min before learning); subtask during which silencing was applied indicated in bold. "IDS" indicates that cues are as in IDS, but previous history is distinct from IDS.
g: Summary of PreL and IL roles in IEDS learning.
Error bars: SEM; one-way ANOVA followed by Dunnet's *post hoc*; p<0.05 (*),0.001 (**), 0.0001 (***).

IL→PreL neurons are required for IL driven shifting in IEST

We then determined whether and which aspect of reciprocal PreL-IL connectivity might be required in IEST learning. For these experiments, we inhibited IL→PreL or PreL→IL projecting neurons (**Fig. 1A**) specifically during IDS, IDSRe or EDS learning (total of six different experimental groups of mice). Like IL silencing using pharmacogenetic PV-neuron activation, inhibiting IL→PreL projection neurons using DREADDs accelerated learning in IDS (**Fig. 3A**), and suppressed learning in IDSRe (**Fig. 3B**) and EDS (**Fig. 3C**). By contrast, inhibiting PreL→IL projection neurons had no effect on IDS (**Fig. 3A**), IDSRe (**Fig. 3B**) or EDS learning (**Fig. 3C**). Therefore, IL→PreL projection neurons are specifically important during new learning involving the function of IL in IEST learning, whereas PreL→IL projection neurons are not. Furthermore, neither IL→PreL nor PreL→IL connectivity appeared to be important to mediate the roles of PreL in IEST learning.

To investigate the notion that IL might influence learning by counteracting PreL-mediated application of a previously learned rule, we carried out projection neuron activation experiments during IDS, IDSRe and EDS learning. This again involved six different groups of experimental mice. Indeed, activating IL→PreL projection neurons at IDS (strong inhibition; **Fig. 3D**) or IDSRe learning (marked facilitation; **Fig. 3E**) faithfully reproduced the effects of PreL inhibition on set shifting learning. Unlike PreL inhibition, activation of IL→PreL projection neurons did not affect performance in EDS learning, consistent with the notion that enhancing the impact of IL on PreL was not sufficient to reproduce the effects of PreL silencing on EDS learning (**Fig. 3F**). Taken together, these results provided evidence that the output of IL to PreL is specifically important for the role of IL during IEST learning.

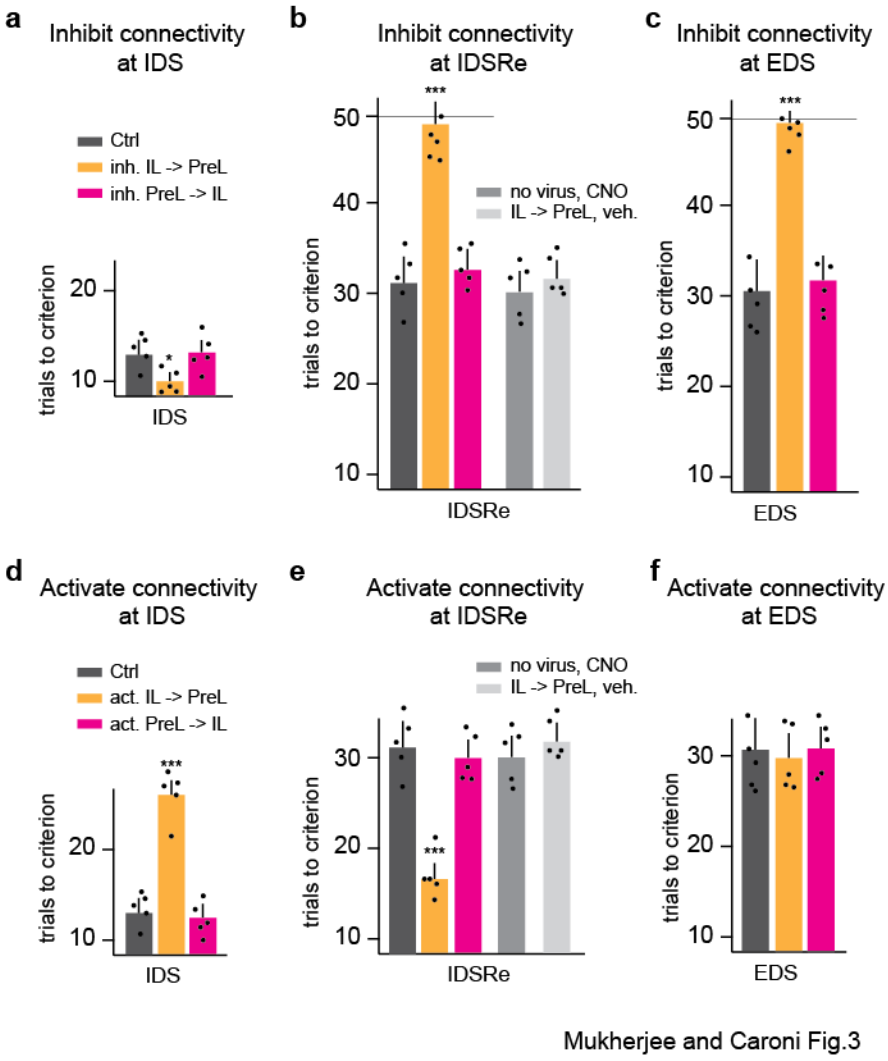

Figure 3. IL→PreL neurons are required for IL driven shifting in IEST.

a-c: Silencing IL->PreL, but not PreL->IL projection neurons during IDS (**a**; n=5 each; F (2, 12) = 6.64, *P = 0.011), IDSRe (**b**; n=5 each; F (4, 20) = 17.08, ***P), or EDS (**c**; n=5 each; F (2, 12) = 17.89, ***P) learning reproduces the effect of IL silencing during the same IEST subtasks. These experiments involved inhibitory DREADDS into IL or PreL projection neurons, and delivery of CNO or vehicle 20min before learning; CNO ligand alone or virus alone had no impact on IDSRe learning (**b**).
d, e: Activating IL->PreL, but not PreL->IL projection neurons during IDS (**d**; n=5 each; F (2, 12) = 25.39, ***P) or IDSRe (**e**; n=5 each; F (4, 20) = 20.01, ***P) reproduces the effect of silencing PreL during the same subtasks.
f: Activating IL->PreL projection neurons during EDS has no detectable impact on learning performance (n=5 each; F (2, 12) = 1.08, P = 0.371 *ns*). These experiments involved excitatory DREADDS into IL or PreL projection neurons, and delivery of CNO or vehicle 20min before learning. CNO ligand alone or virus alone had no impact on IDSRe learning (**e**).
Error bars: SEM; one-way ANOVA followed by Dunnet's *post hoc*; p<0.05 (*), 0.001 (**), 0.0001 (***).

PreL promotes fear learning and IL required for its extinction

To investigate whether relative roles of PreL and IL, and of IL→PreL connectivity in learning can be generalized beyond IEST, we turned to Pavlovian fear conditioning

and its extinction, comparatively simple learning forms in which PreL and IL have been reported to have opposite roles, and where extinction learning could be considered alternative learning (Sierra-Mercado et al., 2011; Courtin et al., 2013; Giustino and Maren, 2015). We investigated mice that underwent trace fear conditioning (tFC) (**Fig. 4A, Fig. S4**), a form of Pavlovian associative learning involving several brain areas, including medial prefrontal cortex (Gilmartin et al., 2013; Raybuck and Lattal, 2014). Silencing PreL at acquisition led to absence of freezing at recall one day after conditioning, whereas silencing IL at acquisition had no impact on freezing at recall (**Fig. 4B)**. By contrast, silencing PreL or IL at recall did not affect freezing (**Fig. 4C**). In a positive control experiment to verify that interference with recall could be detected with our procedure (Karunakaran et al., 2016), silencing ventral hippocampus at recall effectively suppressed freezing during recall (**Fig. 4C**). Therefore, PreL supports learning (but not recall) of tFC, whereas IL is not important at acquisition to learn tFC.

We then investigated requirements for PreL or IL in extinction of tFC. Silencing IL at acquisition, which did not affect fear learning, also did not affect extinction of tFC (**Fig. 4D**). By contrast, silencing IL during the extinction protocol effectively prevented extinction learning (**Fig. 4E**). Silencing PreL during extinction learning slightly accelerated loss of freezing, while not preventing return of fear 10d after extinction learning, suggesting that PreL might interfere with extinction learning (**Fig. 4E**; see below). Finally, silencing IL (or PreL) during recall of extinction learning did not affect absence of freezing upon extinction (**Fig. 4F**).

To further investigate the notion that IL is specifically required for extinction learning, we carried out extinction experiments in which we silenced both, IL required for extinction and PreL that might counteract extinction. Silencing of PreL in addition to IL did not noticeably influence how IL silencing interfered with extinction learning (**Fig. 4G**). In additional experiments, we found undistinguishable dependences on PreL and IL in contextual fear conditioning and its extinction (**Fig. S5**). Taken together, these results provided evidence that PreL has a role in promoting learning of Pavlovian fear conditioning, whereas IL is required for extinction learning in this paradigm (**Fig. 4H**).

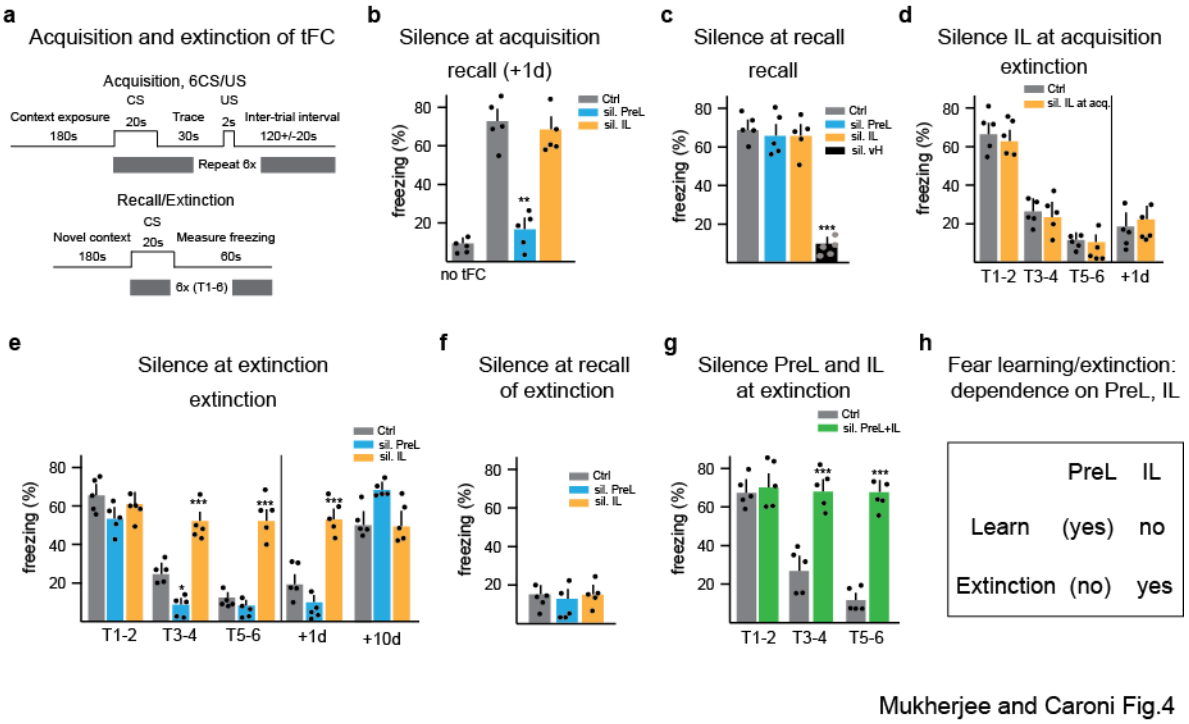

Mukherjee and Caroni Fig.4

Figure 4. PreL promotes fear learning and IL required for its extinction.

In all these experiments: silencing through pharmacogenetic activation of PV neurons 20min before learning (or recall); control: vehicle delivery in virus expressing mice.

a: Schematic of trace fear conditioning (tFC) and extinction protocol.
b: Silencing PreL at acquisition impairs freezing at 24h recall, whereas silencing IL does not (n=5 each; one-way ANOVA: F (2, 12) = 20.67, ***P; Dunnet's *post hoc*).
c: Silencing PreL or IL at recall does not affect freezing. In positive control experiments, silencing ventral hippocampus (vH) at recall suppresses freezing (n=5 each; one-way ANOVA: F (3, 16) = 31.14, ***P; Dunnet's *post hoc*).
d: Silencing IL at acquisition does not affect extinction learning on the next day (n=5 each; repeat measure two-way ANOVA: silence IL, F (1, 4) = 1.01, P = 0.372 *ns*). For extinction of tFC, data are shown (here and throughout the paper) as average freezing during T1-T2, T3-T4, or T5-T6; for individual freezing values see **Fig. S4**.
e: Silencing during extinction learning: silencing IL suppresses extinction learning, whereas silencing PreL slightly accelerates loss of freezing (n=5 each; repeat measure two-way ANOVA: silence IL vs. PreL, F (2, 8) = 64.75, ***P; Tukey's *post hoc*).
f: Silencing PreL or IL at recall of extinction does not affect recall of extinction learning (n=5 each; one-way ANOVA: F (2, 12) = 0.636, P = 0.546 *ns*).
g: Silencing IL and PreL during extinction learning suppresses extinction learning (n=5 each; repeat measure two-way ANOVA: silence PreL+IL, F (1, 4) = 199.35, ***P; Tukey's *post hoc*).
h: Summary of PreL and IL roles in fear learning and its extinction.
Error bars: SEM. p<0.05 (*), 0.001 (**), 0.0001 (***).

IL→PreL activity required in IL driven extinction learning

We next investigated whether, like in IEST, activity in IL->PreL projection neurons might be specifically required during learning processes that depend on IL in fear and extinction learning. Again, this first involved targeting of specific IL->PreL or PreL->IL connectivity, followed by separate experimental groups of mice, with their controls

(CNO ligand or saline delivered 20min before learning). Inhibiting IL→PreL or PreL→IL projection neurons during acquisition of tFC did not affect freezing to cue-induced recall on the subsequent day (**Fig. 5A**). By contrast, while inhibiting IL→PreL projection neurons during learning of tFC extinction did not affect initial freezing to cue (i.e. recall), it suppressed subsequent extinction (**Fig. 5B**). Furthermore, and in further correspondence to IEST, inhibiting PreL→IL projection neurons at extinction learning did not affect extinction (**Fig. 5B**).

To investigate whether IL→PreL projecting axons are specifically required for extinction learning through their synaptic terminations in PreL, we silenced their terminals specifically in individual target areas. We expressed a presynaptically targeted silencing DREADDs in IL→PreL (or PreL→IL) projecting neurons, and then delivered ligand (CNO) locally to specific target areas (Stachniak et al., 2014) (**Fig. 5C**). Silencing the terminals of IL→PreL projecting axons in PreL during extinction suppressed extinction learning whereas silencing of terminations by the same axons in BLA did not suppress extinction learning (**Fig. 5C**). By contrast, and as predicted, silencing the terminals of PreL-IL projecting axons in IL did not detectably affect extinction learning (**Fig. 5C**). These results provided evidence that for extinction (but not fear) learning to occur, IL→PreL connectivity is specifically required during extinction. Furthermore, the combined results from IEST and fear/extinction learning experiments were consistent with the notion that IL→PreL connectivity is specifically required during learning processes that depend on IL, providing evidence that one synaptic output of IL needed for this process is mediated by their projections to PreL.

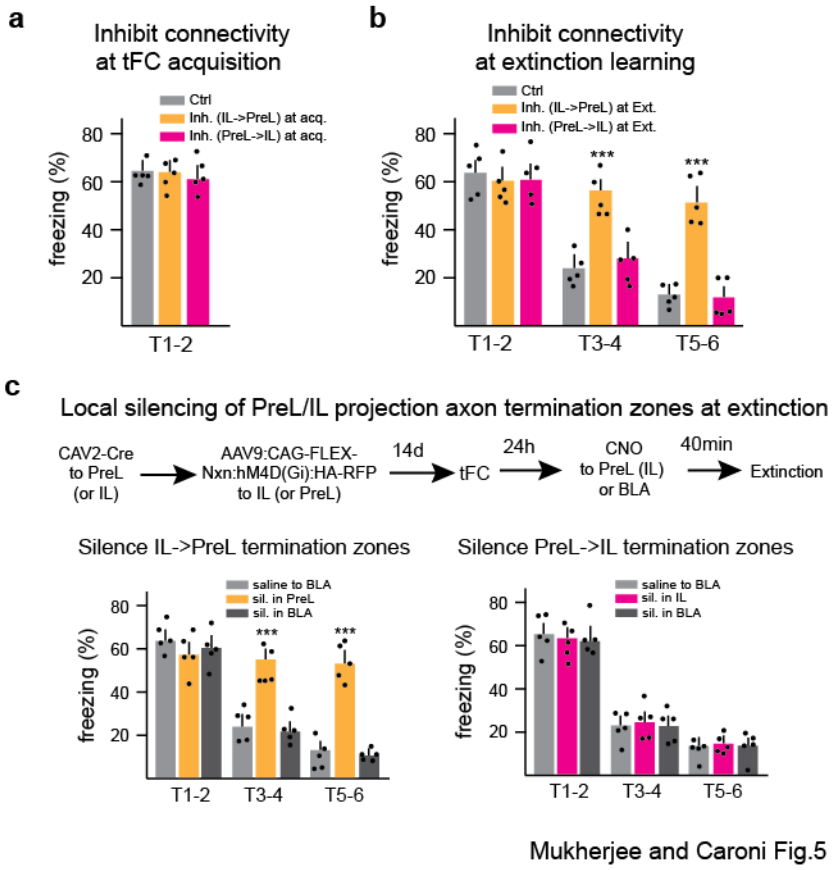

Figure 5. IL→PreL activity required in IL driven extinction learning.

a, b: Impact of inhibiting activity in IL->PreL or PreL->IL projection neurons during acquisition of tFC (T1-2 recall values) (**a**; n=5 each; one-way ANOVA: F (2, 12) = 0.057, P = 0.9446 *ns*) or during extinction learning (**b**; n=5 each; repeat measure two-way ANOVA: Inh. IL→PreL vs. PreL→IL, F (2, 8) = 23.22, ***P).

c: Local silencing of IL->PreL or PreL->IL projecting axon collaterals in their termination zones during extinction learning. Top: schematic of experimental strategy (expression of Neurexin-inhibitory DREADDs fusion protein). Bottom: Suppression of extinction learning by silencing of IL->PreL (n=5 each; repeat measure two-way ANOVA: Inh. Terminals in PreL vs. BLA, F (2, 8) = 58.6, ***P) but not PreL->IL (n=5 each; repeat measure two-way ANOVA: Inh. Terminals in IL vs. BLA, F (2, 8) = 2.81, P = 0.119 *ns*) collateral terminals in PreL (or IL) but not BLA.
Error bars: SEM. Tukey's *post hoc;* p<0.05 (*), 0.001 (**), 0.0001 (***).

Studies of extinction after traumatic experiences in humans have highlighted how extinction protocols are not always effective, and that in some cases extinction can be difficult or even not possible to achieve. Accordingly, we wondered whether under circumstances in which extinction might be more challenging to achieve, extinction learning still specifically depends on activity in IL, and on IL→PreL connectivity (Supplementary Results; **Figs. S6, S7**). We found that fear behavior produced by two tFC protocols delivered on consecutive days (2xtFC) resisted subsequent extinction (**Fig.S6**). Consistent with the notion that silencing PreL can accelerate extinction (**Fig.**

4E), silencing PreL during the extinction protocol of 2xtFC produced robust extinction learning (**Fig. S6**). Silencing of both, PreL and IL during the extinction protocol of 2xtFC again prevented extinction learning, indicating that extinction in the absence of active PreL still depended on active IL (**Fig. S6**). While one extinction session (Ext1) failed to produce detectable extinction of 2xtFC, extinction protocols delivered on three consecutive days (Ext1, Ext2, Ext3) produced robust extinction upon Ext3 (**Fig. S6**). Notably, silencing IL during Ext1, Ext2 or Ext3 suppressed detectable extinction learning upon Ext3, indicating that functional IL at both Ext1 and Ext2 was a prerequisite for extinction learning at Ext3 (**Fig. S6**). Furthermore, activity in IL→PreL projection neurons was specifically required during processes in Ext1-3 extinction learning that depend on IL (**Figs. S6, S7**). Taken together, these results further support the notion that activity in IL→PreL (but not PreL→IL) projection neurons is specifically required during IL-dependent alternative learning.

IL role in extinction set up 12 h after fear learning in IL

We then wondered whether there was a time window during which PreL→IL projection neurons might be important in learning involving communication between PreL and IL. As a prerequisite to address this question, we investigated when PreL and IL might undergo learning-related plasticity in fear/extinction learning. We analyzed contents of cFos+ neurons in PreL and IL cortical layers upon acquisition, recall and extinction of tFC (**Fig. 6A**). Ninety min after acquisition of tFC, cFos+ neuron contents were greatly increased in PreL layer2/3, layer5 and layer6 (**Fig. 6B**). By contrast cFos+ neuron induction in IL upon acquisition ranged from modest (layer2/3) to absent (layer5, layer6) (**Fig. 6B**). Likewise, at recall of tFC (T1-2), cFos+ induction was robust in all PreL layers, but either modest (layer2/3, layer5) or absent (layer6) in IL (**Fig. 6C**). By contrast, and consistent with the notion that IL is specifically involved in extinction learning, extinction of tFC did not produce cFos induction beyond that detected upon recall in PreL, but led to robust induction of cFos expression over recall values in IL (layer2/3, layer6, but not layer5) (**Fig. 6D**).

We next reasoned that IL might either be specifically recruited for learning at the time of extinction, or that, alternatively, acquisition of fear learning might already trigger processes in IL important for IL-dependent extinction, and more generally for

alternative learning. In a search for processes that might anticipate cFos induction in IL upon extinction learning, we analyzed contents of cFos+ neurons in PreL and IL 14h after acquisition (+14h), i.e. around the peak of a long-term memory consolidation time window (+12h-15h) known to involve re-induction of cFos expression (Katche et al., 2013; Karunakaran et al., 2016). Notably, while cFos expression at +14h was not significantly different from that detected upon tFC acquisition in PreL, it was dramatically elevated over acquisition values in IL (**Fig. 6E**). Specifically, cFos+ content values at IL layer2/3 and layer6 resembled those induced upon extinction learning, and those in layer 5 dramatically exceeded those detected upon acquisition, recall or extinction learning (**Fig. 6E**).

To investigate the possible importance of PreL/IL cFos expression at +12h-14h for extinction learning, we delivered a specific small-molecule inhibitor of cFos transcriptional function to either PreL or IL at +12h. While delivering the cFos inhibitor to PreL did not significantly affect freezing during extinction learning, delivery to IL at +12h suppressed subsequent extinction learning (**Fig. 6F**). Therefore, inhibiting cFos from +12h after acquisition in IL resembled the effect of silencing IL during extinction learning.

To determine how activity in IL or PreL at a +12h-14h time window might influence subsequent learning, we carried out silencing experiments in IL or PreL at +12h. Like inhibition of cFos function, silencing IL at +12h suppressed subsequent extinction learning, whereas silencing PreL did not noticeably affect freezing during extinction learning (**Fig. 6G**). In parallel, silencing IL at +12h suppressed cFos induction in IL and led to a marked increase in cFos induction upon the (failing) extinction learning protocol in PreL layer2/3 (**Fig. 6G**). Therefore, interfering with cFos or network activity in IL at a +12h-14h time window after fear learning mimics the impact of IL silencing during extinction learning.

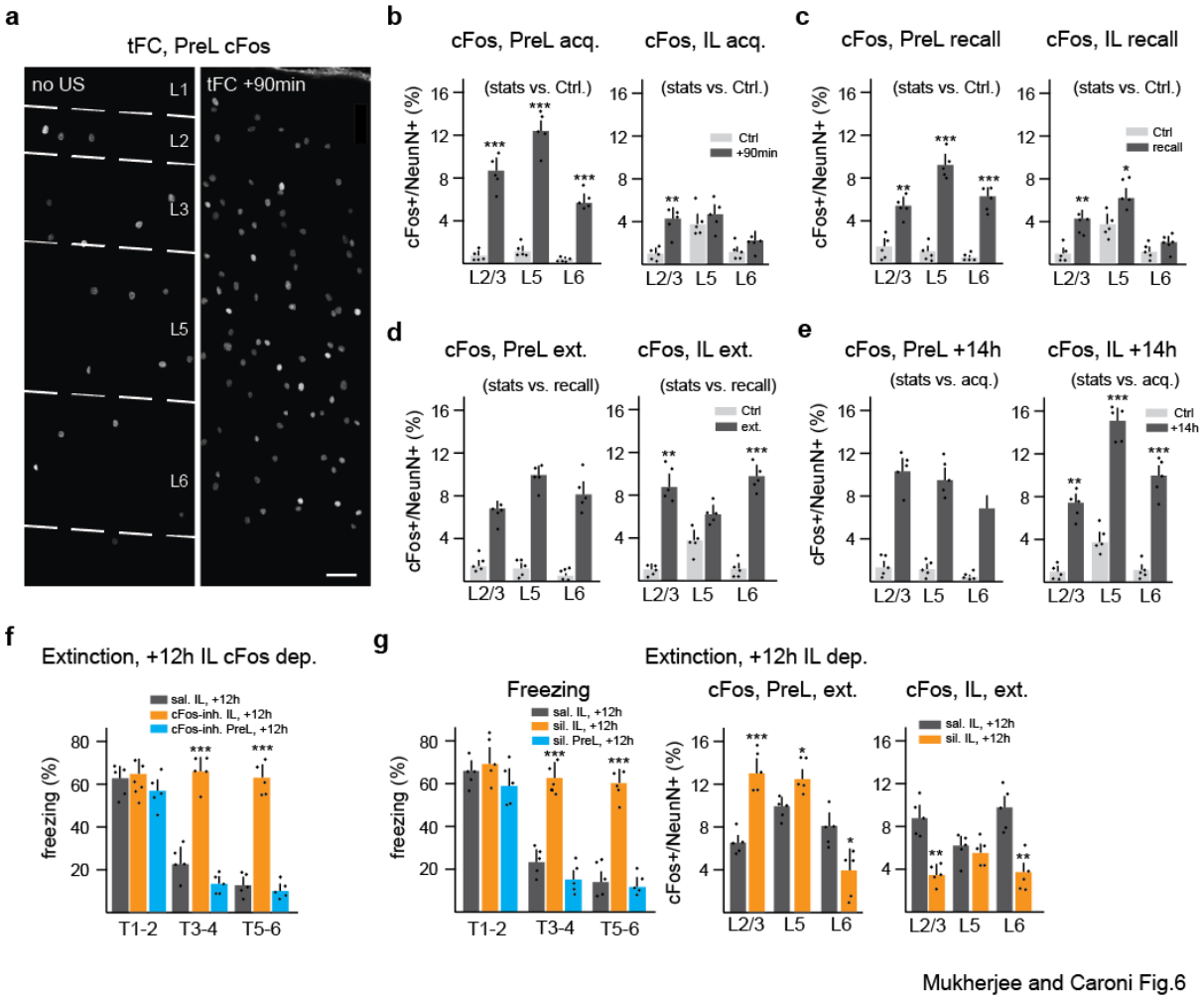

Figure 6. IL role in extinction set up 12 h after fear learning in IL.

a: Representative images of PreL cFos immunoreactivity upon acquisition in control (CS but no US) or tFC mouse. Bar: 50 µm.

b-e: cFos induction in PreL and IL cortical layers upon acquisition (+90min; **b**; statistics comparisons to cage control; n=5 each; two-way ANOVA: PreL, F (1, 24) = 147.5, ***P; IL, F (1, 24) = 22.4, ***P), upon recall (90min after T1-2 recall; **c**; comparisons to cage control; n=5 each; two-way ANOVA: PreL, F (1, 24) = 163.8, ***P; IL, F (1, 24) = 25.94, ***P), upon extinction learning (90min after T1-6; **d**; comparison to recall; n=5 each; two-way ANOVA: PreL, F (1, 24) = 2.252, P = 0.1465 *ns*; IL, F (1, 24) = 29.57, ***P), or at +14h after acquisition (**e**; comparison to acquisition; n=5 each; two-way ANOVA: PreL, F (1, 24) = 0.2994, P = 0.5893 *ns*; IL, F (1, 24) = 120, ***P). Sidak's *post hoc* test for all comparisons in **b-e**.

f: Effect of cFos inhibition in PreL or IL 12h after acquisition on next-day extinction learning. (n=5 each; Repeat measure two-way ANOVA: cFos Inh. IL vs. PreL, F (2, 8) = 33.14, ***P; Tukey's *post hoc*).

g: Effect of PreL or IL silencing 12h after acquisition on next-day extinction learning (left; n=5 each; repeat measure two-way ANOVA: sil. +14h IL vs. PreL, F (2, 8) = 47.4, ***P; Tukey's *post hoc*), or on cFos induction 90min after extinction learning in PreL (center; n=5 each; two-way ANOVA: F (1, 24) = 8.523, **P ; Sidak's *post hoc*) or in IL (right; n=5 each; two-way ANOVA: F (1, 24) = 26.79, ***P; Sidak's *post hoc*).

Error bars: SEM; p<0.05 (*), 0.001 (**), 0001 (***).

Reciprocal PreL↔IL activity at +12h-14h drives IL function

We then determined whether activity in IL→PreL and/or in PreL→IL projection neurons 12h after acquisition might affect subsequent fear memory recall and extinction learning. Inhibiting IL→PreL projection neurons at +12h after fear learning did not affect subsequent fear responses to tone (T1-2), but specifically suppressed extinction of tFC (**Fig. 7A**). Inhibiting IL→PreL projection neurons at +1h or at +16h after fear learning failed to suppress extinction (**Fig. 7A**), consistent with the notion that functional interactions between IL and PreL were specifically required during a +12h-14h time window to produce IL-dependent extinction. Notably, inhibiting PreL→IL projection neurons at +12h after fear learning also specifically suppressed extinction of tFC (**Fig. 7B**), suggesting that IL-dependent extinction learning depended on reciprocal exchange of information between PreL and IL 12h-14h after acquisition of fear learning, much in contrast to the unilateral IL→PreL requirement during extinction learning.

To investigate whether IL→PreL and/or PreL→IL projecting axons are required at +12h-14h for extinction learning specifically through their terminations in PreL (respectively IL), we silenced their terminals specifically in individual target areas(method as in Fig. 5c, but CNO or vehicle locally at +12h after fear learning). Silencing the terminals of IL→PreL projecting axons in PreL at +12h suppressed subsequent extinction learning whereas silencing of terminations by the same axons in BLA did not suppress extinction learning (**Fig. 7C**). Likewise, silencing the terminals of PreL-IL projecting axons in IL at +12h suppressed extinction learning, whereas silencing them in BLA did not affect extinction (**Fig. 7C**). Therefore, reciprocal PreL↔IL connectivity is specifically important 12h after fear learning for subsequent IL-dependent extinction learning.

Consistent with the notion that activity in PreL↔IL reciprocal connectivity at +12h was specifically required for IL-dependent extinction learning, inhibiting PreL→IL or IL→PreL projection neurons at +12h led to a complete loss of cFos expression in IL, and to enhanced layer2/3 cFos expression in PreL upon the extinction protocol (**Fig.**

S8). Furthermore, and as might have been expected given the close correspondence between cFos expression at +14h and upon extinction, inhibiting PreL→IL projection neurons at +12h produced a complete loss of cFos induction at +14h in IL (**Fig. S8**). In addition, inhibiting PreL→IL projection neurons at +12h strongly reduced cFos expression in PreL at +14h (**Fig. S8**).

Finally, we determined whether activity in PreL↔IL projection neurons 12h-14h after acquisition was also specifically required for the role of IL in set-shifting learning. To address this question we inhibited IL→PreL or PreL→IL at +12h after CD, IDS or IDSRe and monitored the impact of these interventions on subsequent IDS, IDSRe or EDS. As predicted, and closely mimicking the effects of IL silencing during learning, inhibiting IL→PreL or PreL→IL at +12h after CD improved subsequent IDS learning, whereas inhibiting IL→PreL or PreL→IL at +12h after IDSRe suppressed subsequent EDS learning (**Fig. 7D**). The impact of inhibition at +12h after IDS on IDSRe learning was slightly less pronounced than when IL was silenced during IDSRe learning, but the direction of the change (worsening) was the same as upon IL silencing (**Fig. 7D**).

Taken together, these results provided evidence that activity in reciprocal PreL↔IL connectivity during a +12h-14h time window after acquisition is essential to set up how IL influences subsequent learning.

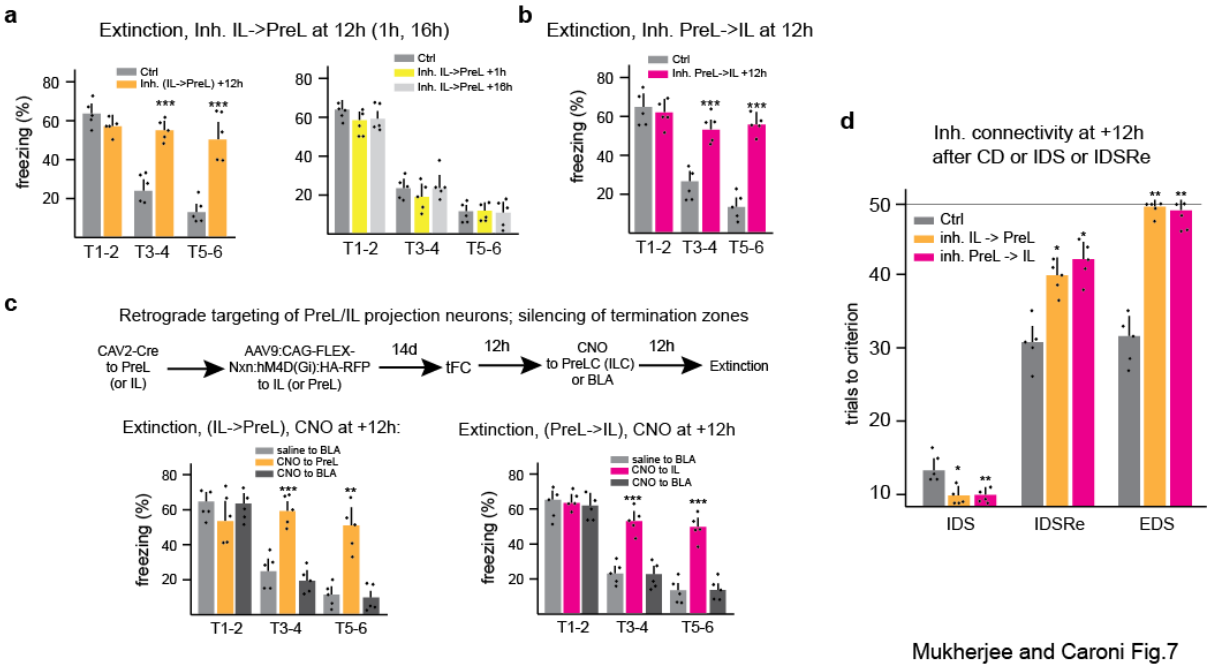

Mukherjee and Caroni Fig.7

Figure 7: Reciprocal PreL↔IL connectivity required at +12h-14h to set up role of IL in learning.

a, b: Impact of inhibiting IL->PreL (**a**) or PreL->IL (**b)** projection neurons at +12h after acquisition on subsequent extinction learning. Repeat measure two-way ANOVA; **a**: n=5 each; Cntrl vs +12h, F (1, 4) = 13.63, **P; **b**: Cntrl vs +12h, F (1, 4) = 19.21, **P. Silencing IL->PreL at +1h or +16h after acquisition did not affect subsequent extinction learning (**a**; n=5 each; repeat measure two-way ANOVA: +1h vs. +16h, F (2, 8) = 1.869, P = 0.197 *ns*). Sidak's *post hoc* test for **a, b**.
c: Local silencing of IL->PreL or PreL->IL projecting axon collaterals in their termination zones at +12h after acquisition of tFC. Top: schematic of experimental strategy (expression of Neurexin-inhibitory DREADDs fusion protein). Bottom: Suppression of extinction learning by silencing of IL->PreL or PreL->IL collateral terminals in PreL (or IL) but not BLA. Repeat measure two-way ANOVA; n=5 each; IL->PreL: Inh. PreL vs. BLA, F (2, 8) = 97.73, ***P; PreL->IL: Inh. IL vs. BLA, F (2, 8) = 85.86, ***P. Tukey's *post hoc* test for C.
d: Impact of silencing IL->PreL or PreL->IL projection neurons at +12h after CD, IDS or lDSRe learning on subsequent IDS, lDSRe or EDS learning. Repeat measure two-way ANOVA; n=5 each; Inh. IL→PreL vs PreL→IL, F (2, 8) = 36.61, ***P; Tukey's *post hoc*.
Error bars: SEM; *post hoc;* p<0.05 (*), 0.001 (**), 0.0001 (***).

Discussion

We have investigated how two distinct but functionally related prefrontal cortical areas, mouse PreL and IL, exert complementary and possibly opposite roles to support learning. We provide evidence of direct reciprocal PreL↔IL layer5/6 connectivity, and show that in new learning activity in PreL is important to promote application of previously learned associations, whereas activity in IL is required to learn alternatives to previous associations. Activity in PreL and IL are specifically important when new learning is required, whereas neither activity in PreL nor IL is required for recall of previously learned associations. We further show that activity in IL→PreL connectivity is specifically required during IL-dependent alternative learning, whereas reciprocal PreL↔IL connectivity is specifically required during a time window 12-14h after learning to set up the role of IL in subsequent alternative learning. Taken together, our results define specific and opposite roles of PreL and IL to flexibly support new learning, and provide circuit-level evidence that direct reciprocal PreL↔IL connectivity is important for activity in IL to mediate learning of associations alternative to those supported by PreL (**Fig. S9**).

The results of our set-shifting experiments suggest that PreL supports new learning by promoting application of relevant previously learned associations. In this way, PreL appears to account for a key aspect of adaptive behavior, allowing to take advantage

of previous related experience to efficiently learn new but related tasks. Our results further show that IL is specifically required to learn alternatives to PreL-promoted associations. Together, PreL and IL appear to represent complementary and opposing components of a top-down system to support experience-based flexible goal-oriented learning.

The results of our fear learning and extinction experiments provide further support for the notion that PreL and IL have opposite roles specifically in new learning. Unlike the set-shifting experiments, fear conditioning and its extinction do not directly address rule application and learning of alternative associations under conditions of choice. Accordingly, our results involving such different learning settings cannot be related to one another in every respect. Nevertheless, extinction learning can be considered as learning of an alternative to the CS-US association in Pavlovian fear conditioning, and our results provide evidence that this alternative learning again depends on activity in IL and on IL→PreL connectivity.

Our conclusions are in good agreement with those of a previous lesion study in rats addressing relative roles of PreL and IL in a Y-maze shifting task (Oualian and Gisquet-Verrier, 2010). Our results are further consistent with previous reports that activity in dorsolateral PFC is correlated to the reward value of action choices (Tanji and Hoshi, 2008; Kim and Shadlen, 1999; Morris et al., 2014), and that medial PFC has critical roles for flexible behavior, particularly strategy shifting (Rich and Shapiro, 2009), in humans, monkeys and rodents. Previous reports on learning flexibility have focused on the role of IL in promoting flexible behaviors in extinction and addiction (Peters et al., 2009; Sotres-Bayon and Quirk, 2010; Barker et al., 2014; Giustino and Maren, 2015), and our findings are consistent with the conclusions of those previous studies. Our study does not address how IL is involved in habit learning (Killeross and Coutureau, 2003; Gourley and Taylor, 2016). However, while that likely involves circuits (e.g. prefrontal-striatal) and mechanisms not addressed in this study (Smith and Graybiel, 2013), a possibility consistent with our findings is that context-related shifting away from PreL-promoted goal-directed behavior might favor habitual reward seeking. Taken together, our findings using set shifting and fear/extinction learning protocols lend support to those previous studies that have assigned opposite roles to PreL and IL in tasks involving flexible goal-oriented learning. By showing how the role

of IL in alternative learning depends first on activity in reciprocal PreL→IL and IL→PreL projection neurons 12h-14h after association learning, and then specifically on activity in IL→PreL projections during alternative learning, our results suggest a circuit-level mechanism for how PreL and IL interact to exert opposite influences on learning.

Our finding that IL is required for extinction learning is consistent with the results of previous studies on fear conditioning and its extinction (Peters et al., 2009; Sotres-Bayon and Quirk, 2010; Giustino and Maren, 2015). Generally, our findings do not support the notion that IL might mediate learning just opposite to that promoted by PreL. This is most evident in EDS learning, which depended on activity in both IL and PreL. Our findings concerning extinction-resistant fear learning suggest that IL-dependent alternative learning is influenced by the strength of previous PreL-dependent learning (see also Sparta et al., 2014). Along similar lines, the results of previous studies involving set-shifting tasks have suggested that if some of the subtasks (e.g. IDSRe) are omitted, EDS can be learned more readily than in the protocol applied in our study, suggesting that the extent of previous reinforcement is important in set-shifting (Birgman et al., 2005; Garner et al., 2006). Taken together, these considerations suggest a conceptual framework in which how application and perseverance with previously learned associations is balanced against alternation and shifting in learning is influenced by the combined outcome of previous learning experiences, possibly including the relative strengths of PreL- and IL-dependent memories. However, how sequences of learning sessions are integrated to influence subsequent learning, and the extent to which PreL, IL as well as further prefrontal areas such as anterior cingulate and orbitofrontal cortex might be involved remains to be determined.

A key result of our study is that PreL and IL exhibit direct reciprocal layer5/6 connectivity, and that this connectivity is critically important for IL-dependent alternative learning. The specific requirement for activity in IL→PreL, but not PreL→IL connectivity during IL-dependent learning suggests that PreL has an important role in IL-dependent learning, and that PreL and IL might have antagonistic roles in controlling flexible learning. Consistent with this notion, inhibition of IL→PreL connectivity prevented IL-dependent learning, whereas activation of IL→PreL connectivity during IEST learning mimicked PreL silencing. How IL→PreL connectivity

might be recruited to interfere with PreL-mediated perseverance and promote alternative learning remains to be determined. Furthermore, our results make no specific predictions as to how connectivity to and from downstream brain areas mediates the distinct effects of activity in PreL and IL on learning.

The reciprocal connectivity between PreL and IL mainly involving layer5/6 can potentially complicate the interpretation of our interference experiments. Thus, for example, influencing activity in IL->PreL connectivity might, in turn, influence activity in PreL->IL connectivity, making it difficult to disentangle specific roles of these individual circuitries in learning. Our study does not address how activity in PreL->IL or in IL->PreL projection neurons influences local circuit activity in their respective target areas. However, the behavioral outcomes of our manipulations provide evidence for striking functional asymmetries in the impact of PreL->IL and of IL->PreL connectivity on learning. Thus, inhibiting IL->PreL connectivity activity by either specifically inhibiting the projection neurons themselves, or by inhibiting activity in the corresponding collaterals specifically in their target area in PreL closely mimicked the effects of inhibiting activity in IL as a whole (thereby presumably suppressing all outputs from IL). Furthermore, enhancing activity in IL->PreL projection neurons mimicked effects of inhibiting activity in PreL as a whole, suggesting that activity in IL->PreL connectivity is critically and specifically important to support IL-promoted alternative learning, as opposed to PreL-promoted rule application. By contrast, inhibiting activity in PreL-IL connectivity not only did not mimic the effects of inhibiting PreL (i.e. we found no symmetry to the outcome of the IL->PreL interference experiments), but it specifically interfered with subsequent IL-dependent alternative learning when carried out during a memory consolidation time window 12-14h after acquisition. These findings are consistent with a conceptual framework in which rule learning occurs first (PreL-dependent), and the role of IL in learning alternatives to that rule is set up subsequently, in a process that involves activity in PreL->IL projection neurons. Our findings are further consistent with the possibility that activity in IL->PreL projection neurons might control subpopulations of neurons in PreL with a specific role in steering IL-dependent learning. One possible model consistent with our findings could involve projections from PreL and IL to shared downstream areas in which behaviorally important learning processes might occur in a PreL and/or IL-directed manner, and in which the corresponding memories would be stored for behavioral

recall. In such a model, some of the projections from PreL to downstream areas might interfere with IL-dependent alternative learning, and the interference might be suppressed by IL->PreL connectivity. This arrangement would be consistent with our finding that inhibiting activity in PreL or IL had no detectable behavioral impact during recall of previous learning. The hypothetical model does not imply that activity in IL->PreL connectivity is the only route through which PreL and IL influence each other's impacts in new learning, and additional systems, e.g. involving cortico-striatal-thalamic circuitry might also be involved. In sum, our results provide evidence for specific roles of PreL->IL and IL->PreL connectivity to support IL-promoted learning of alternatives to PreL-promoted associations. Elucidating the precise circuit mechanisms and the broader systems arrangements through which PreL and IL influence rule application versus shifting in flexible learning will, however, require further research.

A key result of our study is that the role of IL in promoting learning of alternative associations is set up during a time window 12-14h after acquisition of the original association. Such 12-14h time windows are thought to be important for long-term memory consolidation through processes involving coordinated activity between distributed networks (Girardeau et al., 2009; Carr et al., 2011). Information exchange between PreL and IL might therefore occur in the context of such systems-wide processes, and the direct layer5/6-derived connectivity between PreL and IL might not be the only route through which balances between PreL and IL memories are established to modulate the outcome of rule application versus alternative associations in learning (Sotres-Bayon and Quirk, 2010; Gilmartin et al., 2014; Herry and Johansen, 2014; Song et al., 2015). The late time frame for setting up systems balances that define subsequent learning might ensure that relevant information obtained before or after the initial acquisition can be included into an updated representation of learned rules and their values. The mechanisms through which activity at +12h-14h is specifically required to establish PreL/IL balances that regulate persistence versus alternative learning remain to be determined.

In more general terms, our results highlight unique roles of late memory consolidation processes at +12h-14h in flexible learning. Our results suggest that balancing the relative importance of future conflicting strategies might require integration processes best achieved during off-line memory consolidation processes. Elucidating the

systems and circuit mechanisms and logic underlying these integrations should provide novel fundamental insights into learning and memory.

Supplementary figures

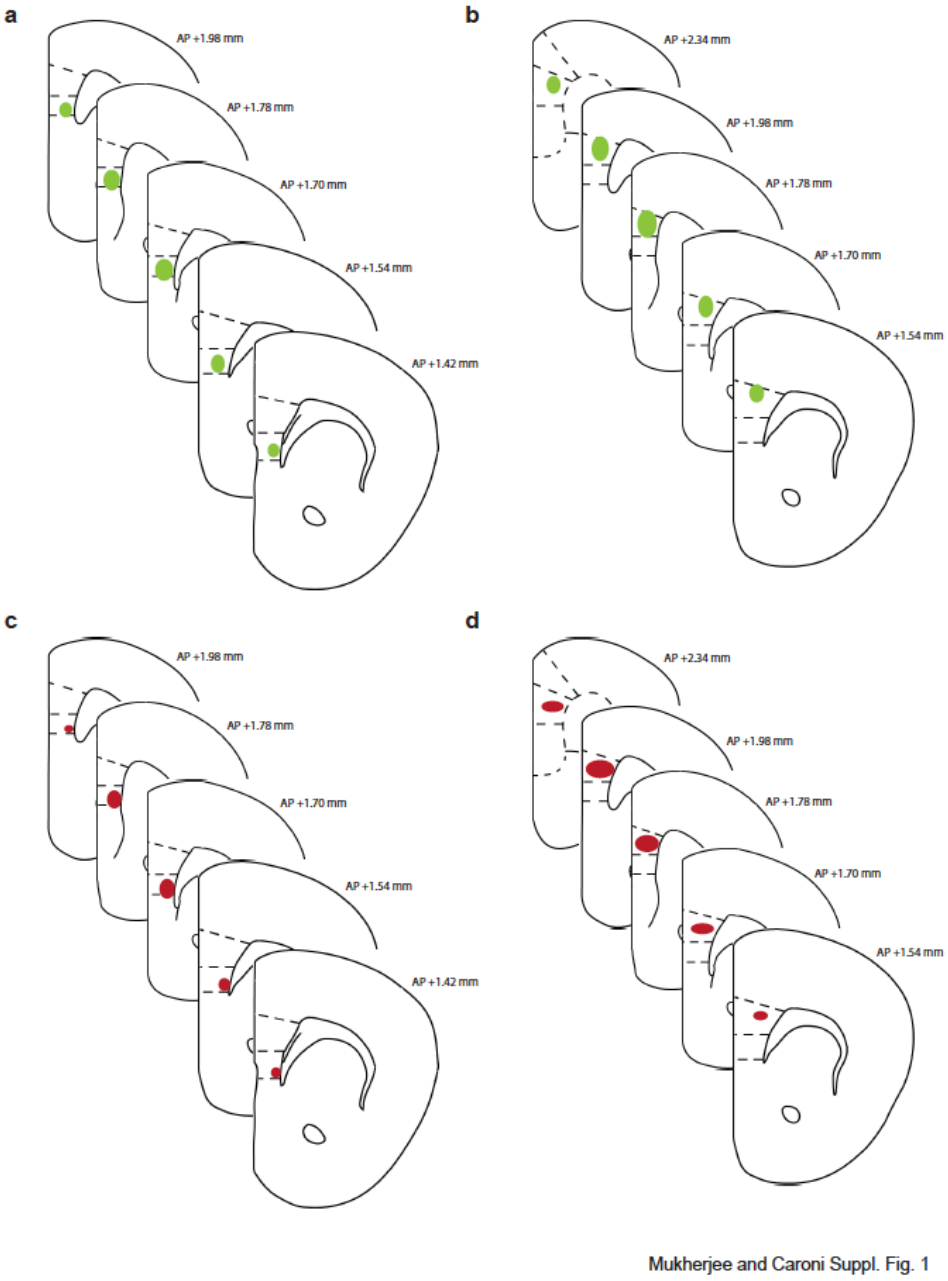

Figure S1: Local viral targeting of PreL or IL neurons for silencing and connectivity experiments. Representative examples of virus spread range (**a, b**) and of retrograde projection neuron targeting (**c, d**).

a, b: Schematic representations of virus labeling (green, Bungarotoxin488 signal) in IL (**a**) or PreL (**b**) in PV-Cre mice. Such mice were used for IL or PreL silencing experiments.

c, d: Schematic representations of retrograde projection neuron labeling (red, mCherry signal) in IL->PreL (**c**) and PreL->IL (**d**) targeting experiments. Such mice were used for the analysis and manipulation of IL->PreL and PreL->IL projection neurons.

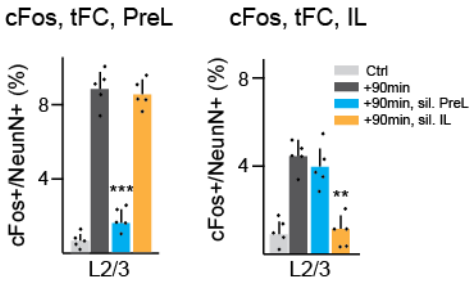

Mukherjee and Caroni Suppl. Fig. 2

Figure S2: Local silencing of PreL or IL: impact on cFos expression. Silencing through pharmacogenetic PV-neuron activation in PV-Cre mice during acquisition of trace fear conditioning (tFC). cFos+ neuron contents 90 min after acquisition in PreL or IL. Note loss of cFos+ neurons specifically in PreL upon PreL silencing (blue; n=5 each; F (3, 16) = 36.84, ***P), and in IL upon IL silencing (orange; n=5 each; F (3, 16) = 28.73, ***P). One-way ANOVA followed by Dunnet's *post hoc*; p<0.01 (**), 0.001 (***).

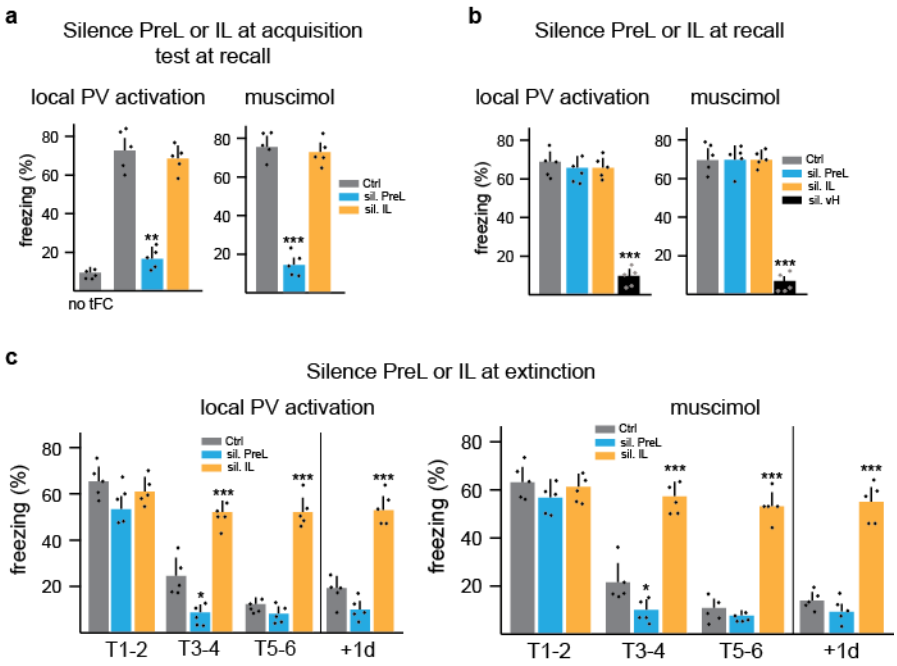

Mukherjee and Caroni Suppl. Fig. 3

Figure S3: Local PreL or IL silencing through PV-neuron activation or muscimol: comparison of behavioral impact.
a-c: Silencing PreL or IL during acquisition (**a**), recall (**b**) or extinction (**c**) of tFC. Silencing through local pharmacogenetic PV-neuron activation or muscimol had undistinguishable effects: silencing PreL at acquisition specifically impairs freezing at 24h recall (**a**; n=5 each; one-way ANOVA Muscimol: F (2, 12) = 21.85, ***P; Dunnet's *post hoc);* neither PreL nor IL are involved in recall of tFC (**b**; n=5 each; one-way ANOVA: Muscimol F (3, 16) = 29.83, ***P; Dunnet's *post hoc*); silencing IL specifically interferes with extinction learning (**c**; n=5 each; repeat measure two-way ANOVA: Muscimol, F (2, 8) = 61.83, ***P. Error bars: SEM; p<0.05 (*), 0.001 (**), 0001 (***).

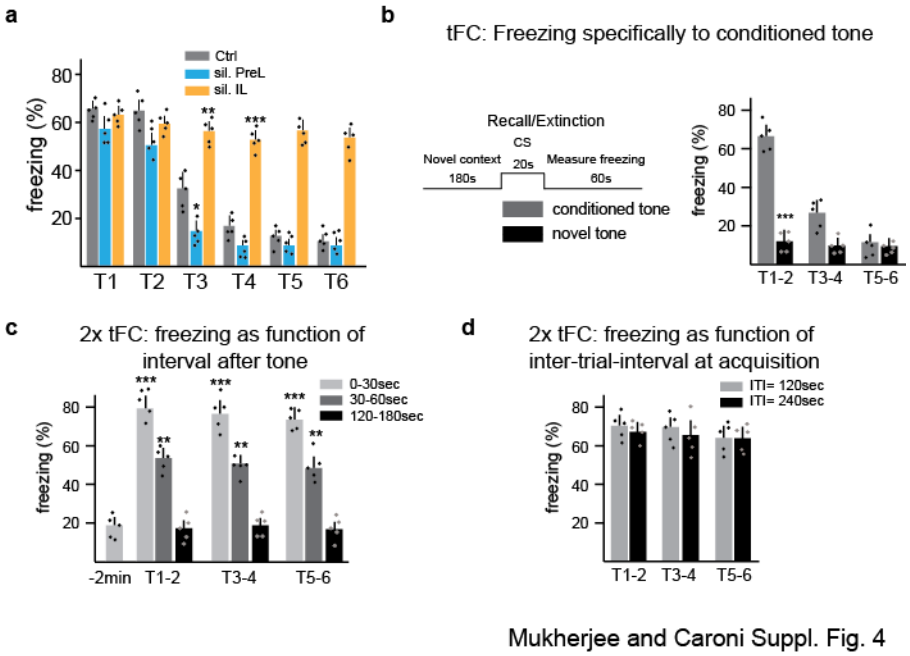

Mukherjee and Caroni Suppl. Fig. 4

Figure S4: Validation of tFC/extinction protocol.
a: Individual T1-T6 freezing values for extinction experiment as shown in **Fig. 4e**. n = 5 each; Repeat measure two-way ANOVA: Sil. PreL vs. IL F (2, 8) = 96.57, ***P
b: Upon tFC, mice do not freeze to a novel (unconditioned) tone. Recall/extinction protocol. n = 5 each; Repeat measure two-way ANOVA: F (1, 4) = 204.33, ***P
c, d: Freezing as a function of time interval after the tone at recall (**c**), or as a function of inter-trial-interval at acquisition (**d**). Extinction protocol upon 2x tFC (Ext1, no extinction; see **Fig. 5a**). Freezing is highest during the first 30sec after the tone, and absent 120-180sec after the tone (**c**, n = 5 each; Repeat measure two-way ANOVA: F (2, 8) = 188.62, ***P); longer inter trial-intervals at acquisition (240sec instead of 120sec) do not affect freezing at recall (**d**). Two-way ANOVA followed by Tukey's *post hoc*; p<0.05 (*), 0.01 (**), 0.001 (***).

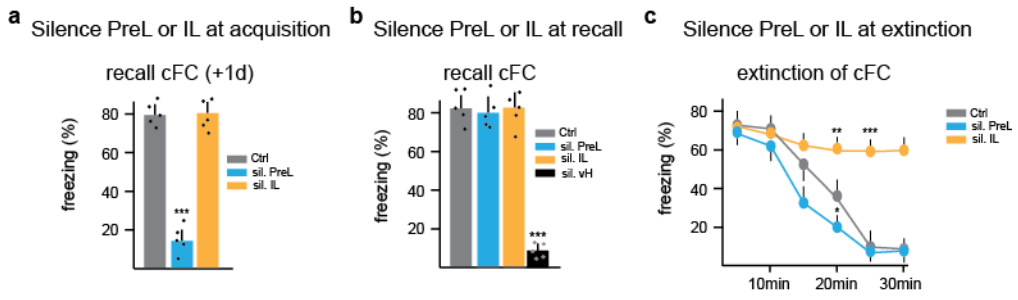

Mukherjee and Caroni Suppl. Fig. 5

Figure S5: PreL promotes contextual fear learning (cFC), IL required for extinction of contextual fear learning.
Like in tFC, activity in PreL (but not IL) is important at acquisition of cFC for freezing at 24h recall (**a**; n = 5 each; one-way ANOVA: F (2, 12) = 148.9, ***P), neither PreL nor IL is important at recall of cFC (**b**; n = 5 each; one-way ANOVA: F (3, 16) = 97.78, ***P), and activity in IL is required during learning of cFC extinction (**c**; n = 5 each; Repeat measure two-way ANOVA: Sil. PreL vs IL, F (2, 8) = 89.35, ***P). Dunnet's *post hoc* (Tukey's *post hoc* in **c**); p<0.05 (*), 0.01 (**), 0.001 (***).

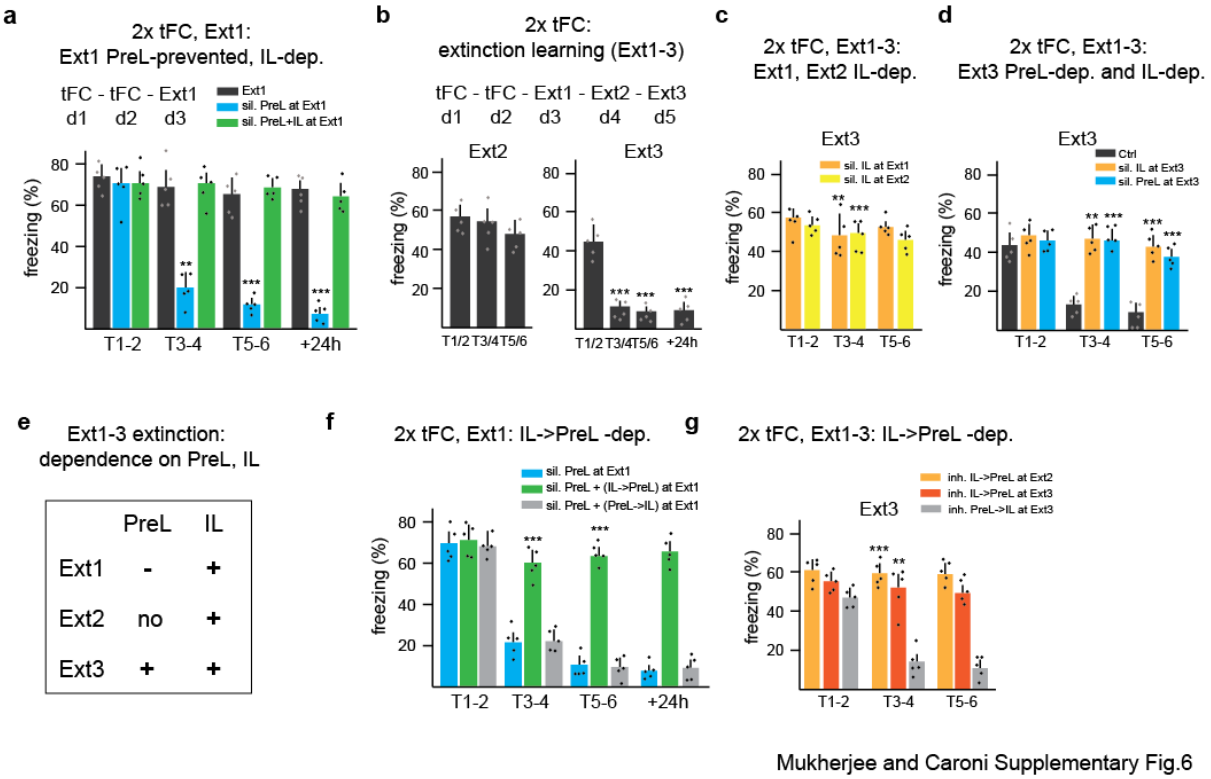

Mukherjee and Caroni Supplementary Fig.6

Figure S6: From IL-dependent to IL- and PreL-dependent extinction learning.
a: tFC protocols on two consecutive days (2x tFC) lead to PreL-prevented, IL-dependent extinction learning (Ext1). In Ext1, extinction learning is prevented by PreL (blue, silencing PreL), and dependent on IL (green, PreL and IL silenced) (n = 5 each; repeat measure two-way ANOVA: Silence PreL vs PreL+IL, F (2, 8) = 33.28, ***P).
b: Ext1-3 learning upon 2x tFC protocol (n = 5 each; one-way ANOVA: Ext3, F (3, 16) = 25.82, ***P).
c: Silencing of IL at Ext1 or Ext2 learning suppresses detectable extinction learning at Ext3 (n = 5 each; repeat measure two-way ANOVA: Sil. At Ext1 vs. Ext2, F (2, 8) = 17.47, *P).
d: Detectable extinction learning at Ext3 depends on both, IL and PreL (n = 5 each; repeat measure two-way ANOVA: Silence. IL vs. PreL, F (2, 8) = 13.55, *P).
e: Summary of PreL and IL roles in Ext1-3 extinction learning. IL is required during Ext1, Ext2, and Ext3 learning. Activity in PreL prevents extinction learning at Ext1; silencing PreL has no detectable effect during Ext2 learning, but it suppresses extinction learning at Ext3.
f: Silencing IL->PreL, but not PreL->IL projection neurons during Ext1 learning suppresses facilitation of PreL silencing, during Ext1 learning (n = 5 each; repeat measure two-way ANOVA: Inh. IL->PreL vs. PreL->IL, F (2, 8) = 49.87, ***P).
g: Silencing IL->PreL, but not PreL->IL projection neurons during Ext2 or Ext3 learning reproduces the effect of IL silencing on Ext3 learning (n = 5 each; repeat measure two-way ANOVA: F (2, 8) = 35.23, ***P).
Error bars: SEM. Tukey's *post hoc* (Dunnet's *post hoc* in **b, c**); p<0.05 (*), 0.001 (**), 0.0001 (***).

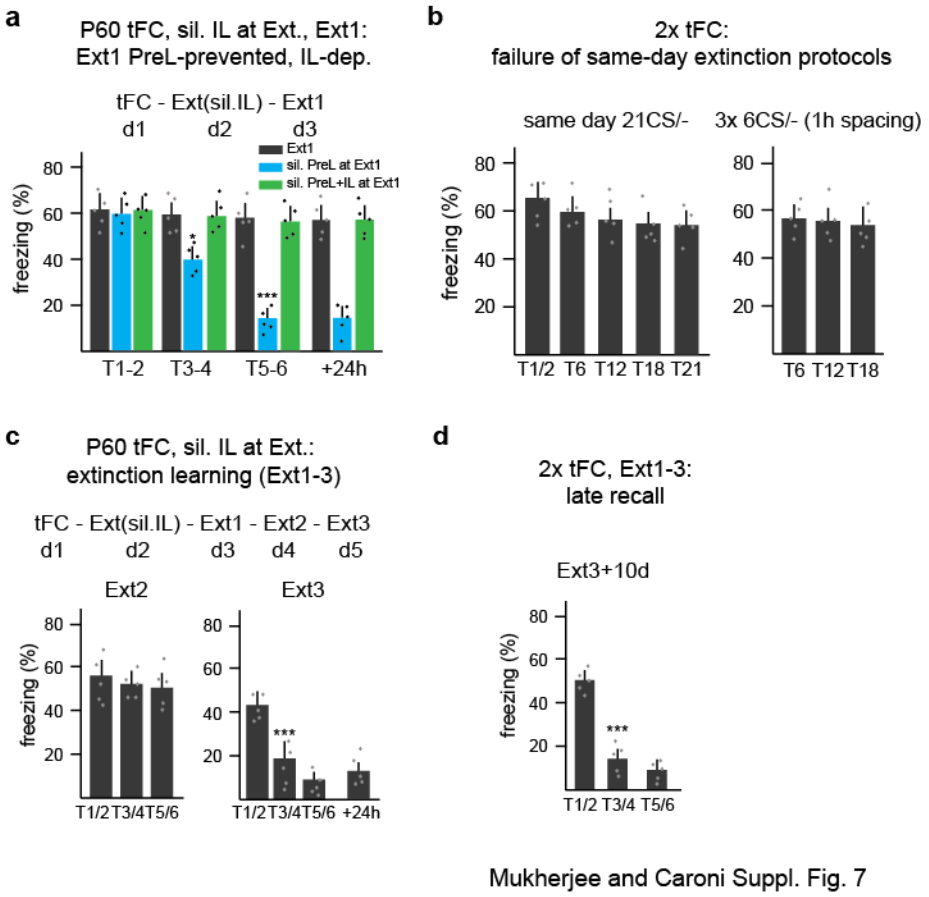

Figure S7: Extinction protocols in extinction-resistant mice.
a: Silencing IL during extinction learning produces PreL-prevented, IL-dependent extinction (Ext1). n = 5 each; Repeat measure two-way ANOVA: F (2, 8) = 27.38, ***P.
b: Extinction learning protocols in mice that underwent 2x tFC. 21 CS/- (left) or 3x 6CS/- (center) delivered on the same day fail to produce detectable extinction learning.
c: Ext1-3 learning upon tFC followed by IL silencing during extinction protocol as in (**a**). Right; n = 5 each; one-way ANOVA: F (3, 16) = 46.87, ***P.
d: Savings upon Ext1-3 learning. Mice that underwent 2x tFC followed by an Ext1-3 protocol rapidly learn to extinguish again upon return of fear (10d). n = 5 each; one-way ANOVA: F (2, 12) = 77.77, ***P. Dunnet's *post hoc* (Tukey's *post hoc* in **a**); p<0.05 (*), 0.01 (**), 0.001 (***).

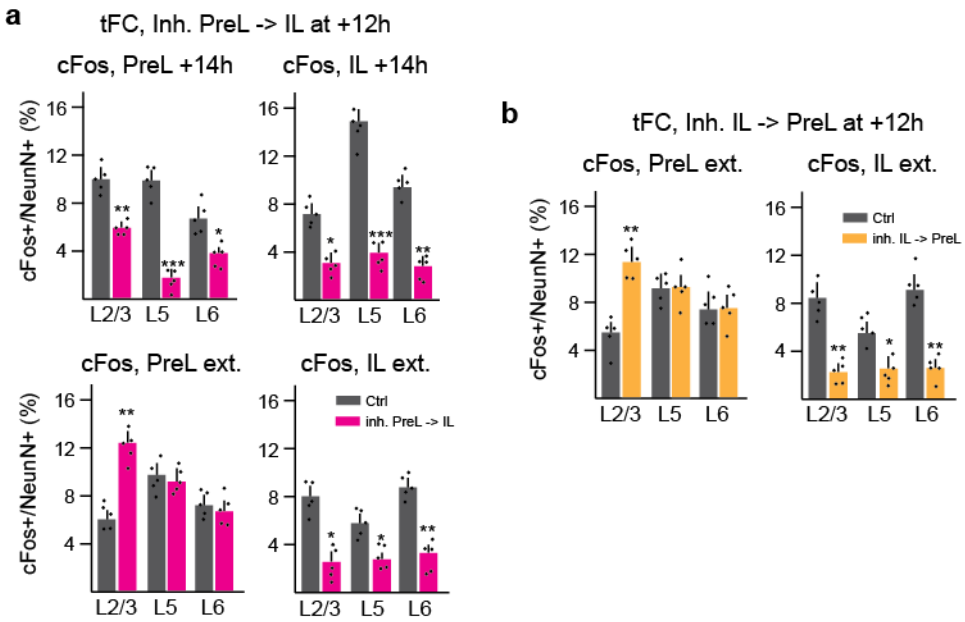

Mukherjee and Caroni Suppl. Fig. 8

Figure S8: Activity in PreL->IL and in IL->PreL projecting neurons required at +12h-14h after fear learning acquisition to set up role of IL in extinction learning.
a: Impact of PreL->IL projection neuron silencing at +12h after acquisition on induction of cFos in PreL and IL at +14h after acquisition and upon extinction protocol. n = 5 each; Two-way ANOVA: PreL +14h, F (1, 24) = 38.04, ***P; IL +14h, F (1, 24) = 106, ***P; PreL Ext, F (1, 24) = 5.49, *P; IL Ext, F (1, 24) = 40.57, ***P.
b: Impact of IL->PreL projection neuron silencing at +12h on induction of cFos in PreL and IL upon extinction protocol. n = 5 each; Two-way ANOVA: PreL Ext, F (1, 24) = 11.97, **P; IL Ext, F (1, 24) = 30.68, ***P. Sidak's *post hoc*.
Error bars: SEM; p<0.05 (*), 0.01 (**).

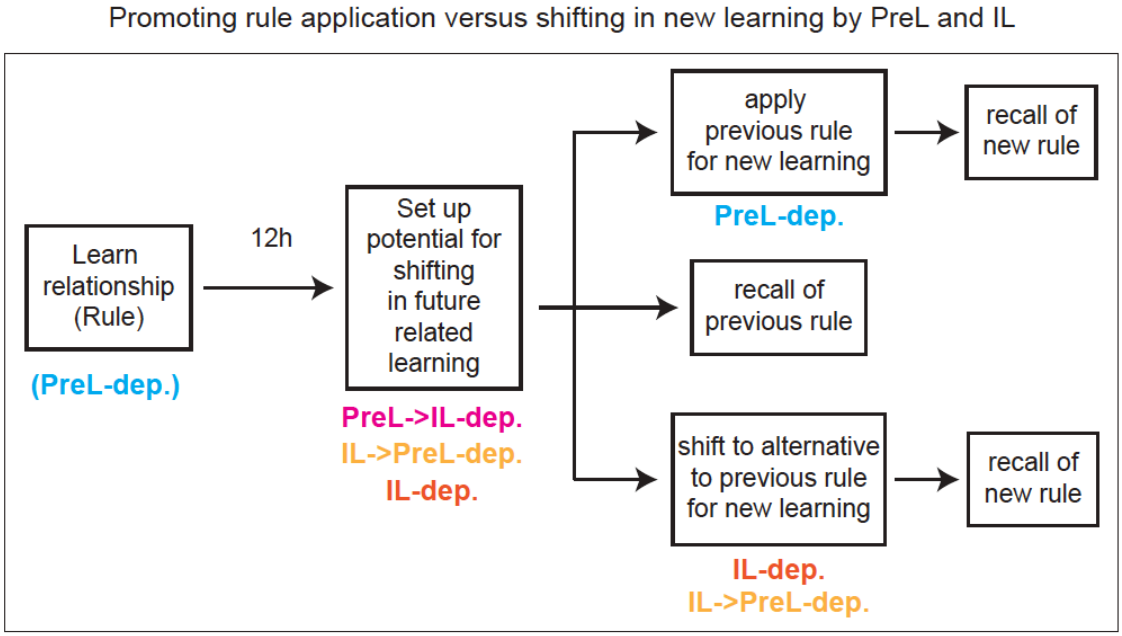

Mukherjee and Caroni, Suppl. Fig. 9

Figure S9: Summary of main findings in the study. Requirements for activity in PreL, IL, PreL→IL connectivity, and IL→PreL connectivity during different phases of learning/recall were investigated through pharmacogenetic silencing/inactivation during the learning/recall phase to be tested. The schematic shows how learning through application of a previous rule depends on activity in PreL (cyan), learning requiring shifting to an alternative to the previous rule depends on activity in IL (orange-red) and IL→PreL connectivity (orange), whereas recall of previous learning does not depend on activity in PreL, IL, IL→PreL or PreL→IL connectivity. Activity in IL→PreL and in PreL→IL (magenta) connectivity were both required during a time window approximately 12h after rule learning to set up the role of IL in subsequent alternative learning.

Experimental procedures

Mice

PV-Cre mice were from Jackson laboratories (129P2-Pvalbtm1 (cre)Arbr/J) were a kind gift from S. Arber (Friedrich Miescher Institut). Mice were kept in temperature-controlled rooms on a constant 12h light-dark cycle, and all experiments were conducted at approximately the same time of the light cycle. Before the behavioral experiment, mice were housed individually for 3-4d and provided with food and water *ad libitum* unless otherwise stated. All animal procedures were approved and performed in accordance with the Veterinary Department of the Kanton Basel-Stadt.

Behavioral procedures

All experiments were carried out with male mice. At the onset of the experiments P60 mice were 55-65d old.

For trace fear conditioning (tFC) (Raybuck and Lattal, 2014), animals were placed in the training context (Habitest Unit, Coulbourn Instruments, Allentown, PA) and were given a 180s habituation period. Conditioning trials began with a 20s mixed-frequency tone (CS), followed by a 30s trace period before the animal received a 2s (0.8 mA) foot shock (US). The conditioning trial was followed by a pseudo-random inter-trial interval (ITI) of 120 +/- 20s. The conditioning trials were repeated 6 times to get a robust CS-US association. To assess retrieval of trace fear memory the animals were placed in a novel context (a white circular enclosure in a separate noise proof cabinet) and given a 180s habituation period. Retrieval trials began by presentation of a 20s tone and freezing was measured for 60s post tone presentation, in the absence of foot shock. In extinction experiments this was repeated 6 times with a variable ITI of 90+/-

30s to get 6 independent measures of freezing and a gradual extinction curve. Identities of the contexts were maintained with the presence of distinct odors; 2% acetic acid for training context and 0.25% benzaldehyde for retrieval context. The training and retrieval chambers were cleaned with 70% ethanol before and after each session. Control mice were subjected to the same procedure without receiving foot shocks. Freezing was defined as complete absence of somatic mobility other than respiratory movements.

Contextual fear conditioning experiments were carried out as described (Donato et al., 2013). Briefly, mice were allowed to explore the training context for 2.5min, and then received five foot shocks (1s and 0.8mA each, inter-trial interval: 30s). Control mice were subjected to the same procedure without receiving foot shocks. We assessed contextual fear memory by returning mice to the training chamber after fear conditioning during 5min, and analyzing freezing during a test period of 4min (first min excluded). In extinction experiments mice were kept in the training chamber for 30min without foot shocks.

For Intradimension / Extradimension set shift task (IEST), mice were trained to dig in plastic food bowls, with an internal diameter of 40mm and a depth of 40mm and filled with wood chips, to retrieve a food reward buried at the bottom of the bowl. The reward was one-third of a Honey Nut Loop (Kellogg, Manchester, UK). The outer surface of the bowl was covered with a texture and the rim of the bowl was coated with an odor. The test apparatus was a rectangular Plexiglas box with panels that divided one-third of its length into two sections of equal proportions. The digging bowls were placed in these sections and two doors with independent access separated the mouse from the two sections where the bowls were placed. The doors could be slid open to give the mouse access to the food bowls or closed rapidly to prevent access to the other bowl after an error. The mice were food restricted from a day before the habituation phase till the end of the experiment. Each day, after the end of testing, mice were given access to 1g of a mash made of crushed food pellets mixed with water. The habituation phase consisted of 3 days; each day mice were given access to 2 bowls filled with wood chips and baited with reward. Mice were allowed to dig in both the bowls for the reward following which the bowls were re-baited for a second time. During test phases, trials were initiated by opening both doors simultaneously to give the mouse access to the two digging bowls, only one of which was baited. The first four trials were

exploratory trials, where the mouse was allowed to dig in both the bowls and an error was recorded if the mouse dug first in the un-baited bowl. On subsequent trials access to the other bowl was occluded as soon as the mouse began digging in one of the bowls. A correct trial was recorded when the mouse dug in the baited bowl to collect the reward. A trial was terminated when the mouse dug in the correct bowl and collected the reward, or dug in the un-baited bowl and left the chamber. Testing continued until the mouse reached a criterion level defined as 8 correct trials out of the last 10 trials. IEST consisted of 5 testing sessions spread over five days, each involving a different type of discrimination. In simple discrimination the bowls differed along the odor dimension only. For compound discrimination a second dimension (textures) was introduced, but correct and incorrect odors remained constant. For intra-dimensional shift a new pair of odors and textures were introduced and the mouse had to learn a new odor-reward association using the odor rule learnt previously. For intra-dimensional shift reversal the odor and texture cues remained unchanged but the mouse had to learn that the previously correct odor-reward association was now incorrect and the previously incorrect odor now predicted reward. Finally, for the extra-dimensional shift a new pair of odors and textures were introduced and the previously relevant dimension (odor) was now irrelevant whereas the previously irrelevant dimension (texture) now predicted reward. The order of the discriminations was always the same, but the dimensions and the pairs of cues were equally represented within groups and counterbalanced between groups.

Immunocytochemistry and histology.

Antibodies used were as follows: goat anti-PV (Swant biotechnologies, PVG-213) 1:5000; rabbit anti-cFos (Santa Cruz biotechnology, sc-52) 1:8000; mouse anti-NeuN (Millipore, MAB377) 1:1000; α-Bungarotoxin, Alexa 488 Conjugate (Molecular Probes, Life Technologies, B-13422) 1:500; mouse α-cMyc (ATCC, CRL-1729) 1:1000. Secondary antibodies were Alexa Fluor 488 (Molecular Probes; A150077), or 647 (Molecular Probes; A150131, A150107); 1:500. Prelimbic and Infralimbic were at +1.8mm to +1.95mm from bregma while Basolateral Amygdala and Nuclear Accumbens were at +1.8mm and +0.8mm from bregma respectively. Samples belonging to the same experiment (for example, from the mice of a given time point, with their controls) were acquired in parallel and with the same settings on an LSM700

confocal microscope (Zeiss) using an EC Plan-Neofluar340/1.3 oil-immersion objective (Zeiss). cFos immunohistochemistry and intensity analysis were done as described in Karunakaran et al., 2016. For c-Fos analysis, mice were returned to their home cage for 90min or till the relevant time point after the training session and then perfused (transcardially with 4% PFA in PBS, pH 7.4). Brains were kept in fixation solution overnight at 4°C and cryostat sections were processed for immuno-cytochemistry. All c-Fos and/or NeuN immunopositive cells were quantified using an automatic spot-detection algorithm (Imaris 7.0.0, Bitplane AG; expected radius, 10mm; quality level, 7). cFos induction was quantified as a fraction of cFos positive cells over the total neuronal population expressing NeuN. In experiments involving injections with picospritzer or Hamilton needles, brains were collected at the end of the experiments for histological analysis (e.g. **Fig. 2A**). Serial slices were imaged at 10x or at 4x to locate the injection site and the extent of volume spread. To that end, all microinjections were controlled using a vital stain, Hoechst 33342 (Invitrogen, H3570) as a proxy for drug spread into the cells. All viral expression spread were controlled with α-Bungarotoxin staining for PSAM channel or mCherrry signal for the DREADDS. Occasional mice in which the injections had also targeted neighboring areas were excluded from the analysis.

Stereotaxic surgery:

All surgeries were conducted under aseptic conditions using a small animal stereotaxic instrument (David Kopf Instruments). Mice were anaesthetized with isoflurane (4% for induction, 1.5–2.0% afterward) in the stereotaxic frame for the entire surgery and body temperature was maintained with a heating pad. Local drug treatments were carried out with a 33-gauge needle coupled to a 5ul syringe (Hamilton, Reno, NV) while viruses were delivered using glass pipettes (tip diameter 10–20 µm) connected to a picospritzer (Parker Hannifin Corporation). Coordinates relative to bregma are as follows: PreL (anteroposterior (AP) +2.0mm, mediolateral (ML) ±0.5mm, dorsoventral (DV, relative to dura) -2.1mm); IL (angle (ML-DV plane; away from mid-line) 10°, AP +1.8mm, ML ±1.0mm, DV -2.95mm); ventral hippocampus (AP -3.0mm, ML ±2.9mm, DV -3.5mm) and BLA (AP -1.6mm, ML +3.0mm, DV -4.3mm). For drug injections the needle was slowly lowered to 0.1mm beyond the required DV co-ordinate and quickly pulled up to the original co-ordinate

to create a pocket for injection of the drug. This prevented backflow of the drug and undesirable spread into neighboring areas. Drugs were injected at the rate of 100nl/min to a final maximum volume of ~200nl. After completion of injection the needle was left in its place for 5 min to allow for diffusion of the drug and then slowly withdrawn. For virus injections the glass pipette was inserted at the desired co-ordinate and ~200nl of the virus preparation was slowly pressure injected using a picospritzer over a period of 10 min. After the end of the injection the pipette was left in its place for a further 10 min to allow for diffusion of the virus. All drugs and viruses were injected bilaterally in the PreL, IL, vH and BLA. Post-surgical recovery was monitored daily until the start of behavioral protocols. All injections were paired with saline injected control animals to account for any effect due to tissue damage or surgical procedure.

Pharmacology in vivo

Drugs were used bilaterally as follows: Muscimol (50ng/side prepared in buffered saline, Sigma); T-5224 (1ug/side prepared in 20% PVP and 10% DMSO, MedChemExpress; cFos-AP1 inhibitor; Aikawa et al., 2008).

Pharmacogenetic in vivo

For acute silencing of a brain area, we bilaterally delivered floxed PSAM-carrying AAV9 (excitation, rAAV9-CAG-flox-PSAM(Leu41Phe,Tyr116Phe)5HT3-WPRE) in PV-Cre mice (Donato et al., 2013; Karunakaran et al., 2016; Magnus et al., 2011). To allow for transgene expression, mice were kept under home cage conditions for 7-9d before any behavioral experiment. The PSAM agonist, PSEM308 was injected i.p. at 5mg/kg of animal weight to activate the PSAM channels (Magnus et al., 2011). All silencing experiments were done 20mins before the behavior.
For PreL->IL or IL->PreL activation/silencing experiments a canine adenovirus 2 (CAV2) carrying Cre-recombinase (IGMM, France) was injected bilaterally in the PreL (or IL). Concurrently, a FLEXed DREADD-carrying AAV8 (Sternson and Roth, 2014) (B. Roth, UNC Vector Core; activation, rAAV8-hSyn-DIO-hM3D(Gq)-mCherry; silencing, rAAV8-AAV-hSyn-DIO-hM4D(Gi)-mCherry) was injected in the IL (or PreL). To visualize collaterals and terminals of IL->PreL or PreL->IL projections, beyond the

prefrontal cortex, a similar approach as above was taken. Here instead of DREADDs a FLEXed Synaptophysin-cMyc carrying AAV9 (a kind gift from S. Arber, FMI) and a FLEXed GFP carrying AAV8 (B. Roth, UNC Vector Core) was co-injected into the IL (or PreL). Thus, we could follow the projection fibers using the GFP signal and their synaptic terminals by immunostaining for cMyc. For chemogenetic synaptic silencing of the projection neurons a FLEXed synaptically targeted silencing DREADD (Stachniak et. al., 2014) was used. To allow for transgene expression, mice were kept under home cage conditions for 12-14 days before any behavioral experiment. Selective activation of the DREADD receptors was achieved by administering the DREADD agonist, clozapine-N-oxide (CNO; 5mg/kg, i.p, Tocris; Sternson and Roth, 2014). For synaptic silencing CNO (0.3μM) was administered through a Hamilton needle at target regions. All DREADD activation experiments were done 30mins before the behavioral procedure. Post experiment brains were dissected and serial slices were imaged at 10x to verify correct projection neuron labelling using the mCherry signal.

Statistical analysis

All statistical analyses were based on two-tailed comparisons and were done using GraphPad Prism (GraphPad software. Inc.). Results are presented as mean ± s.e.m. The sample size per group is mentioned in the respective figure legends. Number of animals to be used for a standard behavioral analysis was determined based on our preliminary behavioral experiments across different investigators in the laboratory. We paid particular attention to the magnitude of difference between groups tested apart from the statistical significance across groups. Data distributions were assumed to be normal but this was not formally tested. Male mice of closely comparable age were assigned randomly to experimental groups. Intensity analysis and freezing data were verified by a co-worker blind to experimental conditions.

Data availability

All relevant data files, namely video recordings and image files are available from the authors upon request.

Acknowledgments

We thank S. Arber (FMI) for valuable comments on the manuscript. This work was supported in part by a Swiss National Fund grant to P.C. and by the NCCR Synapsy. The Friedrich Miescher Institut is part of the Novartis Research Foundation.

Author contributions

A.M. devised and carried out all the experiments. P.C. helped devise the experiments and wrote the manuscript. All authors discussed the results and commented the manuscript.

Supplementary information includes a supplementary results section and 9 supplementary figures with their legends.

References

Aikawa, Y., Morimoto, K., Yamamoto, T., Chaki, H., Hashiramoto, A., Narita, H., Hirono, S., and Shiozawa, S. (2008). Treatment of arthritis with a selective inhibitor of c-Fos/activator protein-1. Nat. Biotechnol. *26*, 817-823.

Barker, J.M., Taylor, J.R., and Chandler, L.J. (2014). A unifying model of the role of the infralimbic cortex in extinction and habits. Learning Mem. *21*, 441-448.

Birgman, J.L., Bussey, T.J., Saksida, L.M., and Rothblat, L.A. (2005). Discrimination of multidimensional visual stimuli by mice: intra- and extra-dimensional shifts. Behav. Neurosci. *119*, 839-842.

Birrell, J.M., and Brown, V.J. (2000). Medial frontal cortex mediates perceptual attentional set shifting in the rat. J. Neurosci. *20*, 4320-4324.

Bissonette, G.B. Martins, G.J., Franz, T.M., Harper, E.S., Schoenbaum, G., and Powell, E.M. (2008). Double dissociation of the effects of medial and orbital prefrontal cortical lesions on attentional and affective shifts in mice. J. Neurosci. *28*, 11124-11130.

Brady, A.M., and Floresco, S.B. (2015). Operant procedures for assessing behavioral flexibility in rats. J. Vis. Exp. *96*, e52387.

Carr, M.F., Jadhav, S.P., and Frank, L.M. (2011). Hippocampal replay in the awake state: a potential substrate for memory consolidation and retrieval. Nat. Neurosci. *14*, 147-153.

Courtin J., Bienvenu T. C., Einarsson E. O., and Herry C. (2013). Medial prefrontal cortex neuronal circuits in fear behavior. Neuroscience *240*, 219–242.

Courtin J., Chaudun F., Rozeske R. R., Karalis N., Gonzalez-Campo C., Wurtz H., et al. (2014). Prefrontal parvalbumin interneurons shape neuronal activity to drive fear expression. Nature 505, 92–96.

David-Pereira, A., Puga, S., Goncalves, S., Amorim, D., Silva, C., Pertovaara, A., Almeida, A., and Pinto-Ribeiro, F. (2016). Metabotropic glutamate 5 receptor in the infralimbic cortex contributes to descending pain facilitation in healthy and arthritic animals. Neuroscience *15*, 108-119.

Donato, F., Rompani, S.B. and Caroni, P. (2013). Parvalbumin-expressing basket-cell network plasticity induced by experience regulates adult learning. Nature *504*, 272–276.

Fitzgerald, P.J., Giustino, T.F., Seemann, J.R., and Maren, S. (2015). Noradrenergic blockade stabilizes prefrontal activity and enables fear extinction under stress. Proc. Natl. Acad. Sci. U.S.A. *112*, E3729-E3737.

Fuchikami, M., Thomas, A., Liu, R., Wohleb, E.S., Land, B.B., DiLeone, R.J., Aghajanian, G.K., and Duman, R.S. (2015). Optogenetic stimulation of infralimbic PFC reproduces ketamine's rapid and sustained antidepressant actions. Proc. Natl. Acad. Sci. USA *112*, 8106-8111.

Garner, J.P., Thogerson, C.M., Würbel, H., Murray, J.D., and Mench, J.A. (2006). Animal neuropsychology: validation of the intra-dimensional extra-dimensional set shifting task for mice. Behav. Brain Res. *173*, 53-61.

Gilmartin M. R., McEchron M. D. (2005). Single neurons in the medial prefrontal cortex of the rat exhibit tonic and phasic coding during trace fear conditioning. Behav. Neurosci. *119*, 1496–1510.

Gilmartin, M.R., Miyawaki, H., Helmstetter, F.J. and Diba, K. (2013). Prefrontal activity links non-overlapping events in memory. J. Neurosci. *33*, 10910-10914.

Gilmartin, M.R., Balderston, N.L., and Helmstetter, F.J. (2014). Prefrontal cortical regulation of fear learning. Trends Neurosci. *37*, 455-464.

Girardeau, G., Benchenane, K., Wiener, S.I., Buzsáki, G., and Zugaro, M.B. (2009). Selective suppression of hippocampal ripples impairs spatial memory. Nat. Neurosci. *12*, 1222-1233.

Giustino, T.F. and Maren, S. (2015). The role of the medial prefrontal cortex in the conditioning and extinction of fear. Front. Behav. Neurosci. *9*, 298.

Giustino, T.F., Fitzgerald, P.J., and Maren, S. (2016). Fear expression suppresses medial prefrontal cortical firing in rats. PLoS One *11*, e0165256.

Glickfeld, L.L., Andermann, M.L., Bonin, V., and Reid, R.C. (2013). Cortico-cortical projections in mouse visual cortex are functionally target specific. Nat. Neurosci. *16*, 219-226.

Gonzalez, M.C. Kramar, C.P., Tomaiuolo, M., Katche, C., Weisstaub, N., Cammarota, M., and Medina, J.H. (2014). Medial prefrontal cortex dopamine controls the persistent storage of aversive memories. Front. Behav. Neurosci. *8*, 408.

Gourley, S.L. and Taylor, J.R. (2016). Going and Stopping: dichotomies in behavioral control by the prefrontal cortex. Nat. Neurosci. *19*, 656-664.

Groenewegen H. J., Uylings H. B. M. (2000). The prefrontal cortex and the integration of sensory, limbic and autonomic information. Prog. Brain Res. *126*, 3–28.

Hamilton, D.A., and Brigman, J.L. (2015). Behavioral flexibility in rats and mice: contributions of distinct frontocortical regions. Genes Brain Behav. *14*, 4-21.

Herry, C., and Johansen, J.P. (2014). Encoding of fear learning and memory in distributed neuronal circuits. Nat. Neurosci. *17*, 1644-1654.

Hoover W. B., Vertes R. P. (2007). Anatomical analysis of afferent projections to the medial prefrontal cortex in the rat. Brain Struct. Funct. *212*, 149–179.

Hok, V., Save, E., Lenck-Santini, P.P., and Poucet, B. (2005). Coding for spatial goals in the prelimbic/infralimbic area of the rat prefrontal cortex. Proc. Natl. Acad. Sci. U.S.A. *102*, 4602-4607.

Huxter, F.J., Conway, M.W., Lowry, J.P., Tricklebank, M.D. and Gilmour, G. (2014). Differential contributions of infralimbic prefrontal cortex and nucleus accumbens during reward-based learning and extinction. J. Neurosci. *34*, 596-607.

Ito, H.T., Zhang, S.-J., Witter, M.P., Moser, E.I., and Moser, M.-B. (2015). A prefrontal-thalamo-hippocampal circuit for goal-directed spatial navigation. Nature *522*, 50-55.

Ji, G., and Neugebauer, V. (2012). Modulation of medial prefrontal cortical activity using in vivo recordings and optogenetics. Mol. Brain *5*, 36.

Katche, C., Cammarota, M., and Medina, J.H. (2013). Molecular signatures and mechanisms of long-lasting memory consolidation and storage. Neurobiol. Learn. Mem. *106*, 40-47.

Karunakaran, S., Chowdhury, A., Donato, F., Quairiaux, C., Michel, C.M., and Caroni, P. (2016). PV plasticity sustained through D1/5 dopamine signaling required for long-term memory consolidation. Nat. Neurosci. *19*, 454-464.

Killcross S., Coutureau E. (2003). Coordination of actions and habits in the medial prefrontal cortex of rats. Cereb. Cortex *13*, 400–408.

Kim, J.N., and Shadlen, M.N. (1999). Neural correlates of a decision in the dorsolateral prefrontal cortex of the macaque. Nat. Neurosci. *2*, 176-185.

Knapska, E., Macias, M., Mikosz, M., Nowak, A., Owczarek, D., Wawrzyniak, M., Pieprzyk, M., Cymerman, I.A., Werka, T., Sheng, M. *et al.* (2012). Functional anatomy of neuronal circuits regulating fear and extinction. Proc. Natl. Acad. Sci. U.S.A. *109*, 17093-17098.

Kolling, N., Behrens, T.E.J., Mars, R.B., and Rushworth, M.F.S. (2012). Neural mechanisms of foraging. Science *336*, 95-98.

Kremer, E.J., Boutin, S., Chillon, M. and Danos, O. (2000). Canine adenovirus vectors: an alternative for adenovirus-mediated gene transfer. J. Virol. *74*, 505-512.

Laurent, V., and Westbrook, R.F. (2009). Inactivation of the infralimbic but not the prelimbic cortex impairs consolidation and retrieval of fear extinction. Learn. Mem. *16*, 520-529.

Little J. P., Carter A. G. (2013). Synaptic mechanisms underlying strong reciprocal connectivity between the medial prefrontal cortex and basolateral amygdala. J. Neurosci. *33*, 15333–15342.

Magnus, C.J., Lee, P.H., Atasoy, D., Su, H.H., Looger, L.L., and Sternson, S.M. (2011). Chemical and genetic engineering of selective ion channel-ligand interactions. Science *333*, 1292–1296.

Miller, E.K., and Cohen, J.D. (2001). An integrative theory of prefrontal cortex function. Ann. Rev. Neurosci. *24*, 167-202.

Morris, R.W., Dezfouli, A., Griffiths, K.R., and Balleine, B.W. (2014). Action-value comparisons in the dorsolateral prefrontal cortex control choice between goal-directed actions. Nat. Commun. *5*, 4390 (2014).

Peters, J., Kalivas, P.W. and Quirk, G.J. (2009). Extinction circuits for fear and addiction overlap in prefrontal cortex. Learn. Mem. *16*, 279-288.

Qualian, C. and Gisquet-Verrier, P. (2010). The differential involvement of the prelimbic and infralimbic cortices in response conflict affects behavioral flexibility in rats trained in a new automated strategy-switching task. Learn. Mem. *17*, 654-668.

Rich, E.L., and Shapiro, M.L. (2007). Prelimbic/infralimbic inactivation impairs memory for multiple task switches, but not flexible selection of familiar tasks. J. Neurosci. *27*,

4747-4755.

Rich, E.L. and Shapiro, M. (2009). Rat prefrontal cortical neurons selectively code strategy switches. J. Neurosci. *29*, 7208-7219.

Rushworth, M.F.S., Noonan, M.P., Boorman, E.D., Walton, M.E., and Behrens, T.E. (2011). Frontal cortex and reward-guided learning and decision making. Neuron *70*, 1054-1069.

Saffari, R. Teng, Z., Zhang, M., Kravchenko, M., Hohoff, C., Ambrée, O. and Zhang, W. (2016). NPY+, but not PV+-GABAergic neurons mediated long-range inhibition from infra- to prelimbic cortex. Transl. Psychiatry *6*:e736.

Sangha, S., Robinson, P.D., Greba, Q., Davies, D.A., and Howland, J.G. (2014). Alterations in reward, fear and safety cue discrimination after inactivation of the rat prelimbic and infralimbic cortices. Neuropsychopharmacology *39*, 2405-2413.

Santini, E., Quirk, G.J., and Porter, J.T. (2008). Fear conditioning and extinction differentially modify the intrinsic excitability of infralimbic neurons. J. Neurosci. *28*, 4028-4036.

Sierra-Mercado, D., Padilla-Coreano, N., and Quirk, G.J. (2011). Dissociable roles of prelimbic and infralimbic cortices, ventral hippocampus, and basolateral amygdala in the expression and extinction of conditioned fear. Neuropsychopharmacology *36*, 529-538.

Smith K.S., Virkud A., Deisseroth K., Graybiel A.M. (2012). Reversible online control of habitual behavior by optogenetic perturbation of medial prefrontal cortex. Proc Natl Acad Sci U S A *109(46)*, 18932-7.

Smith K.S., Graybiel A.M. (2013). A dual operator view of habitual behavior reflecting cortical and striatal dynamics. Neuron *79(2)*, 361-74

Soler-Cedeno, O., Cruz, E., Criado-Marrero, M., and Porter, J.T. (2016). Contextual fear conditioning depresses infralimbic excitability. Neurobiol. Learn. Meme. *130*, 77-82.

Sparta D.R., Hovelsø N., Mason A.O., Kantak P.A., Ung R.L., Decot H.K., Stuber G.D. (2014). Activation of prefrontal cortical parvalbumin interneurons facilitates extinction of reward-seeking behavior. J. Neurosci. *34*, 3699-705.

Stachniak, T.J., Gosh, A., and Sternson, S.M. (2014). Chemogenetic synaptic silencing of neural circuits localizes a hypothalamus -> midbrain pathway for feeding behavior. Neuron *82*, 797-808.

Sternson, S.M., and Roth, B.L. (2014). Chemogenetic tools to interrogate brain functions. Ann. Rev. Neurosci. *37*, 387-407.

Song, C., Ehlers, V.L., and Moyer, J.R.Jr. (2015). Trace fear conditioning differentially modulates intrinsic excitability of medial prefrontal cortex-basolateral complex of amygdala projection neurons in infralimbic and prelimbic cortices, J. Neurosci. *35*, 13511-13524.

Sotres-Bayon, F., and Quirk, G.J. (2010). Prefrontal control of fear: more than just extinction. Curr. Op. Neurobiol. *20*, 231-235.

Suto N., Laque A., De Ness G.L., Wagner G.E., Watry D., Kerr T., Koya E., Mayford M.R., Hope B.T., Weiss F (2016). Distinct memory engrams in the infralimbic cortex of rats control opposing environmental actions on a learned behavior. eLife. 5, e21920.

Raybuck, J.D., and Lattal, K.M. (2014). Bridging the interval: theory and neurobiology of trace conditioning. Behav. Processes *101*, 103-111.

Tanji, J., and Hoshi, E. (2008). Role of the lateral prefrontal cortex in executive behavioral control. Physiol. Rev. *88*, 37-57.

Tsutsui-Kimura I., Ohmura, Y., Izumi, T., Matsushima, T., Amita, H., Yamaguchi, T., Yoshida, T., and Yoshioka, M. (2016). Neuronal codes for the inhibitory control of impulsive actions in the rat infralimbic cortex. Behav. Brain Res. *296*, 361-372.

Vertes R.P. (2004). Differential projections of the infralimbic and prelimbic cortex in the rat. Synapse. *51*, 32-58.

Van Aerde, K.I., Heistek, T.S., and Mansvelder, H.D. (2008). Prelimbic and infralimbic cortex interact during fast network oscillations. PLoS ONE *3*, e2725.

2.2

A sensitive period for long-lasting rescue in a genetic model of Schizophrenia

Arghya Mukherjee and Pico Caroni

To be submitted to Cell

Introduction

Schizophrenia is a psychiatric illness that affects roughly 1% of the global population and emerges between the ages of 18 to 25 years in human patients. The disease is characterized by three classes of symptoms namely, positive (delusions, hallucinations and disorganized speech), negative (social withdrawal, avolition and anhedonia) and cognitive (poor working memory). While the psychotic symptoms are used to make a clinical diagnosis of the disorder, the cognitive deficits manifest much earlier in the etiology of the disease (Elvevag and Goldberg, 2000). These cognitive impairments, a lot of which are primarily prefrontal and hippocampal in origin, are now recognized to be the core domain of the illness and is the focus of this study.

Our understanding of the neurobiological underpinnings of the cognitive deficits in schizophrenia has progressed considerably over the years. Altered excitatory/inhibitory balance, deficits in neuromodulatory systems, disrupted connectivity and network synchrony have all been identified through research in human patients and rodent models (Lewis, 2014; Uhlhaas and Singer, 2010; Sigurdsson and Duvarci, 2016). Additionally, neurodevelopmental changes at the level of genetic mutations and cellular events have also been identified (Poels et al., 2014a; 2014b). However, the diversity and heterogeneity of these deficits across patient groups and various rodent models (Clementz et al., 2016) have precluded a simple model of the disorder at the level of genetic and molecular changes. In recent years, dysfunction in the Parvalbumin (PV) interneuron network has emerged as a core substrate underlying the pathophysiology of the cognitive symptoms in the disease (Lewis, 2014) and support a circuit dysfunction hypothesis for the disorder (Arguello and Gogos, 2010). Research in rodents and other higher order model organisms have shown that PV neurons provide powerful local feedforward and feedback inhibition onto the perisomatic region of pyramidal neurons (Freund & Katona, 2007). These neurons have been shown to synchronize network activity, supporting different types of neuronal network oscillations, such as gamma and theta oscillation, ripple and spindle activity (Amilhon et al., 2015; Royer et al., 2012; Stark et al., 2014; Lapray et al., 2012; Cardin, 2009). Thereby, they play an important role in the stable formation and consolidation of cell assemblies to support learning and behavior (Karunakaran et al., 2016). Moreover, learning-related plasticity of PV basket cells has been reported

to transiently shift PV cell networks into configurations either supporting or suppressing further plasticity and learning (Donato et al., 2013). Two recent studies in mouse models of schizophrenia have shown that these neurons in the Prefrontal cortex and hippocampus are dysfunctional in their functional properties leading to aberrant neural synchrony and poor performance in cognitive tasks similar to human schizophrenic patients (Cho et al., 2015; Piskorowski et al., 2016). Thus, understanding the dysfunctions in prefrontal and hippocampal PV neuronal networks and their maturation may provide us with novel therapeutic strategies towards the cognitive symptoms of Schizophrenia.

In this study, we set out to explore the Parvalbumin neuronal network state and behavioral deficits in a mouse model of 22Q11.2DS. These mice (from now on referred to as LgDel +/-) have a heterozygous microdeletion on the mouse chromosome number 16 spanning all but 1 of the 27 genes deleted in human 22Q11.2DS (Stark et al., 2008). This genetic deletion has the highest risk factor for schizophrenia in humans with 30% of individuals carrying the deletion developing schizophrenia or schizoaffective disorder. Moreover de novo deleltions of the 22q11.2 locus accounts for 1 to 2 % of all schizophrenia cases (Xu et al., 2008). In human patients cognitive deficits in 22Q11.2DS are most severe in the executive function domain including working memory and attention (Woodin et al., 2001; Campbell et al., 2010, Karayiorgou et al., 2010). LgDel+/- mice have been previously shown to have deficits in emotional behaviour, sensorimotor gating, spatial working memory and reversal learning (Stark et al., 2008; Sigurdsson et al., 2010; Meechan et al., 2015). We found that the PV network in the prefrontal cortex of these mice fail to mature to an adult state. This deficit is accompanied by altered baseline neural synchrony and behavioral deficits. We also show that the deficits in the PV neurons can be rescued within a specific window of treatment during early adulthood. This rescue also improves performance of the LgDel+/- animals in cognitive tasks and lasts for a long duration post rescue. Finally our rescue strategy has a strong potential for translational application in human patients to ameliorate the cognitive symptoms of te disorder.

Results

LgDel+/- mice show deficits in Parvalbumin neuronal network

We examined Parvalbumin neuron and protein distribution in different areas of prefrontal cortex and hippocampus of P60 LgDel+/- mice. Previously it has been shown that based on their PV protein expression levels, PV neurons can be classified into two distinct subpopulations expressing high (high-PV neurons) and low levels (low-PV neurons) of PV protein (Donato et. al., 2013). Compared to age matched wild type controls LgDel+/- mice (n=5 for each) showed a shift towards excessive levels of low-PV neurons and a smaller decrease of high-PV neurons of prelimbic cortex (PreL), infralimbic cortex (IL), ventro-orbital cortex (VLO), anterior cingulate cortex(Cg1), dorsal hippocampus CA3 (dH) and ventral hippocampus CA3 (vH) (**Figure 1A**). In contrast, no changes were observed in the density of PV neurons in the same brain regions of LgDel +/- mice (**Figure 1B,**). We further determined which PV subpopulation was specifically affected in LgDel+/- mice. Lineage tracing experiments show that the high-PV (early born) and low-PV (late-born) sub-populations are born at different days during embryonic development and are controlled by excitation and inhibition respectively (Donato et. al., 2015). Through similar lineage tracing experiments, we observed that the increase in the low PV population is restricted to the early born subpopulation (**Figure 1C**) while the late born subpopulation remains unaffected. Therefore, in LgDel+/- mice there is a deficit in parvalbumin expression in both the PFC and Hippocampus. This deficit is restricted to the early born subpopulation of PV neurons, which are regulated by excitation.

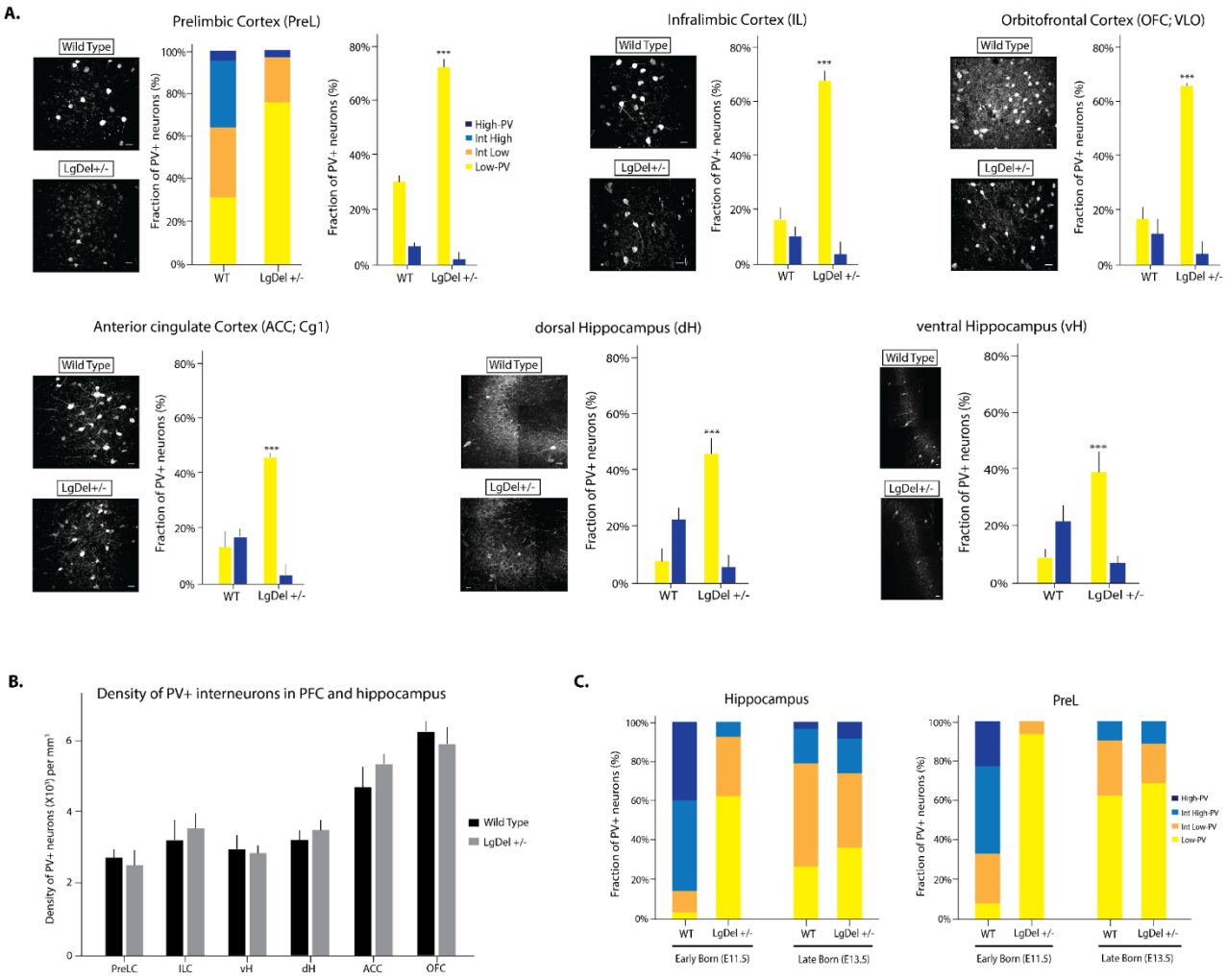

Figure 1. LgDel+/- mice show deficits in Parvalbumin neuronal network. (A) Representational images of PV network state in the prefrontal areas and hippocampus of wild type and Lgdel +/- mice (n=5 each). Quantification of High-PV and low-PV distribution in those areas showing increased low-PV population in LgDel+/- animals. Scale: 20um. Error bars show SEM. **(B)** Quantification of density of PV neurons in the same areas show that cell densities does not change in LgDel+/- (n=5 each). **(C)** Lineage tracing experiment showing early born PV neurons which are usually high-PV in WT animals have low-PV expression in LgDel+/- mice in hippocampus as well as Prelimbic cortex (n=5 each) while the late born neurons are unaffected (n=5 each). ***p<0.0001; analyzed using two-tailed Students T-test comparing low-PV or high-PV of WT vs Lgdel+/-.

Altered baseline gamma oscillations in LgDel+/- mice

It has been reported that PV interneurons are central to the generation of local gamma oscillations. To evaluate functional properties of PV neurons in Lgdel+/- mice, we implanted intra-cranial recording electrodes covering both PreL and IL. We measured the baseline power of various known oscillations in freely moving mice while they

explored an open field. We found that in comparison to WT (n=5), P60 LgDel+/- animals (n=5) had an increase in mPFC baseline gamma power in the low gamma band (30-48Hz) while high gamma oscillations (52Hz-90Hz) were unaffected (**Figure 2A**). On the other hand, oscillatory power in theta (4-10Hz) and beta bands (15-30Hz) showed no differences between LgDel+/- and WT animals **(Figure 2B**). Surprisingly, in adult LgDel+/- mice (P120, n=5) we observed a reduction in baseline spectral power in only in the high gamma range (**Figure 2C**) while the low gamma oscillations remained unaffected. Similar to younger P60 mice, older P120 mice had no observable deficits in oscillations in other frequencies (**Figure 2D**). These results show that LgDel+/- have altered baseline gamma activity in PreL and IL which parallels the deficits seen in the PV expression.

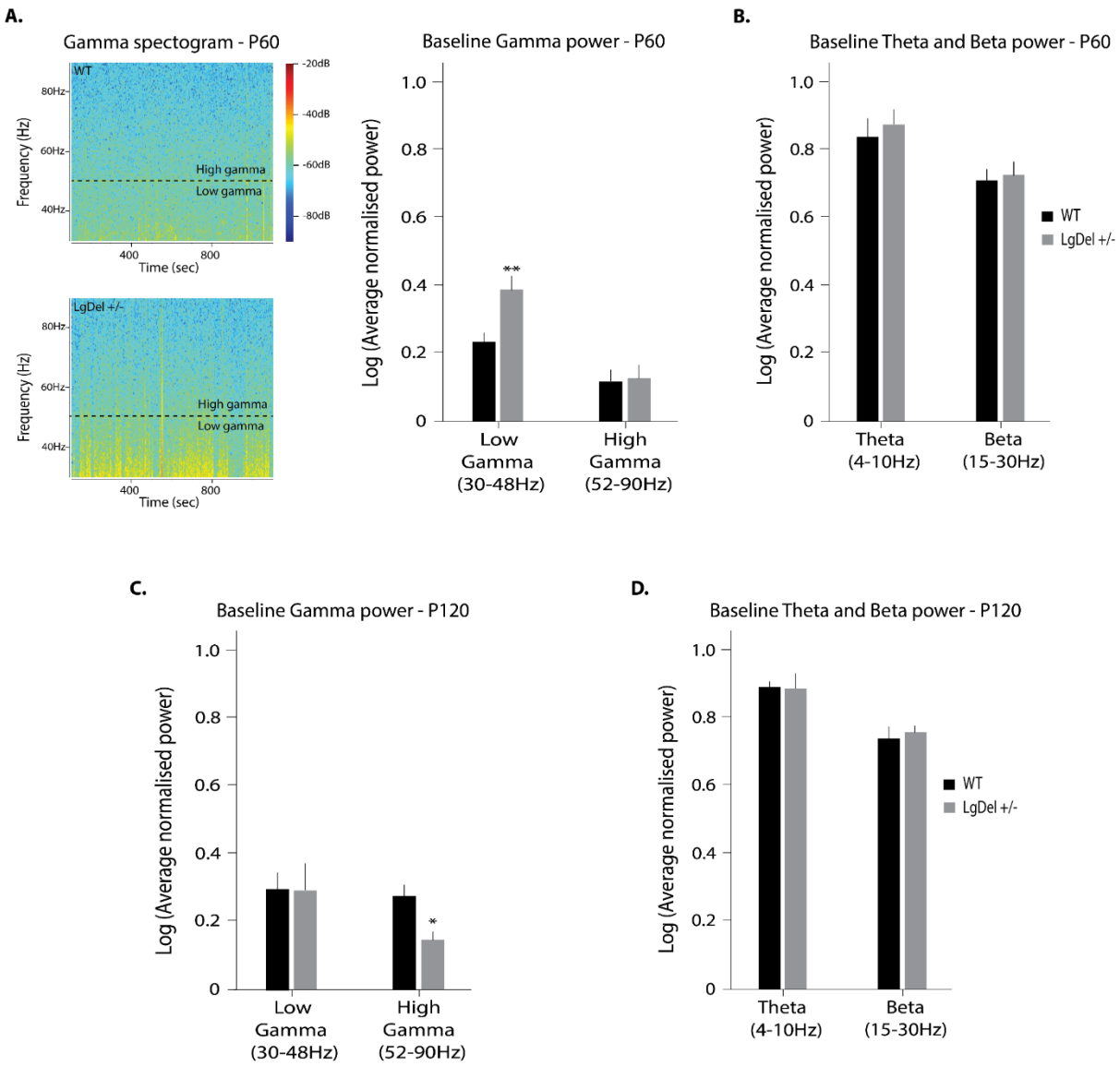

Figure 2. Altered baseline gamma oscillations in LgDel+/- mice. (A) Spectrogram of log power of oscillations in the gamma frequency range of freely exploring P60 WT and LgDel+/- mice in an open field, measured over a 20-minute window. Black dashed line separates the high gamma band from the low gamma band. P60 LgDel+/- animals show an increase in power of baseline low gamma oscillations compared to wild types (n=5 each). (B) Power of Beta and theta oscillations are comparable across P60 wild type and LgDel+/- animals (n=5 each). (C) Freely exploring, P120 Lgdel+/-, animals show reduced baseline power in the high gamma band while the low gamma band is unaffected in comparison to age-matched wild types (n=5 each). (D) Power of baseline theta and beta oscillations remain unaffected in P120 LgDel+/- mice. *p<0.01; **p<0.001; analyzed using two-tailed t-test comparing each frequency band of WT vs Lgdel+/- for P60 and P120 separately.

Impaired cognitive functions in LgDel+/- mice

Our next experiments assayed whether the network and cellular changes in PV interneurons were accompanied by cognitive deficits in prefrontal and hippocampal dependent tasks. To assess prefrontal function we used the intradimensional/extradimensional set shifting task (IEST) as described before (Bisonette et al., 2008) (**Figure 3A**). The task is divided into 5 distinct phases, each administered one day after the other. On each trial mice are presented with two bowls and must choose to dig in one bowl to find a food reward. Each bowl contains a different odor and a different texture around the bowl, and the odor-texture combinations vary from trial to trial. In the first phase, simple discrimination (SD), the mice have to learn an odor association, where a food reward is paired with only one odor out of an odor pair. The following day new textures are introduced as distractors and mice are tested on their ability to remember the learnt odor association (complex discrimination; CD). Both P60 and P120 LgDel +/- mice (n=8) learn the SD in similar number of trials as age matched WT controls (n=8) suggesting that the LgDel+/- mice have no deficits in learning an association (**Figure 3B**). However, during CD, in the presence of distractors, Lgdel+/- mice of both ages take significantly more number of trials to reach performance criterion compared to age matched controls (**Figure 3B**). In the subsequent Intra dimensional shift (IDS), which is a rule following step, the animals have to follow the rule of ‘odors predict the reward’ to learn a new odor association with new odors and textures. Interestingly, P60 LgDel+/- mice learn this phase as fast as their wild type counter parts while P120 LgDel+/- show a significant impairment (**Figure 3C**). Following this, animals were taught to perform a reversal (IDS Reversal; IDSRe) where the cues remained the same but the odor association

was reversed and the reward was paired with the previously unrewarded odor. Again compared to age matched WT animals, P60 LgDel+/- animals show no deficit in performance in IDSRe while P120 animals show a small impairment (**Figure 3D**). In the final and hardest stage of the task called extra dimensional shift (EDS) new odors and textures are presented where the reward is now paired with one of the two textures while the odor dimension is irrelevant. Thus, the animals have to perform a rule shift and learn that the odors no longer predict the reward and instead the textures predict the reward. During EDS the P60 LgDel+/- animals show a strong deficit in performance compared to their WT counterparts (**Figure 3E**). P120 Lgdel+/- as well as WT mice are unable to mediate this rule shift and do not learn the EDS shift in fifty trials (**Figure 3E**). Taken together these results demonstrate that LgDel+/- mice have severe deficits in a prefrontal dependent cognitive task. To account for a bias in perception of sensory modalities, in separate cohort of animals of both ages, the order of presentation of the rewarded and unrewarded dimensions were reversed with the textures being presented first in SD and the odors being rewarded in EDS. The LgDel+/- animals continued to have the same age specific deficits under this condition (**Figure S2A**)

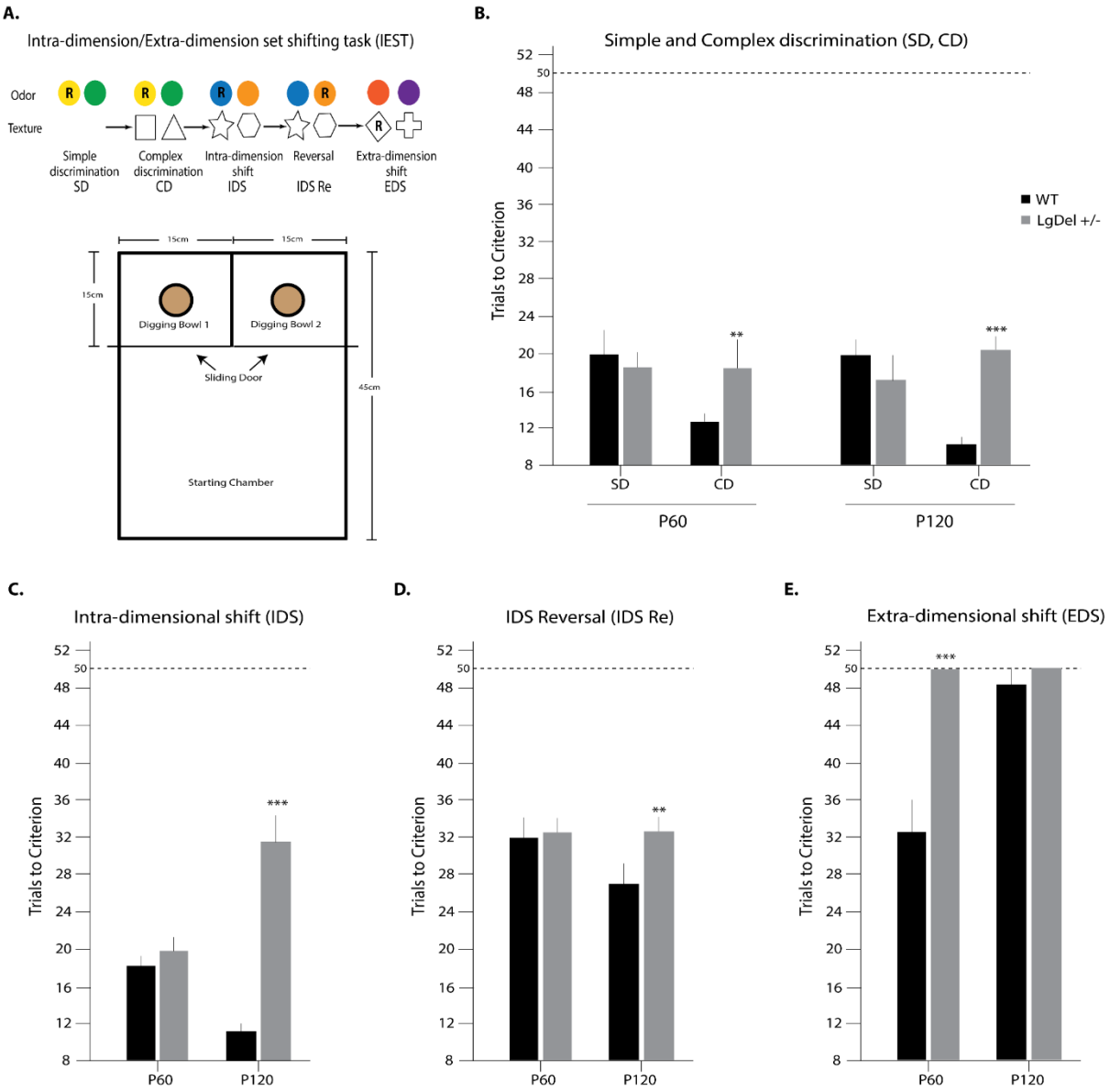

Figure 3: Impaired cognitive functions in LgDel+/- mice. (A) Schematic representation of ID/ED task (top) and setup (bottom). Mice have to choose between one of the two baited bowls for a food reward based on learnt rules involving odors and textures. See results text for more details. **(B)** LgDel+/- mice of both ages (P60 and P120) show no deficits in the simple discrimination phase (SD) (n=8). In the complex discrimination phase, in the presence of distractors, LgDel+/- animals show deficits in performance and take more trials to reach criterion. **(C)** In the rule following IDS phase, only P120 Lgdel+/- animals show a deficit in learning compared to age matched wild type animals (n=8). Performance of P60 Lgdel+/- animals are comparable to age matched wild types (n=8). **(D)** In the reversal task only P120 Lgdel+/- animals show a small deficit in performance while P60 LgDel+/- animals perform like wild types (n=8). **(E)** In the rule-shifting EDS phase, P60 Lgdel+/- animals fail to learn within 50 trials compared to their age matched controls. P120 animals cannot be compared in their performance due to ceiling effect of the task (n=8). *p<0.01; **p<0.001; ***p<0.0001; analyzed using two-tailed t-test comparing number of trials taken to reach criterion in each phase between age-matched WT and Lgdel+/- animals.

We also compared the performance of the animals in a hippocampus dependent social recognition memory task (SRT) adapted from Piskowrowski et. al., 2016. For this test, the subject mouse (LgDel+/- or WT) is first exposed to an unfamiliar WT mouse for five minutes. An hour post the first exposure the subject mouse is re-exposed to either the familiar mouse encountered before or a novel mouse. WT and LgDel+/- mice (n=6 each) of both ages show similar exploration when a novel mouse is presented in both phases of the task (**Figure S3C**). On re-exposure to the familiar mouse, P60 LgDel+/- mice spent less time interacting with the familiar mouse, like their WT counterparts (**Figure S3D**). However, older P120 LgDel+/-, unlike WT controls, did not show a reduction in time spent exploring a familiar mouse (**Figure S3E**). This shows that P120 LgDel+/- animals have a deficit in hippocampal dependent social recognition memory as reported before (Piskowrowski et al., 2016). Therefore, LgDel+/- mice show age dependent deficits in cognitive tasks involving the PFC or the Hippocampus.

PV neuron phenotype is a property of their network configuration

Having identified PV interneuron network deficits in LgDel mice, we wanted to determine whether these neurons could respond like WT PV+ neurons. Here we made use of a PV-Cre line crossed with LgDel+/- animals to derive a LgDel+/-:PV-cre colony. We injected an adeno-associated virus (AAV) bearing a FLEXed chemogenetic activating ligand-gated ion channel (LIGC) (PSAM(Leu41Phe,Tyr114Phe)5HT3; Magnus et al., 2011), in the PreL of P90 mice, to specifically target the parvalbumin neurons for stimulation using a non-biologically available ligand (PSEM308, 50mg/Kg i.p.) (**Figure 4A**). We observed that in WT PV-Cre animals (n=6), acute stimulation of the PV neurons resulted in a transient shift of the PV network to a high-PV configuration (**Figure 4B**) 6 hours post stimulation. Surprisingly in Lgdel+/-:PV-Cre animals, acute chemogenetic stimulation of PV neurons failed to induce a high PV shift, unlike that of WT animals (n=6) (**Figure 4B**).

Next, we wanted to determine whether the failure to induce a shift towards high-PV was due to excessive inhibitory D2 receptor distribution in the PreL of LgDel+/- mice. So, we injected a specific D2 receptor antagonist, Eticlopride (1ug/side), in the PreL or dorsal hippocampus of WT and LgDel+/- mice. We observed a complete but transient rescue (up to 48h post injection) of the PV distribution in LgDel+/- mice

resulting in a high-PV / low-PV neuron proportions similar to WT animals at baseline while WT animals showed no alteration of their PV network state (n=6 each) (**Figure 4C**). To see if the transient rescue with D2 receptor antagonism also recued normal functioning of the PV network, we first injected Eticlopride in the PreL of Lgdel+/-: PV-Cre and only PV-Cre mice followed by chemogenetic stimulation of the PV network 6hours later. Pre-treatment with the drug enabled a complete shift of the Parvalbumin network to a high-PV state in the Lgdel+/- mice; comparable to age matched PV-Cre controls (**Figure 4C**) (n=6). However, this rescue was transient, as when checked 48 hours later, the PV network had shifted back to the pathological low-PV state (**Figure 4C)**. To see if a similar transient rescue could be mediated using a clinically approved drug, we substituted Eticlopride with Haloperidol (120ng/side), a clinically approved drug used to manage psychotic breaks. Haloperidol treatment also rescued the PV network in Lgdel+/- mice to WT baseline and lead to a normal high-PV shift on subsequent chemogenetic stimulation (n=6) (**Figure 4D**). To see if the transient rescue of the PV network also have a behavioral effect we evaluated the LgDel+/- mice in a contextual fear conditioning protocol (cFC). On fear memory retrieval the next day, Lgdel+/- mice freeze like their WT counterparts (n=6 each). However, when tested 7 days post fear conditioning these animals show poor retrieval of the fear memory. In contrast, when LgDel+/- mice are pre-injected with Haloperidol 6 hours before fear conditioning they show a rescue of the freezing behavior when tested 7 days later (**Figure 4E**). Taken together, these results suggest that the low-PV state as observed in LgDel+/- animals could be a consequence of excessive inhibition on the parvalbumin cells through overexpression of D2 receptors and an acute pharmacological inhibition of these receptors lead to normal learning.

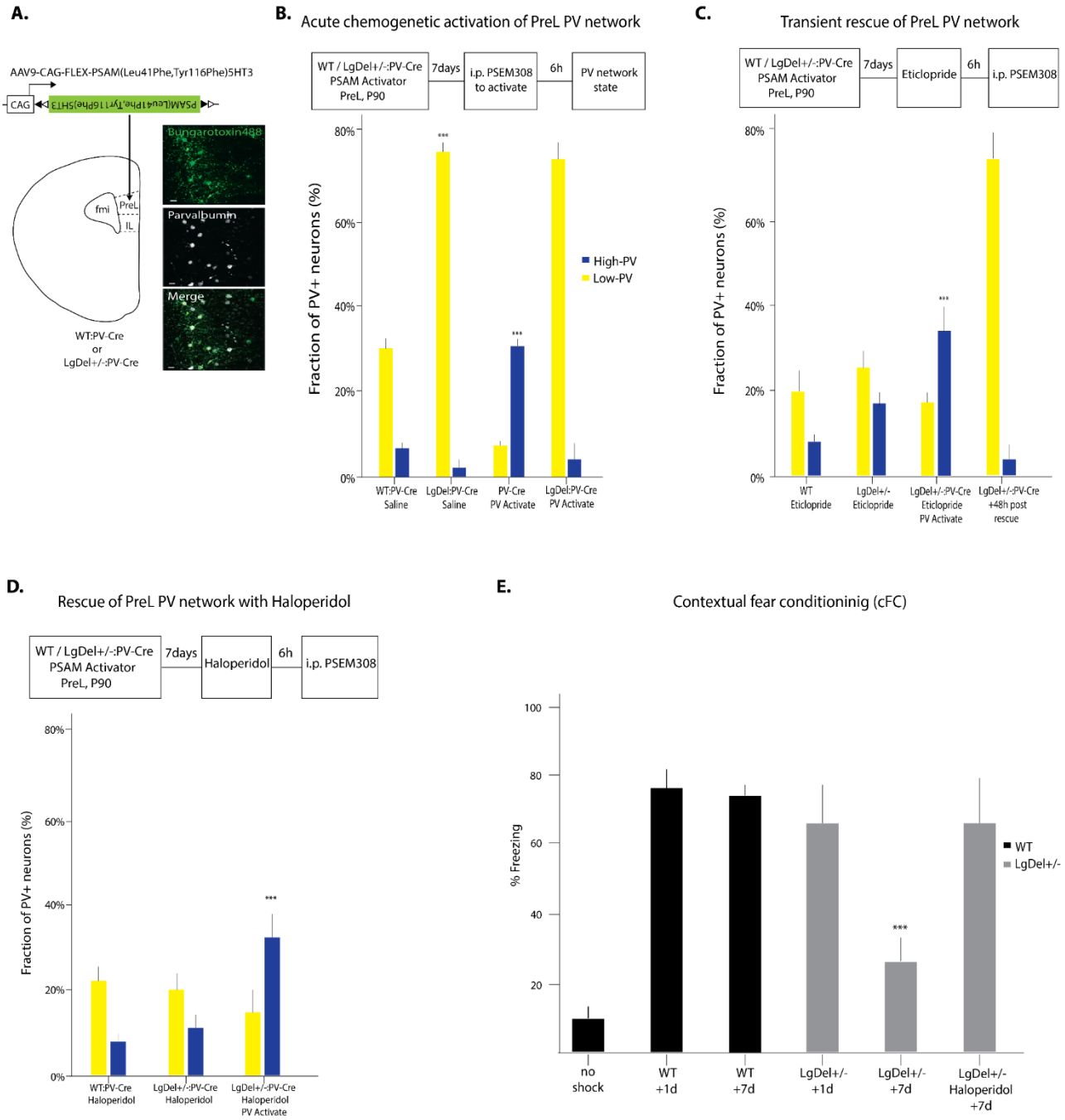

Figure 4: PV neuron phenotype is a property of their network configuration. (A) Left: Schematic representation of chemogenetic stimulation of PV network. A FLEXed AVV bearing an activating PSAM LGIC is bilaterally injected in the PreL of WT:PV-Cre or LgDel+/-:PV-Cre animals. After virus expression PSEM308 is injected i.p. to activate the PSAM LGIC and in turn the infected neuron. Right: Example labelling, where Bungarotoxin-488 (green) marks the cells expressing PSAM. PV neurons are immunolabelled in while and show a complete overlap with green showing specific infection of PV neurons. Scale: 20um. **(B)** Acute stimulation of PreL PV neurons by a single delivery of PSEM308 induce a high-PV shift in WT:PV-Cre animals, 6h post stimulation (n=6). This fails to induce a high-PV shift in LgDel+/-:PV-Cre animals (n=6). **(C)** Topical bilateral delivery of a specific D2 receptor antagonist, Eticlopride, shifts the increased low-PV state in LgDel+/- animals to WT baseline within 6h post injection. Chemogenetic stimulation of the PV network post Eticlopride injection induces a high-PV shift in LgDel+/- animals. The PV network in LgDel+/- mice revert to the increased low-PV state by 48h

post injection (n=6). **(D)** Haloperidol induces a transient high-PV state like Eticlopride (n=6). **(E)** Transient rescue of the PreL PV network in LgDel+/- mice allows normal learning of cFC comparable to WT animals (n=6). ***p<0.0001; analyzed using two-tailed t-test, compared between WT and Lgdel+/- groups for all measures.

A sensitive window for long-term rescue of PV network state in LgDel+/- mice.

To better understand the etiology of the PV dysfunction in Lgdel+/- mice we looked at plasticity and maturation of the PreL PV network. We used immunohistochemistry to analyze the baseline expression of PV in the PreL at ages P30, P45, P55, P60, P90 and P120 (n=4 each age and genotype). Young P30 WT animals showed 68% of cells in the low-PV state, suggesting a still maturing PreL, which reduced to 59% by P45 and finally by P55, the PreL parvalbumin network transitioned into a stable adult baseline state of 30% low-PV. (**Figure 5A**). Similar to WT, P30 LgDel+/- animals also showed that 70% of the PV+ neurons in the PreL are initially in the low PV state. However, contrary to WT, LgDel+/- animals remained in this low-PV state even at P60 and beyond (**Figure 5A**). Therefore, suggesting that, in Lgdel+/- the PreL PV network fails to mature like WT animals. In a different set of experiments, we subjected animals of age P40, P60, P90, P120 and P180 to an environment enrichment protocol (EE), which has been used previously to induce plasticity in the brain. In response to EE hippocampal and cortical areas usually induce a low-PV network state which facilitates new learning (Donato, 2013). However, unlike other areas EE could only induce a low-PV state in the PreL when done at the ages of P40 and P60 (**Figure 5B**). EE at older ages (P90 and above) failed to induce a low-PV state in the PreL although low PV induction could be seen in the ACC or motor cortex (M1) (**Figure 5B**).

In human schizophrenic patients, the first episode of psychosis (FEP) usually occurs in early adulthood. Since the PV network in mice reaches an adult like configuration at P60 and shows experience dependent plasticity only around P60, we decided to target this age for a long-term rescue strategy for the PreL PV network in LgDel+/- mice. We used our previously described chemogenetic approach to chronically stimulate the PV network over multiple days. We expressed the PSAM activator channel in the PreL PV neurons of LgDel+/-:PV-Cre and WT:PV-Cre animals (n=6 each) and stimulated the PV network once daily for 10 days between P60-70 with i.p.

delivery of the ligand PSEM308. The treated mice were left undisturbed in their home cages until P120, where they were sacrificed to assess baseline PV network state. When done in the PreL, daily stimulation over these 10 days resulted in a rescue of the LgDel PV network to a WT adult baseline state (30% low PV) (**Figure 5C**). WT PV-cre mice showed normal baseline PV network state compared to saline injected controls (**Figure 5C**). Surprisingly, this rescue lasted up to 6 months beyond the treatment window (last time point evaluated) (**Figure 5C**). Moreover, the rescue targeted to PreL also rescued the PV network in the IL, dH and vH (**Figure 5D**).

To verify if the rescue of PV levels as observed by immunochemistry also resulted in a functional rescue of the PreL network, we looked at baseline gamma oscillations in freely exploring mice. We found that chronic stimulation of the PreL PV network restored the baseline low power of high gamma oscillations in Lgdel+/- mice to the WT state, when tested at P120 (**Figure 5E**). Preceding results have shown that a D2 receptor antagonist (Eticlopride or Haloperidol) could transiently (48hrs) rescue the PV network state in LgDel animals to WT state. Thus, we hypothesized that chronic delivery of Haloperidol between P60-70 to PreL could also result in long-term rescue of the PV network and behavioral deficits. We bilaterally cannulated the P60 mice in the PreL (n=6) and injected Haloperidol (0.1ug/side) once every alternate day over the P60-P70 window. Similar to the chemogenetic stimulation, Haloperidol also mediated a long-term rescue of the PV network state up to 6 months post treatment (**Figure 5F**).

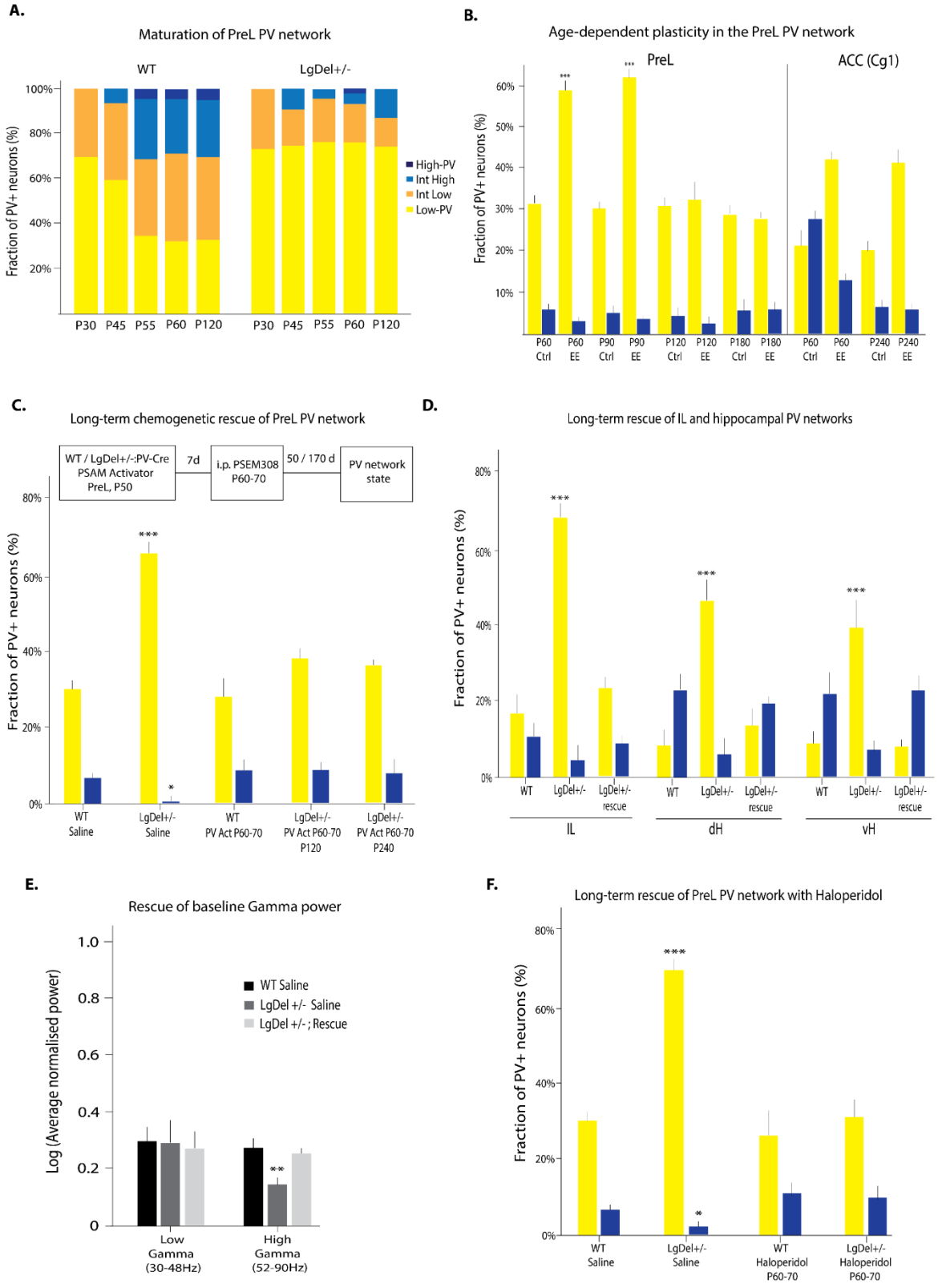

Figure 5: A sensitive window for long-term rescue of PV network state in LgDel+/- mice. (A) Immature PV neurons in WT animals show low levels of PV in the PreL. With increasing age the PV intensities increase and stabilize at 30% low-PV by P60. The PreL PV network of LgDel+/- animals fail to show an age dependent shift in PV intensities and continue to have 70% low-PV at P60 and beyond (n=4 each age and genotype). **(B)** Wild type animals show age dependent plasticity of the PreL PV

network where environmental enrichment can induce a low-PV shift only around P60 and not beyond (P90 onwards) (n=6). **(C)** Repeated chemogenetic stimulation of the PreL PV network in LgDel+/- animals over 10 days between P60-70 normalized the PreL PV network and maintains it long term, P240 (n=6). **(D)** Chronic stimulation of PreL PV network also rescues the PV network in IL, dH and vH. **(E)** Reduced baseline power in the high gamma band as seen in LgDel+/- animals is restored post chronic stimulation of PreL PV network (n=6). **(F)** Chronic delivery of Haloperidol in the PreL between P60-70 also restores the pathological low-PV state in LgDel+/- animals to a WT baseline and maintained it long term (n=6). *p<0.01; **p<0.001; ***p<0.0001; analyzed using two-tailed Students T-test, compared between WT and Lgdel+/- groups for all measures.

Therapeutic rescue of PV network state also ameliorates behavioral deficits in LgDel+/- mice.

Next, we checked if our long-term rescue strategy also shows therapeutic benefits in the cognitive deficits seen in LgDel+/- mice. We first tested performance in the social recognition test (SRT). LgDel+/- animals, which underwent our long-term rescue treatment, improved their performance in their recognition of a familiar mouse (**Figure 6A**). We also assayed the performance of rescued animals in the CD phase and the rule following IDS stage of IEST in which untreated P120 LgDel+/- animals are deficient. Strikingly and in agreement with the PV network rescue, PreL treated animals also showed a long-term rescue in performance, which lasted up to 6 months post treatment (**Figure 6B**) (n=8). P120 WT PV-Cre animals, which underwent chronic stimulation of the PreL PV network at P60-70, showed no observable changes in performance compared to saline injected controls (n=8) (**Figure 6B**). Furthermore, Haloperidol (120ng/side) injected through bilateral cannulas in PreL at P60 to 70 also rescued behavioral performance in SRT as well as the CD and IDS phases of IEST (**Figure 6C, D**) up to 6 months post treatment. Finally, systemic (i.p.) Haloperidol injections (0.1ug in 300ul of sunflower oil) once every alternate day between P60 to 70 also rescued behavioral performance in IEST (**Figure 6E**). Haloperidol treatment in WT animals, i.p. or through targeted cannulations does not result in observable behavioral performance (**Figure 6C, D**). Therefore, our chemogenetic and

pharmacological therapeutic strategy provides long-term cognitive benefits to LgDel+/- animals.

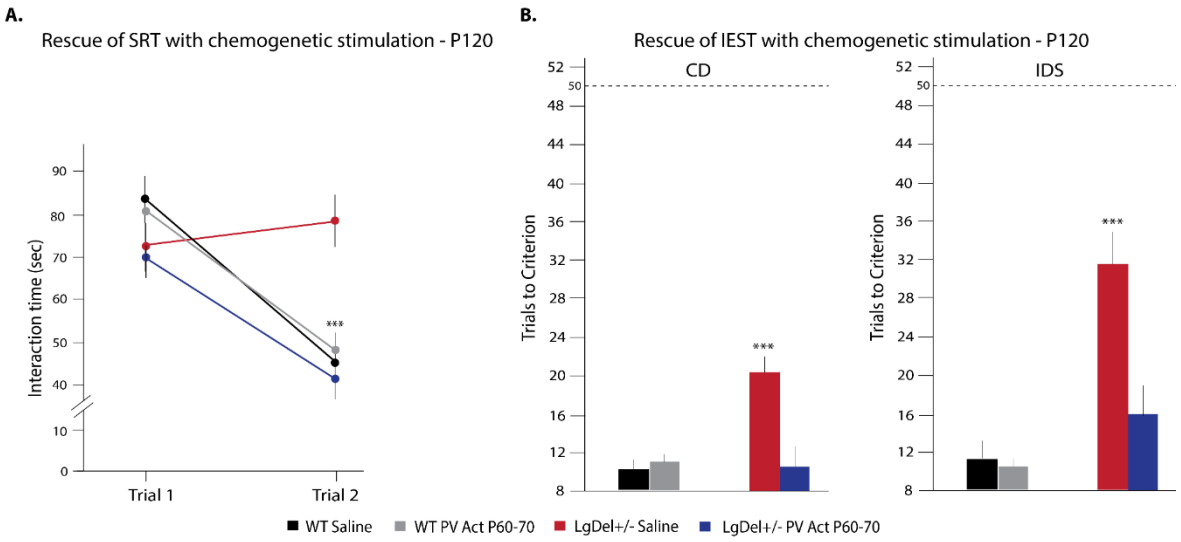

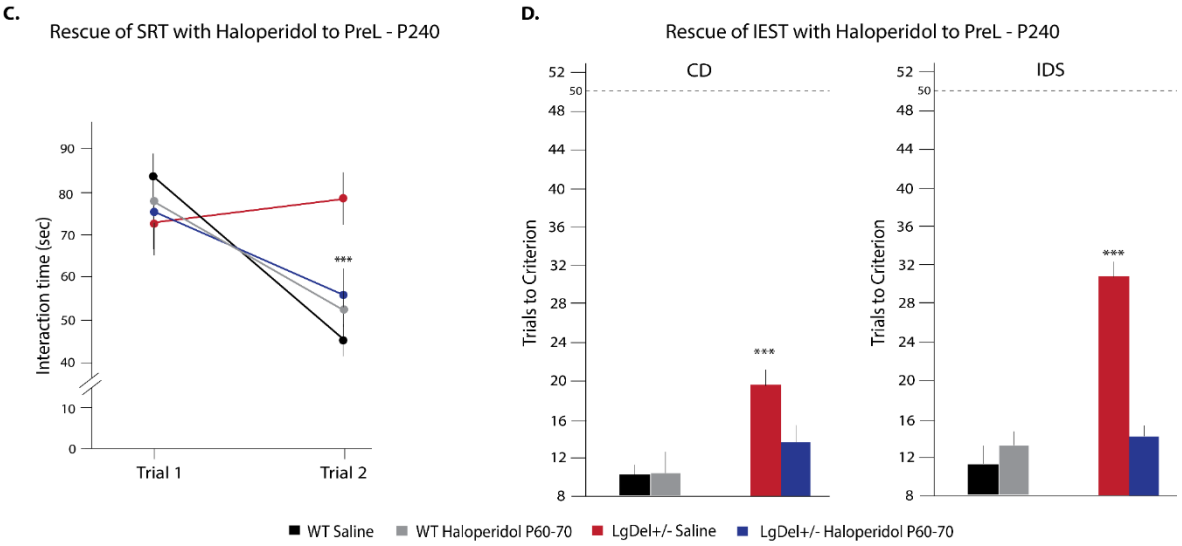

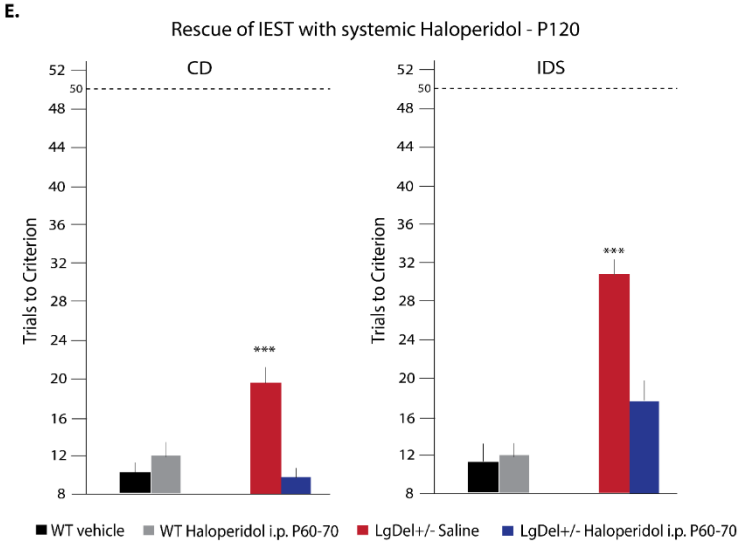

Figure 6: Therapeutic rescue of PV network state also ameliorates behavioral deficits in LgDel+/- mice. (A) Long-term rescue of the PreL PV network also normalizes performance of LgDel+/- mice in the social recognition memory task (n=6). **(B)** Chronic PreL PV network stimulation at P60-70 also rescues performance in IEST in P120 LgDel+/- animals (n=8). **(C)** Repeated Haloperidol delivery in the PreL of LgDel+/- mice between P60-70 also rescues performance in SRT long-term (n=6). **(D)** Haloperidol mediated long-term rescue improves performance of LgDel+/- animals in the IEST task (n=6) **(E)** Systemic delivery of Haloperidol between P60-70 also mediates long term rescue of LgDel+/- mice in the IEST task (n=6). ***p<0.0001; analyzed using two-tailed t-test, compared between WT and Lgdel+/- groups for all measures.

Functional rescue of PV network state and behavior in LgDel mice works through vH-PreL Axis

Previous research has shown that the vH-PreL axis, which is monosynaptically connected from the vH to the PreL, is important for spatial working memory and is dysfunctional in a mouse model of Schizophrenia homologous to the LgDel model (Sigurdsson et al., 2010). Thus, we tried to see if the PV network function and cognitive dysfunction in LgDel+/- mice could be also rescued through the ventral hippocampus. Using our chemogenetic strategy, we stimulated the vH PV network in Lgdel+/-:PV-Cre mice from P60-70. Chronic stimulation of the vH PV network at P60-70 led to a long-term rescue of PV (P120) network state in both PreL and vH (n=6) (**Figure 7A**). Additionally, low baseline power of high gamma oscillations in the PreL was also restored to WT levels (**Figure 7B**). Finally, the treatment also improved performance in the SRT task (**Figure 7D**) and the CD and IDS phases of the IEST task (**Figure 7C**).

Next, we wanted to see if the behavioral rescue required a rescue of the vH-PreL axis. We used two different chemogenetic constructs, which are activated by different ligands, to simultaneously silence (Gi DREADD; Sternson and Roth, 2014) and active (PSAM activator) PreL and vH PV neurons respectively or vice versa. In the first experiment, the Gi DREADD was bilaterally injected in the PreL and the PSAM Activator was injected in the vH. By delivering the two ligands CNO and PSEM308 daily, between P60 to 70, we could simultaneously silence the PreL PV network and activate the vH PV network. Additionally, CNO (2.5mg/100ml) was administered via drinking water to ensure complete silencing of the PreL PV network for the entire

duration of the treatment. When the treated LgDel+/-:PV-Cre mice (n=6) were tested at P120 in the ID/ED task, we found no improvement in behavioral performance (**Figure 7E**). In a conceptually related experiment, we reversed the delivery of the two chemogenetic constructs in the PreL and vH of P50 LgDel+/-:PV-Cre and WT:PV-Cre mice (n=5 each). Again, with simultaneous delivery of CNO and PSEM308 we could do the reverse experiment and silence the vH PV network while stimulating the PreL PV network. This treatment too led to no improvement in the behavioral performance of treated LgDel+/-:PV-Cre mice (**Figure 7F**). Therefore long-term cognitive rescue in LgDel+/- animals require a rescue of the entire vH-PreL axis.

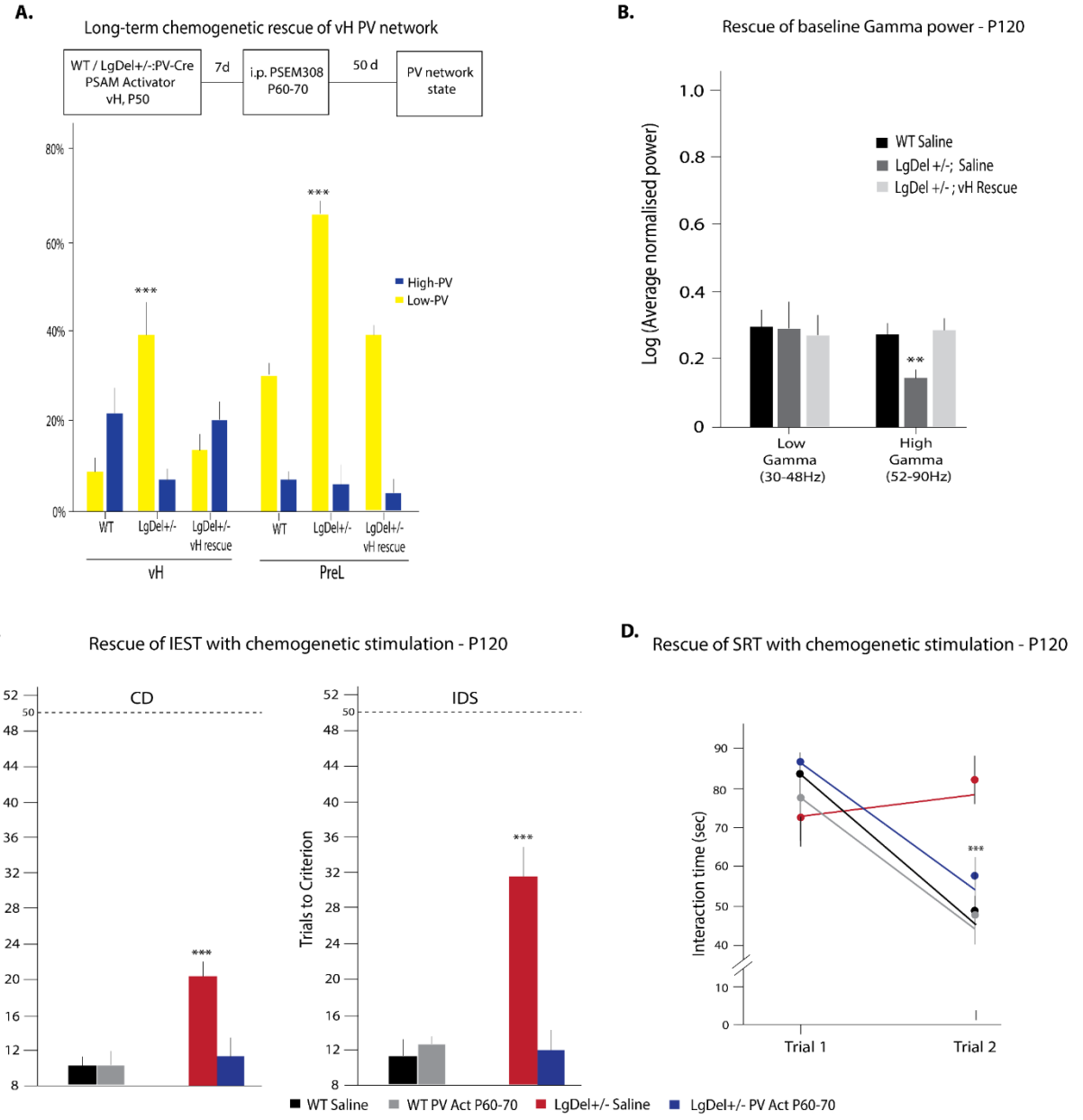
A.
Long-term chemogenetic rescue of vH PV network
WT / LgDel+/-:PV-Cre
PSAM Activator
vH, P50
7d
i.p. PSEM308
P60-70
50 d
PV network state
80%
60%
40%
20%
0%
***
***
High-PV
Low-PV
WT
LgDel+/-
LgDel+/- vH rescue
WT
LgDel+/-
LgDel+/- vH rescue
vH
PreL
B.
Rescue of baseline Gamma power - P120
Log (Average normalised power)
1.0
0.8
0.6
0.4
0.2
0
**
WT Saline
LgDel +/-; Saline
LgDel +/- ; vH Rescue
Low Gamma (30-48Hz)
High Gamma (52-90Hz)
C.
Rescue of IEST with chemogenetic stimulation - P120
CD
IDS
Trials to Criterion
52
50
48
44
40
36
32
28
24
20
16
12
8
***
***
WT Saline
WT PV Act P60-70
LgDel+/- Saline
LgDel+/- PV Act P60-70
D.
Rescue of SRT with chemogenetic stimulation - P120
Interaction time (sec)
90
80
70
60
50
40
10
0
***
Trial 1
Trial 2
E.
Failed Rescue of IEST with PreL PV network silenced
IDS
Trials to Criterion
52
50
48
44
40
36
32
28
24
20
16
12
8
***
WT Saline
WT PV Act P60-70
LgDel+/- Saline
LgDel+/- PV Act vH P60-70
PV Inh PreL P60-70
F.
Failed Rescue of IEST with vH PV network silenced
IDS
Trials to Criterion
52
50
48
44
40
36
32
28
24
20
16
12
8
***
WT Saline
WT PV Act P60-70
LgDel+/- Saline
LgDel+/- PV Act PreL P60-70
PV Inh vH P60-70

Figure 7: Functional rescue of PV network state and behavior in LgDel mice works through vH-PreL Axis. (A) Chronic chemogenetic stimulation of the vH PV network within the sensitive period also rescues the PV network in both vH and PreL (n=6). **(B)** Baseline power of high gamma oscillations are restored in LgDel+/- mice post vH PV network stimulation. **(C)** Performance in IEST task is also rescued post-therapeutic rescue of vH PV network. **(D)** Performance in SRT task is restored in Lgdel+/- mice post chemogenetic therapeutic rescue of vH PV network. **(E)** Chemogenetic rescue of the vH PV network fails to mediate behavioral rescue if the PreL PV network is silenced in the entire duration of stimulation (n=5). **(F)** Chemogenetic rescue through the PreL PV network fails if the vH PV network is silenced during the stimulation window (n=5). **p<0.001; ***p<0.0001; analyzed using two-tailed t-test, compared between WT and Lgdel+/- groups for all measures.

Characterizing the sensitive window for rescue in Lgdel mice - Time of rescue and dosage

To further define the length of the treatment window that could still successfully effect a rescue we stimulated the PreL PV network of LgDel+/- mice for 10 days at other ages before and after P60-70. Specifically, we stimulated the PV network in the PreL between the ages of P75-85, P120-130 and P180-190 (n=6 for each window). None of these treatment windows were able to mediate a rescue of IEST performance when tested 50 days post treatment (**Figure 8A**). In addition, i.p Haloperidol treatment between P45-55 and P120-P130 (n=5, each treatment window) also failed to mediate any behavioral rescue in LgDel+/- animals (**Figure 8B**).

Lastly, we calibrated the minimum number of days of treatment required, within this P60 to 70 window, for a long-term rescue. We performed 4 days of chemogenetic stimulation of the PreL PV network between P60-63 or P67-P70 in LgDel+/-:PV-Cre mice (n=6, each window). Both stimulations failed to mediate any rescue (**Figure 8C**) in the IDS phase of the IEST task. On the other hand, 6 days of chemogenetic stimulation of PreL PV network between P60-P65 or P65-P70 in LgDel+/-:PV-cre mice mediated behavioral rescue indistinguishable from a P60-P70 rescue (**Figure 8E**) (n=6, each window). Thus, the sensitive window for PreL mediated rescue is very narrow and located within P60 to P70 and requires a minimum of 6 days of treatment.

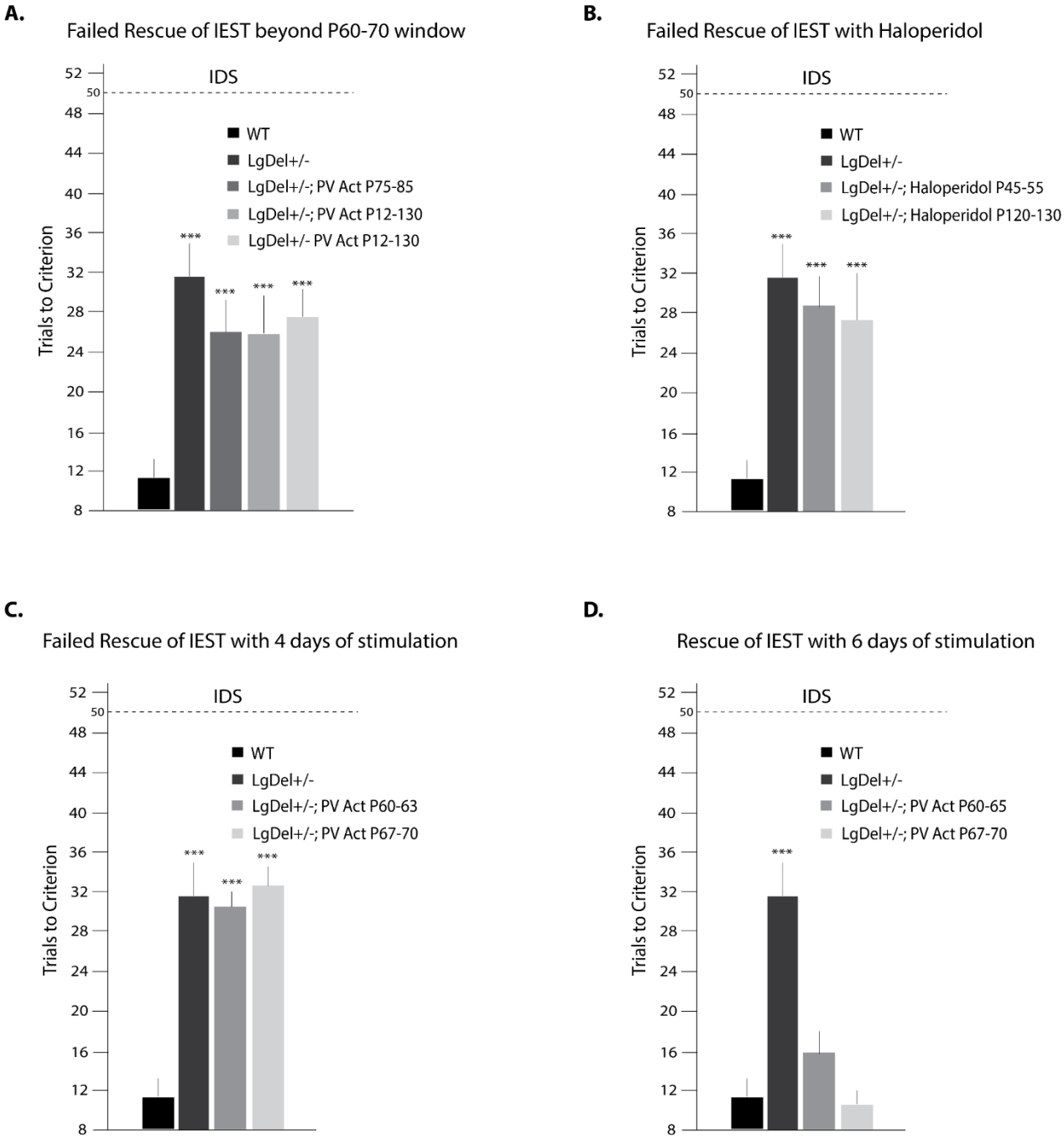

Figure 8: Characterizing the sensitive window for rescue in Lgdel mice - Time of rescue and dosage. (A) Chemogenetic rescue of PreL PV network targeted at windows beyond P60-70 fails to rescue performance in IEST in LgDel+/- animals (n=6). **(B)** i.p. Haloperidol treatment between P45-55 or P120-130 fails to rescue performance of LgDel+/- animals in the IEST task (n=5). **(C)** Four days of chemogenetic stimulation of the PreL PV network fails to rescue performance in LgDel+/- mice (n=6). **(D)** Six days of stimulation of the PreL PV network is sufficient to result in a behavioral rescue in LgDel+/- mice (n=6). ***p<0.0001; analyzed using two-tailed t-test, compared between WT and Lgdel+/- groups for all measures.

Discussion

In this study, we have investigated the Parvalbumin interneuron network and cognitive deficits in the 22q11.2 deletion mouse model of schizophrenia. We have revealed the existence of a therapeutic window around early adulthood in which modulation of the PFC and hippocampal PV network can lead to long-term amelioration of cognitive deficts and a rescue of the PV interneuron network. Specifically, our results show a dramatic shift towards increased fractions of low-PV/GAD67 neurons in the PFC and hippocampus of LgDel+/- mice. However, the density of PV neurons themselves remain unaffected. The deficit in PV expression is reflected in aberrant baseline power of gamma oscillations in the LgDel+/- animals. We also show that the increased low PV fractions seen in adult LgDel+/- animals have a neurodevelopmental origin where the PV neurons in LgDel+/- fail to increase their Parvalbumin content with maturation. In parallel, the LgDel+/- animals have severe deficits in PFC and hippocampus dependent cognitive tasks such as the Intra-dimension/Extra-dimension set shifting task and Social recognition memory task. Our results show that the PV network in the Prelimbic cortex exhibits a sensitive period of increased plasticity at early adulthood. Finally, direct stimulation of the PV network or D2R antagonism within this sensitive period can rescue the PV network deficits in LgDel+/- mice and rescue performance in cognitive tasks. Remarkably, this rescue lasts for months post treatment thus providing a therapeutic window and translational strategy for long-term amelioration of the cognitive symptoms of schizophrenia.

Significance of PV network dysfunction in LgDel+/- animals.

We show that Lgdel+/- mice have a large increase in low-PV population in all prefrontal areas and the hippocampus but the density of PV neurons remain unaffected. Our findings also show that the deficit in PV expression in LgDel+/- animals is restricted to a subpopulation of PV neurons, which are born early in life and normally express high levels of PV. Previous studies from our group has shown that the early-born subpopulation (E9.5-E11.5) is regulated by excitation and is required for completion of learning. Consistent with our findings a decreased expression of PV mRNA and protein but not the number of Parvalbumin interneuron themselves has been observed in the dorsolateral prefrontal cortex of human schizophrenic patients (Lewis et al.,

2012; Hashimoto et al., 2003). Human patients show further dysfunctions of the PV network, namely reduction of PV immune-reactive terminals onto pyramidal neurons (Lewis et al., 2001), reduction in the mRNA of $GABA_A$ receptor α1 and β2 subunits in pyramidal neurons (Beneyto et al., 2011; Akbarian et. al., 1995). This change in PV expression is one of the most reproducible anatomical hallmark of the disease.

Functionally PV neurons play a critical role in generation of local gamma oscillations (Cardin et al., 2009; Sohal et al., 2009, Gulyas et al., 2010). Moreover, schizophrenic patients exhibit altered activation of the dlPFC (Minzenberg et al., 2009) and lower power of gamma oscillations (Cho et al., 2006; Minzenberg et al., 2010) during tasks that require cognitive control. Our results show that LgDel+/- animals have altered baseline power in the gamma range while other oscillations are unaffected (**Figure 2**). Interestingly, we see an age dependent change in baseline gamma-power in LgDel+/- animals where younger P60 animals show an increased baseline power of low gamma oscillations while older P120 (and above) animals have a reduction in baseline power in the high gamma range (**Figure 2B, C**). Increases in resting state or baseline gamma power similar to P60 LgDel+/- animals have been previously reported in studies on schizophrenia patients (Spencer et al., 2009, Mulert et al., 2010) as well as rodent models with deficits in interneuron function (Carlen et al., 2012; Del Pino et al., 2013). While the source of this increase remains unclear, one possibility could be altered firing of thalamic PV neurons, which project to the cortex and maintain tonic levels of excitation. Further studies in changes in resting state gamma power can provide us with novel insights in age dependent pathophysiology of the disease.

Animal models with targeted disruption of genes that play a crucial role in circuit integration and functioning of PV neurons in rodents, show cognitive symptoms and PV network deficits similar to those seen in schizophrenia (Fazzari et al., 2010; Hikida et al., 2007; Shen et al., 2008; Marin 2012; Wen et al.; 2010, Cho et al., 2016). In parallel, abuse of drugs like ketamine and phencyclidine cause dysfunctions in PV networks of humans as well as rodents. Both of these drugs are also known to cause psychotic breaks in human users and exacerbates the symptoms of schizophrenia (Frohlich and Van horn, 2014; Morris et al.; 2005; Lahti et al., 2001; Domino and Luby, 2012). Thus, impaired signaling by PV interneurons may form a convergent endpoint of genetic and environmental insults in schizophrenia. However, from animal models

of drug abuse or disruption of PV interneuron maturation and function it is unclear if the PV network deficits are cell intrinsic, i.e. dysfunction inherent to the neurons themselves or a consequence of altered circuit connectivity onto the PV neurons. Previous reports have seen an increased expression of D2 receptors in human patients with schizophrenia (Brisch et al., 2014). We hypothesized that a selective inhibition of these receptors might enable us to understand if the deficits in the PV network are cell intrinsic or not. An acute delivery of an antagonist of D2R receptor, Eticlopride or Haloperidol, transiently unmasks the altered baseline PV network baseline in LgDel+/- animals (**Figure 4C, D**). Remarkably, this treatment also allows a normal induction of a high-PV state on direct stimulation of the PV neurons as well as normal retrieval of fear memory 7 days post acquisition, which is deficient in LgDel+/- animals (**Figure 4D, E**). This suggests that the dysfunction in the PV network in LgDel+/- animals, and possibly in human schizophrenic patients, could be due to altered connectivity onto the PV neurons and modulation of these deficits can unmask normal functioning of the PV neurons, providing a basis for designing novel therapies towards schizophrenia. Currently distribution of the D2 receptors in neuronal subtypes in the prefrontal cortex or hippocampus of schizophrenia patients or rodent models do not exist. Future work directed at altered localization of these and other receptors onto PV neurons and their modulation will shed further light on this question.

Late maturation of the PreL PV network and a sensitive window for therapeutic rescue.

Our findings also reveal a late maturation of the PreL PV network in wild type animals where the levels of PV expression reach a stable state invariant across adulthood at P55 (**Figure 5A**) . This is in good agreement with a recent study in the rat PFC, which showed that the expression of PV increases across adolescence and stabilizes to adult levels by P50 (Caballero et al., 2014). This study also showed a specific increase in glutamatergic inputs originating in the ventral hippocampus and impinging onto PV neurons in the mPFC around P50 and a corresponding increase in local GABergic activity (Cass et al., 2014). This suggests a possibility that the developmental maturation of the mPFC PV network occurs in late adolescence through increased activity drive from the vH onto the mPFC PV neurons. Our results show that the PreL PV network in LgDel+/- animals fail to show an increase in PV expression in their

transition from adolescence to adulthood and continue to express low levels of PV (**Figure 5**), thus suggesting a neurodevelopmental origin of the disorder in LgDel+/- mice. Furthermore, we also saw that the PreL PV network, in wild type animals, has a brief window of experience dependent plasticity upto P60 where environmental enrichment can induce a low-PV state. Surprisingly, adult wild type animals (P90 and above) fail to show this plasticity in the PreL PV network although other cortical areas continue to show PV network plasticity at older ages. Hence, we hypothesized that targeting the PreL PV network in LgDel+/- mice in this sensitive period for direct chronic stimulation might result in a potential rescue. Indeed, chronic stimulation over ten days between P60-70 rescues the LgDel+/- PV network to WT levels which also persists long-term. Remarkably, it also rescues the PV network in distal areas such as the IL, dorsal and ventral hippocampus as well as deficits in resting state gamma power. Moreover, this treatment mediates long-term rescue of performance in hippocampal and prefrontal tasks (**Figure 6**). In human schizophrenic patients, the first episode of psychosis usually manifests around early adulthood. Thus, our therapeutic strategy has an exciting potential for translation to human patients, using non-invasive procedures like transcranial magnetic stimulation (TMS) (George and Post, 2011). In parallel, chronic D2R antagonism during this sensitive window with a clinically approved drug, Haloperidol, also rescued the PV network and behavioral deficits in LgDel +/- mice. Again, this opens up the possibility for a conventional drug based therapy to ameliorate cognitive deficits in human schizophrenic patients. However, our results show that the window of opportunity for rescue is very narrow, between P60-70 and our strategies fail to induce any rescue at later ages. Recent studies have shown that HDAC inhibitors like Valproate can reopen critical period of learning in adult humans (Gervain et al., 2013). Thus, our rescue strategy in combination with such drugs could possibly also ameliorate PV network phenotypes and cognitive performance in older patients beyond the first episode of psychosis. Finally, basic and translation research in this direction could potentially make the cognitive deficits in schizophrenia curable in the near future.

vH-mPFC axis is central to long-term rescue

The hippocampus and the prefrontal cortex are two major seats of learning in the brain and are monosynaptically connected by projections originating in the ventral hippocampus (Vertes et al., 2004; Thierry, 2010). In recent years synchronous activity between the hippocampus and prefrontal cortex has emerged to play a central role in cognitive tasks (Kesner and Churchwell, 2011, Benchenane et al., 2011; Harris and Gordon, 2015; Spelmann et al., 2015). Furthermore, previous research on LgDel+/- animals have also shown a specific deficit in synchrony in the hippocampus-mPFC axis during a spatial working memory task (Sigurdsson et al., 2010). Consistent with these results we saw that long-term rescue of the PreL PV state in LgDel+/- can be mediated through direct stimulation of the vH PV network. This treatment also rescues resting state gamma deficits and cognitive defects in LgDel+/- animals. However if the PreL PV network is silenced during vH stimulation no cognitive rescue is seen. This also holds true for the reverse case where the PreL PV network is stimulated while the vH PV network is silenced. Thus suggesting that long-term rescue of the PV pathology and cognitive deficits in LgDel+/- animals requires a rescue of the hippocampal-prefrontal axis.

In more general terms, our results highlight a sensitive period for long-term rescue of PV dysfunction and cognitive phenotypes in LgDel+/- animals through the hippocampal-prefrontal axis. We also provide therapeutic strategies, which can be translated to ameliorate the cognitive symptoms of the disease in human patients.

Supplementary Figures:

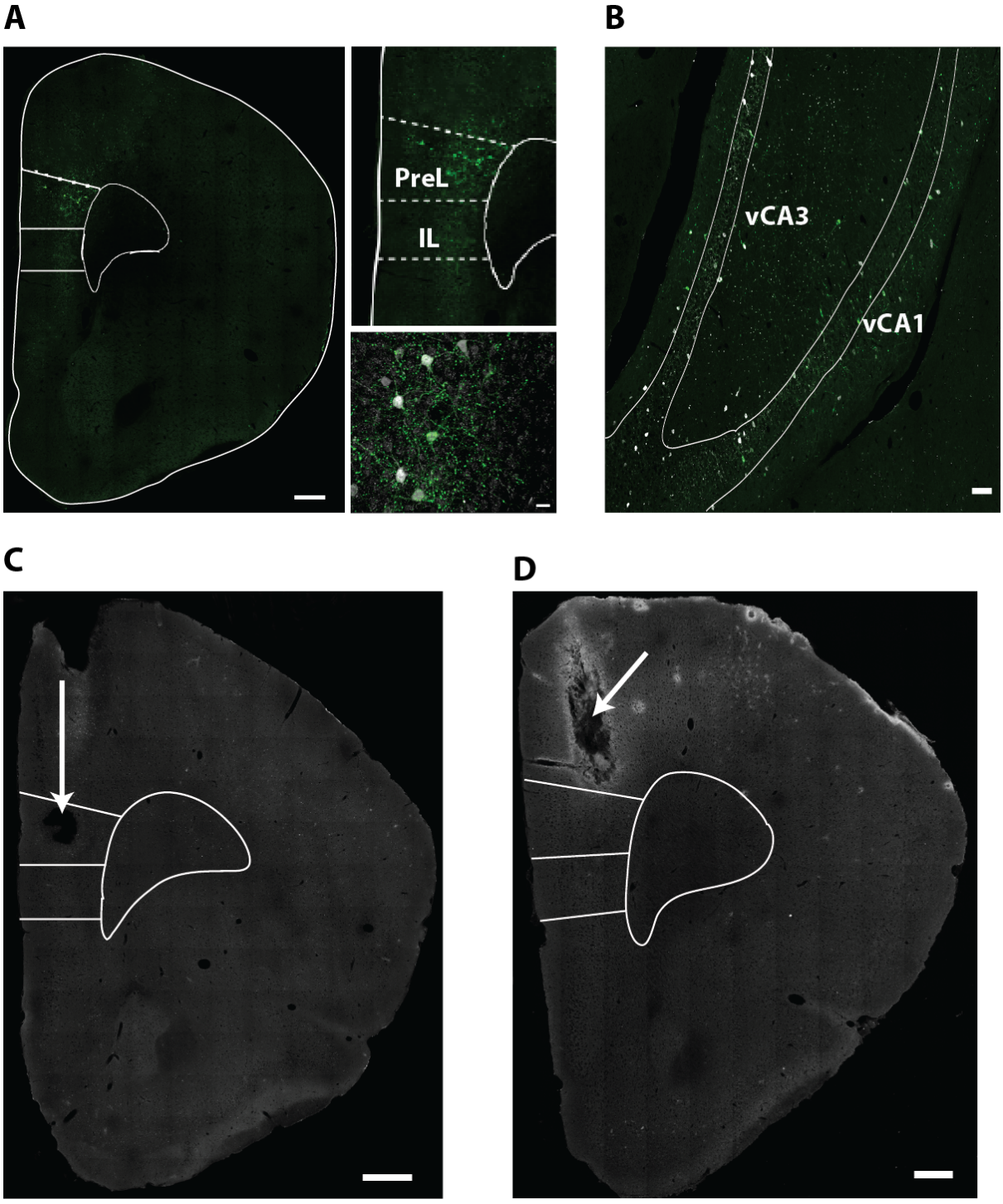

Figure S1: (A, B) Representative images for delivery to PreL (left) or vH (right) of Cre-dependent AAV9-pharmacogenetic activator in LgDel+/-:PV-Cre mice. Bungarotoxin tagged with an Alexa488 dye is used to label the PSAM channels (green) while Parvalbumin is immunostained in white. Bars: 300 (overviews), 30 (insets) μm. **(C)** Representative image of electrode location in the PreL. Arrow marks location of the lesion made with an anodal current post experiment. Bar: 400 μm. **(D)** Representative image of canula tract for chronic injection of Haloperidol. Arrow marks the guide canula track, which ends right above the Prelimbic. Bar: 300 μm.

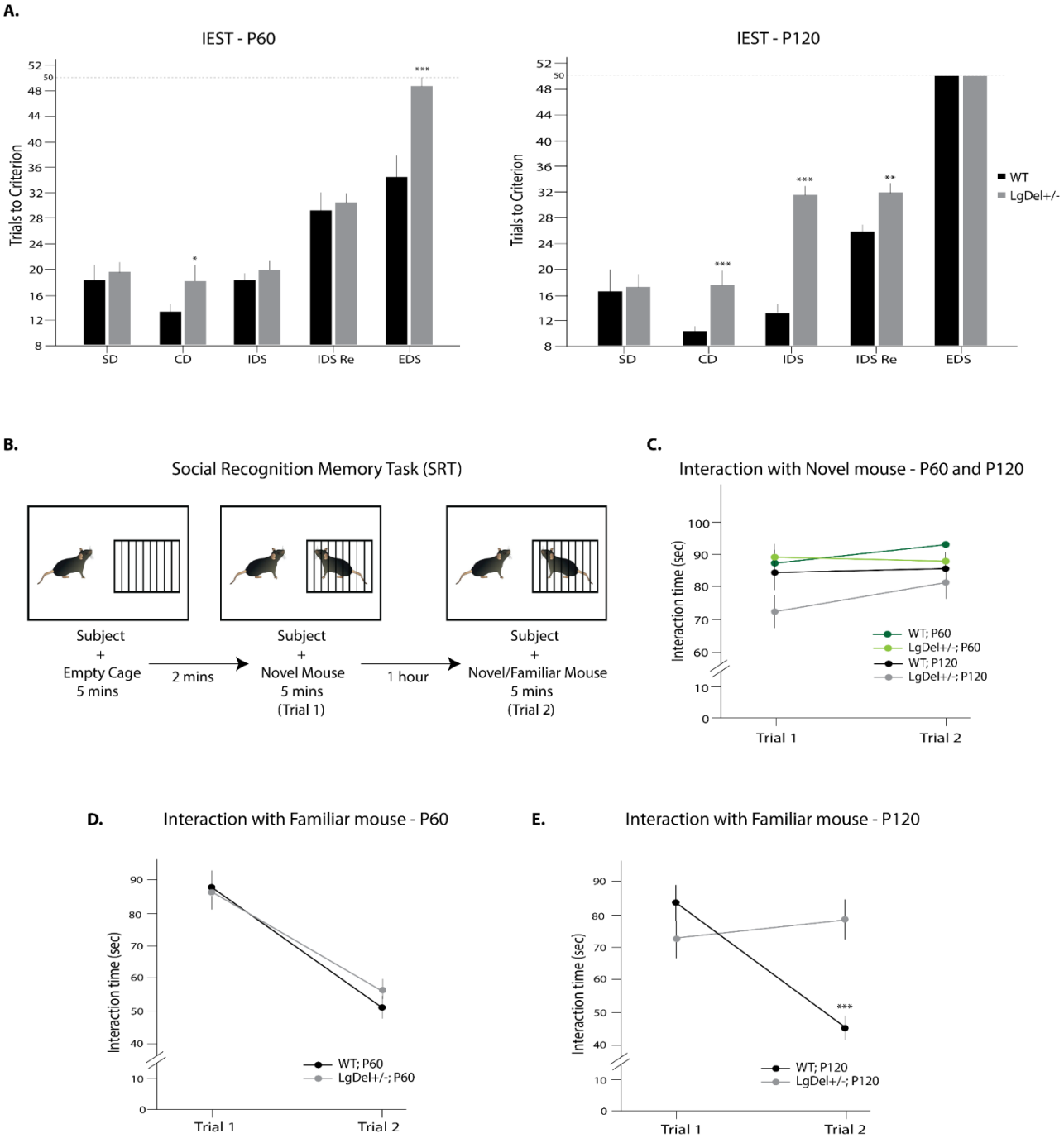

Figure S3: (A) LgDel+/- animals of both ages (P60 and P120) continue to have same age specific deficits in the IEST task when the odor and texture dimensions are flipped across the different task phases showing no bias across sensory modalities (n=4). **(B)** Schematic representation of the social recognition memory task. The subject animal is first exposed to an empty cage (10cmX10cmX10cm) in which an age and gender matched novel mouse is going to be enclosed allowing sniffing and exploration but prevents fighting. After 5 minutes of habituation to the cage a novel mouse is introduced in the cage for exploration by the subject mouse. 1 hour post this exploration a second novel mouse or the previously explored familiar mouse is reintroduced to check for social recognition memory (see methods). **(C)** LgDel+/- mice of both ages show normal exploration of the novel mouse, comparable to WT animals, when encountered in both the trials (n=6). **(D)** P60 LgDel+/- mice show a normal social

recognition memory and reduce their interaction time with a familiar mouse (n=6). **(E)** P120 mice show a deficit in social recognition memory and do not reduce their interaction time with the familiar mouse on trial 2 (n=6).*p<0.01; **p<0.001; ***p<0.0001; analyzed using two-tailed t-test, compared between WT and Lgdel+/- groups for all measures.

Experimental procedures

Mice

PV-Cre mice were from Jackson laboratories (129P2-Pvalbtm1 (cre)Arbr/J) were a kind gift from S. Arber (Friedrich Miescher Institut). LgDel+/- mice (LgDel 129Sv/C57Bl/6/129SvEvTac/FVB/N/SJL) were a kind gift from Novartis Institute for Biomedical Research and were bred in house for 10 generations with C57Bl6/J mice (Janvier) to get a homogenous background. LgDel+/- PV Cre mice were generated in house by crossing the LgDel+/- line with the PV-Cre line. Mice were kept in temperature-controlled rooms on a constant 12h light-dark cycle, and all experiments were conducted at approximately the same time of the light cycle. Before the behavioral experiment, mice were housed individually for 3-4d and provided with food and water *ad libitum* unless otherwise stated. All animal procedures were approved and performed in accordance with the Veterinary Department of the Kanton Basel-Stadt.

Behavioral procedures

All experiments were carried out with male mice. At the onset of experiments, mice were precisely of the age (+/-2 days) as mentioned in the results.

Contextual fear conditioning experiments were carried out as described (Donato et al., 2013). Briefly, mice were allowed to explore the training context for 2.5min, and then received five foot shocks (1s and 0.8mA each, inter-trial interval: 30s). Control mice were subjected to the same procedure without receiving foot shocks. We assessed contextual fear memory by returning mice to the training chamber after fear conditioning during 5min, and analyzing freezing during a test period of 4min (first min excluded).

For Intradimension / Extradimension set shift task (IEST), mice were trained to dig in plastic food bowls, with an internal diameter of 40mm and a depth of 40mm and filled with wood chips, to retrieve a food reward buried at the bottom of the bowl. The reward was one-third of a Honey Nut Loop (Kellogg, Manchester, UK). The outer surface of the bowl was covered with a texture and the rim of the bowl was coated with an odor. The test apparatus was a rectangular Plexiglas box with panels that divided one-third of its length into two sections of equal proportions. The digging bowls were placed in these sections and two doors with independent access separated the mouse from the two sections where the bowls were placed. The doors could be slid open to give the mouse access to the food bowls or closed rapidly to prevent access to the other bowl after an error. The mice were food restricted from a day before the habituation phase till the end of the experiment. Each day, after the end of testing, mice were given access to 1g of a mash made of crushed food pellets mixed with water. The habituation phase consisted of 3 days; each day mice were given access to 2 bowls filled with wood chips and baited with reward. Mice were allowed to dig in both the bowls for the reward following which the bowls were re-baited for a second time. During test phases, trials were initiated by opening both doors simultaneously to give the mouse access to the two digging bowls, only one of which was baited. The first four trials were exploratory trials, where the mouse was allowed to dig in both the bowls and an error was recorded if the mouse dug first in the un-baited bowl. On subsequent trials access to the other bowl was occluded as soon as the mouse began digging in one of the bowls. A correct trial was recorded when the mouse dug in the baited bowl to collect the reward. A trial was terminated when the mouse dug in the correct bowl and collected the reward, or dug in the un-baited bowl and left the chamber. Testing continued until the mouse reached a criterion level defined as 8 correct trials out of the last 10 trials. IEST consisted of 5 testing sessions spread over five days, each involving a different type of discrimination. In simple discrimination the bowls differed along the odor dimension only. For compound discrimination a second dimension (textures) was introduced, but correct and incorrect odors remained constant. For intra-dimensional shift a new pair of odors and textures were introduced and the mouse had to learn a new odor-reward association using the odor rule learnt previously. For intra-dimensional shift reversal the odor and texture cues remained unchanged but the mouse had to learn that the previously correct odor-reward association was now incorrect and the previously incorrect odor now predicted reward.

Finally, for the extra-dimensional shift a new pair of odors and textures were introduced and the previously relevant dimension (odor) was now irrelevant whereas the previously irrelevant dimension (texture) now predicted reward. The order of the discriminations was always the same, but the dimensions and the pairs of cues were equally represented within groups and counter balanced between groups.

The social recognition test was adapted from Piskowrowski et al., 2016 (**Figure S3B**). Briefly, the subject animal is first exposed to a chamber (90cmx45cmx35cm; lbh) with an empty cage (10cmX10cmX10cm) which allows sniffing and exploration but prevents fighting. After 5 minutes of habituation to the cage and the behavioral chamber a novel mouse (age and gender matched) is introduced in the cage for exploration by the subject mouse for another 5 minutes. An hour post this exploration a second novel mouse or the previously explored familiar mouse is reintroduced for 5 minutes to check for social interaction or social recognition memory respectively. Interaction time was measured as a summation of all time intervals spent by the subject mouse in interacting with the novel/familiar mouse over the period of 5 minutes. Only those interactions which were initiated by the subject mouse were counted as true interactions.

Immunocytochemistry and histology.

Antibodies used were as follows: goat anti-PV (Swant biotechnologies, PVG-213) 1:5000; mouse anti-NeuN (Millipore, MAB377) 1:1000; α-Bungarotoxin, Alexa 488 Conjugate (Molecular Probes, Life Technologies, B-13422) Secondary antibodies were Alexa Fluor 488 (Molecular Probes; A150077), or 647 (Molecular Probes; A150131, A150107); 1:500. Prelimbic and Infralimbic were at +1.8mm to +1.95mm from bregma while VLO, Cg1/2, dH and vH were at +2.34mm, +0.9mm, +2.2mm and +2.9mm from bregma respectively. Samples belonging to the same experiment (for example, from the mice of a given time point, with their controls) were acquired in parallel and with the same settings on an LSM700 confocal microscope (Zeiss) using an EC Plan-Neofluar340/1.3 oil-immersion objective (Zeiss). For PV intensity analysis, the dynamic range was set during the acquisition of P60 cage control samples. PV neurons whose soma was included within the tissue sections with optimal staining (dampening of intensity between the first and last confocal plane <15%) were isolated

in 3D (Imaris 7.0.0, Bitplane AG). 3D isosurfaces were created around each PV neuron soma (smoothness: 0.5 µm; quality level: 5) and labeling intensities were quantified automatically in arbitrary units as the mean of all isolated pixels. We set the zero value at pyramidal neuron somas, and the highest treshold so that <20% of the pixels belonging to the brightest PV cells were saturated (ZEN2010 acquisition software, Zeiss). Normalization and recalibration across different experiments was achieved by using internal control animals, which were included in each experiment, and were processed using the same criteria mentioned above. A comparative analysis revealed a cluster of low PV intensities (threshold: 800 arbitrary confocal units (au) that were particularly abundant early during development (P35, PreL), and induced upon EE. The 800au threshold was adopted to classify PV neurons into four subclasses as follows; low-PV: 0-800au; intermediate-low: 800-1600au; intermediate-high: 1600-2400au; high-PV: >2400au.

In experiments involving injections with picospritzer or Hamilton needles or cannulations, brains were collected at the end of the experiments for histological analysis (**Figure S1D**). Serial slices were imaged at 10x or at 4x to locate the injection site and the extent of volume spread. To that end, all microinjections were controlled using a vital stain, Hoechst 33342 (Invitrogen, H3570) as a proxy for drug spread into the cells. All viral expression spread were controlled with α-Bungarotoxin staining for PSAM channel or mCherrry signal for the DREADDS (**Figure S1A, B)**. Occasional mice in which the injections had also targeted neighboring areas were excluded from the analysis.

Stereotaxic surgery:

All surgeries were conducted under aseptic conditions using a small animal stereotaxic instrument (David Kopf Instruments). Mice were anaesthetized with isoflurane (4% for induction, 1.5–2.0% afterward) in the stereotaxic frame for the entire surgery and body temperature was maintained with a heating pad. Local drug treatments were carried out with a 33-gauge needle coupled to a 5ul syringe (Hamilton, Reno, NV) while viruses were delivered using glass pipettes (tip diameter 10–20 µm) connected to a picospritzer (Parker Hannifin Corporation). Repeated drug injections were done through implanted cannulas. Guide cannulae (26G, with dummy

screw caps, Plastics One) were implanted bilaterally to inject below cortical surface. Implants were fixed to the skull with stainless steel screws and dental cement (Paladur, Heraeus). Mice were then given 1 week to recover from surgery. A 33G stainless steel injector attached to 5 µl Hamilton syringe was inserted into the guide cannulae to deliver the drug. Coordinates relative to bregma are as follows: PreL (anteroposterior (AP) +2.0mm, mediolateral (ML) ±0.5mm, dorsoventral (DV, relative to dura) -2.1mm); ventral hippocampus (AP -3.0mm, ML ±2.9mm, DV -3.5mm). For drug injections the needle was slowly lowered to 0.1mm beyond the required DV co-ordinate and quickly pulled up to the original co-ordinate to create a pocket for injection of the drug. This prevented backflow of the drug and undesirable spread into neighboring areas. Drugs were injected at the rate of 100nl/min to a final maximum volume of ~200nl. After completion of injection the needle was left in its place for 5 min to allow for diffusion of the drug and then slowly withdrawn. For virus injections the glass pipette was inserted at the desired co-ordinate and ~200nl of the virus preparation was slowly pressure injected using a picospritzer over a period of 10 min. After the end of the injection the pipette was left in its place for a further 10 min to allow for diffusion of the virus. All drugs and viruses were injected bilaterally in the PreL, IL, dH and vH. Post-surgical recovery was monitored daily until the start of behavioral protocols. All injections were paired with saline injected control animals to account for any effect due to tissue damage or surgical procedure.

Pharmacology in vivo

Drugs were used bilaterally as follows: Haloperidol (0.1ug/side prepared in buffered saline, Tocris). Haloperidol, dissolved in saline, was systemically injected at a dosage of 0.1mg/Kg (i.p.). For intra-cranial delivery to target regions at dosage of 70ng/side was used.

Pharmacogenetic in vivo

For acute or chronic activation of PV neurons , we bilaterally delivered floxed PSAM-carrying AAV9 (excitation, rAAV9-CAG-flox-PSAM(Leu41Phe,Tyr116Phe)5HT3-WPRE) in PV-Cre mice (Donato et al., 2013; Karunakaran et al., 2016; Magnus et al., 2011) in WT:PV-cre or LgDel+/-:PV-cre mice. To allow for transgene expression, mice

were kept under home cage conditions for 7-9d before any behavioral experiment. For chronic stimulation of PV neurons the PSAM agonist, PSEM308 was injected once daily (i.p.) at 5mg/kg of the weight of the animal. The corresponding ligand PSEM308 was injected once daily (5mg/Kg).

For chronic silencing of vH or PreL PV neurons in experiments involving vH-PreL axis we injected a FLEXed DREADD-carrying AAV8 (Sternson and Roth, 2014) (B. Roth, UNC Vector Core; silencing, rAAV8-AAV-hSyn-DIO-hM4D(Gi)-mCherry) bilaterally into vH or PreL. Selective activation of the DREADD receptor and corresponding silencing of the PV neurons was achieved by administering the DREADD agonist, clozapine-N-oxide (CNO; 5mg/kg, i.p, Tocris; Sternson and Roth, 2014) once daily (i.p.) at 5mg/kg of the weight of the animal. Post experiment brains were dissected and serial slices were imaged at 10x to verify correct neuron labelling using either the mCherry signal and staining for the PSAM channel with Bungarotoxin-488.

In vivo Recording with multi-wire electrode arrays:

Animals were anesthetized with isoflurane (induction 4%, maintenance 1.5%) in the stereotaxic frame for the entire surgery and body temperature was maintained with a heating pad. Mice were unilaterally implanted in the PreL (AP: +1.8mm from Bregma, ML: ±0.4 mm from midline, DV: 2.1mm from skull) with a multi-wire electrode. The electrodes consisted of 16 individually insulated nichrome wires (13 µm inner diameter, impedance 30–100 KΩ; Kanthal) contained in a 26 gauge stainless steel guide cannula (Plastics One). The wires were attached to an 18 pin connector (Omnetics). All implants were secured using dental cement (Paladur, Heraeus). After surgery mice were allowed 7 days to recover. Analgesia was applied before, and 1 day after surgery (Metacam, Boehringer). Electrodes were connected to a headstage (Plexon) containing 16 unit-gain operational amplifiers. The headstage was connected to a 16-channel preamplifier (gain 100x, bandpass filter from 0.7 Hz to 170 Hz for field potentials, Plexon).

Local field potentials (LFPs) from channels on which no obvious 50 Hz noise and movement artifacts could be detected and were analyzed using NeuroExplorer software (Plexon). LFP power spectrum density was calculated using Fast Fourier

Transformation (FFT) from the raw LFPs with a hanning window of 250 ms and no overlap. To calculate power of various oscillations of different frequencies, we used a measure of the relative power of the target oscillation (high Gamma: 52-80Hz, low Gamma: 30-48Hz, Theta: 4-10Hz, Beta: 15-30Hz) that corresponds to the ratio of power within the target band to the total power in the power spectrum (0 to 120 Hz) of the raw LFP. This analysis corresponds to a normalization procedure that produces a measure of gamma oscillations completely independent of the large fluctuations of LFP oscillations that can occur in individual animals. Post experiment position of the electrode array was marked by passing anodal current (15 μA for 30 s) through one of the wires (**Figure S1C**).

Statistical analysis

All statistical analyses were based on two-tailed comparisons and were done using GraphPad Prism (GraphPad software. Inc.). Results are presented as mean ± s.e.m. The sample size per group is mentioned in the respective figure legends. Number of animals to be used for a standard behavioral analysis was determined based on our preliminary behavioral experiments across different investigators in the laboratory. We paid particular attention to the magnitude of difference between groups tested apart from the statistical significance across groups. Data distributions were assumed to be normal but this was not formally tested. Male mice of closely comparable age were assigned randomly to experimental groups. Intensity analysis, freezing and interaction time data were verified by a co-worker blind to experimental conditions.

References

Akbarian, S. et al. (1995). GABAA receptor subunit gene expression in human prefrontal cortex: comparison of schizophrenics and controls. Cereb. Cortex 5, 550–560.

Amilhon B, Huh CY, Manseau F, Ducharme G, Nichol H, Adamantidis A, Williams S (2015). Parvalbumin Interneurons of Hippocampus Tune Population Activity at Theta Frequency. Neuron., 86(5):1277-89.

Arguello PA, Gogos JA (2010). Cognition in mouse models of schizophrenia susceptibility genes. Schizophr Bull., 36(2):289-300.

Benchenane K, Tiesinga PH, Battaglia FP (2011). Oscillations in the prefrontal cortex: a gateway to memory and attention. Curr Opin Neurobiol., 21(3):475-85.

Beneyto, M. et al. (2011) Lamina-specific alterations in cortical GABAA receptor subunit expression in schizophrenia. Cereb. Cortex 21, 999–1011.

Bissonette, G.B. Martins, G.J., Franz, T.M., Harper, E.S., Schoenbaum, G., and Powell, E.M. (2008). Double dissociation of the effects of medial and orbital prefrontal cortical lesions on attentional and affective shifts in mice. J. Neurosci. *28*, 11124-11130.

Brisch R, Saniotis A, Wolf R, Bielau H, Bernstein HG, Steiner J, Bogerts B, Braun K, Jankowski Z, Kumaratilake J, Henneberg M, Gos T (2014). The role of dopamine in schizophrenia from a neurobiological and evolutionary perspective: old fashioned, but still in vogue. Front Psychiatry., 5:47.

Caballero, A, Flores-Barrera, E, Cass, DK, Tseng, KY, (2014). Differential regulation of parvalbumin and calretinin interneurons in the prefrontal cortex during adolescence. Brain Struct. Funct., 219, 395–406.

Campbell LE, Azuma R, Ambery F, Stevens A, Smith A, Morris RG, Murphy DG, Murphy KC. (2010). Executive functions and memory abilities in children with 22q11.2 deletion syndrome. Aust N Z J Psychiatry., 44:364–371.

Cardin JA, Carlén M, Meletis K, Knoblich U, Zhang F, Deisseroth K, Tsai LH, Moore CI (2009). Driving fast-spiking cells induces gamma rhythm and controls sensory responses. Nature., ;459(7247):663-7.

Carlen, M., Meletis, K., Siegle, J.H., Cardin, J.A., Futai, K., Vierling-Claassen, D., Ruhlmann, C., Jones, S.R., Deisseroth, K., Sheng, M., et al. (2012). A criticalnrole for NMDA receptors in parvalbumin interneurons for gamma rhythm induction and behavior. Mol. Psychiatry 17, 537–548.

Cass, DK, Flores-Barrera, E, Thomases, DR, Vital, WF, Caballero, A, Tseng, KY (2014). CB1 cannabinoid receptor stimulation during adolescence impairs the maturation of GABA function in the adult rat prefrontal cortex. Mol. Psychiatry19, 536–543.

Cho RY, et al (2006). Impairments in frontal cortical gamma synchrony and cognitive control in schizophrenia. Proc Natl Acad Sci U S A., 103:19878–19883.

Cho KK, Hoch R, Lee AT, Patel T, Rubenstein JL, Sohal VS (2015) γ rhythms link prefrontal interneuron dysfunction with cognitive inflexibility in Dlx5/6(+/-) mice. Neuron 85:1332–1343.

Clementz BA, Sweeney JA, Hamm JP, Ivleva EI, Ethridge LE, Pearlson GD, Keshavan MS, Tamminga CA (2016). Identification of Distinct Psychosis Biotypes Using Brain-Based Biomarkers. Am J Psychiatry.,173(4):373-84.

Del Pino, I., Garcıa-Frigola, C., Dehorter, N., Brotons-Mas, J.R., Alvarez- Salvado, E., Martınez de Lagra´ n, M., Ciceri, G., Gabaldo´ n, M.V., Moratal, D., Dierssen, M., et al. (2013). Erbb4 deletion from fast-spiking interneurons causes schizophrenia-like phenotypes. Neuron 79, 1152–1168.

Domino, EF and Luby, ED (2012). Phencyclidine/Schizophrenia: One View Toward the Past, The Other to the Future. Schizophr Bull., 38(5): 914–919.

Donato, F., Rompani, S.B. and Caroni, P. (2013). Parvalbumin-expressing basket-cell network plasticity induced by experience regulates adult learning. Nature *504*, 272–276.

Donato F, Chowdhury A, Lahr M, Caroni P. Early- and late-born parvalbumin basket cell subpopulations exhibiting distinct regulation and roles in learning. Neuron., 85(4):770-86.

Elvevåg B, Goldberg TE (2000). Cognitive impairment in schizophrenia is the core of the disorder. Crit Rev Neurobiol., 14(1):1-21.

Fazzari, P. et al. Control of cortical GABA circuitry development by Nrg1 and ErbB4 signalling. Nature 464, 1376–1380 (2010).

Freund TF, Katona I (2007). Perisomatic inhibition. Neuron., 56(1):33-42.

Frohlich, J, and Van Horn, JD (2014). Reviewing the Ketamine model for Schizophrenia. J Psychopharmacol., 28(4): 287–302.

Gervain J, Vines BW, Chen LM, Seo RJ, Hensch TK, Werker JF, Young AH (2013). Valproate reopens critical-period learning of absolute pitch. Front Syst Neurosci., 7:102.

George, MS; Post, RM (2011). "Daily Left Prefrontal Repetitive Transcranial Magnetic Stimulation for Acute Treatment of Medication-Resistant Depression". American Journal of Psychiatry. 168 (4): 356–364.

Gulyas, A.I. et al. (2010) Parvalbumin-containing fast-spiking basket cells generate the field potential oscillations induced by cholinergic receptor activation in the hippocampus. J. Neurosci. 30, 15134–15145.

Harris AZ, Gordon JA (2015). Long-range neural synchrony in behavior. Annu Rev Neurosci., 38:171-94.

Hashimoto, T. et al. (2003) Gene expression deficits in a subclass of GABA neurons in the prefrontal cortex of subjects with schizophrenia. J. Neurosci. 23, 6315–6326.

Hikida, T. et al. (2007). Dominant-negative DISC1 transgenic mice display schizophrenia-associated phenotypes detected by measures translatable to humans. Proc. Natl. Acad. Sci. USA 104, 14501–14506.

Vertes RP, Hoover WB, Viana Di Prisco G (2004). Theta rhythm of the hippocampus: subcortical control and functional significance. Behav Cogn Neurosci Rev., 3(3):173-200.

Karayiorgou M, Simon TJ, Gogos JA. (2010). 22q11.2 Microdeletions: linking DNA structural variation to brain dysfunction and schizophrenia. Nat Rev Neurosci. 11:402–416.

Karunakaran, S, Chowdhury, A, Donato, F, Quairiaux, C, Michel, CM, Caroni, P (2016). PV plasticity sustained through D1/5 dopamine signaling required for long-term memory consolidation. Nat. Neurosci. 19, 454–464.

Kesner RP, Churchwell JC (2011). An analysis of rat prefrontal cortex in mediating executive function. Neurobiol Learn Mem. Oct;96(3):417-31.

Lahti AC, Weiler MA, Tamara Michaelidis BA, Parwani A, Tamminga CA (2001). Effects of ketamine in normal and schizophrenic volunteers. Neuropsychopharmacology, 25(4):455-67.

Lapray D, Lasztoczi B, Lagler M, Viney TJ, Katona L, Valenti O, Hartwich K, Borhegyi Z, Somogyi P, Klausberger T (2012). Behavior-dependent specialization of identified hippocampal interneurons. Nat Neurosci., 15(9):1265-71.

Lewis, D.A. et al. (2001) Lamina-specific deficits in parvalbumin immunoreactive varicosities in the prefrontal cortex of subjects with schizophrenia: evidence for fewer projections from the thalamus. Am. J. Psychiatry 158, 1411–1422

Lewis DA, Curley AA, Glausier JR, Volk DW (2012). Cortical parvalbumin interneurons and cognitive dysfunction in schizophrenia. Trends Neurosci., 35(1):57-67.

Lewis DA (2014). Inhibitory neurons in human cortical circuits: substrate for cognitive dysfunction in schizophrenia. Curr Opin Neurobiol., 26:22-6.

Magnus, C.J., Lee, P.H., Atasoy, D., Su, H.H., Looger, L.L., and Sternson, S.M. (2011). Chemical and genetic engineering of selective ion channel-ligand interactions. Science *333*, 1292–1296.

Marin, O (2012). Interneuron dysfunction in psychiatric disorders. Nat. Rev. Neurosci. 13,107–120.

Meechan DW, Rutz HL, Fralish MS, Maynard TM, Rothblat LA, LaMantia AS (2015). Cognitive ability is associated with altered medial frontal cortical circuits in the LgDel mouse model of 22q11.2DS. Cereb Cortex. May;25(5):1143-51.

Minzenberg, M.J. et al. (2009) Meta-analysis of 41 functional neuroimaging studies of executive function in schizophrenia. Arch. Gen. Psychiatry 66, 811–822.

Minzenberg MJ, et al (2010). Gamma oscillatory power is impaired during cognitive control independent of medication status in first-episode schizophrenia. Neuropsychopharm., 35:2590–2599.

Morris, B. J., Cochran, S. M. & Pratt, J. A (2005). PCP: from pharmacology to modelling schizophrenia. Curr. Opin. Pharmacol. 5, 101–106.

Mulert, C., Kirsch, V., Pascual-Marqui, R., McCarley, R.W., and Spencer, K.M. (2010). Long-range synchrony of g oscillations and auditory hallucination symptoms in schizophrenia. Int. J. Psychophysiol. 79, 55–63.

Piskorowski RA, Nasrallah K, Diamantopoulou A, Mukai J, Hassan SI, Siegelbaum SA, Gogos JA, Chevaleyre V (2016). Age-Dependent Specific Changes in Area CA2 of the Hippocampus and Social Memory Deficit in a Mouse Model of the 22q11.2 Deletion Syndrome. Neuron., 89(1):163-76.

Poels EM, Kegeles LS, Kantrowitz JT, Javitt DC, Lieberman JA, Abi-Dargham A, Girgis RR (2014a). Glutamatergic abnormalities in schizophrenia: a review of proton MRS findings. Schizophr Res., 152(2-3):325-32.

Poels EM, Kegeles LS, Kantrowitz JT, Slifstein M, Javitt DC, Lieberman JA, Abi-Dargham A, Girgis RR (2014b). Imaging glutamate in schizophrenia: review of findings and implications for drug discovery. Mol Psychiatry., 19(1):20-9.

Royer S, Zemelman BV, Losonczy A, Kim J, Chance F, Magee JC, Buzsáki G (2012). Control of timing, rate and bursts of hippocampal place cells by dendritic and somatic inhibition. Nat Neurosci., 15(5):769-75.

Shen, S. et al (2008). Schizophrenia-related neural and behavioral phenotypes in transgenic mice expressing truncated Disc1. J. Neurosci. 28, 10893–10904.

Sigurdsson, T., Stark, K.L., Karayiorgou, M., Gogos, J.A., and Gordon, J.A. (2010). Impaired hippocampal-prefrontal synchrony in a genetic mouse model of schizophrenia. Nature 464, 763–767.

Sigurdsson T, and Duvarci, S (2016). Hippocampal-Prefrontal Interactions in Cognition, Behavior and Psychiatric Disease. Front Syst Neurosci., 9: 190.

Spencer, K.M., Niznikiewicz, M.A., Nestor, P.G., Shenton, M.E., and McCarley, R.W. (2009). Left auditory cortex gamma synchronization and auditory hallucination symptoms in schizophrenia. BMC Neurosci. 10.

Sohal, V.S. et al. (2009) Parvalbumin neurons and gamma rhythms enhance cortical circuit performance. Nature 459, 698–702.

Spellman T, Rigotti M, Ahmari SE, Fusi S, Gogos JA, Gordon JA (2015). Hippocampal-prefrontal input supports spatial encoding in working memory. Nature 522:309 –314.

Stark, K.L., Xu, B., Bagchi, A., Lai, W.-S., Liu, H., Hsu, R., Wan, X., Pavlidis, P., Mills, A.A., Karayiorgou, M., and Gogos, J.A. (2008). Altered brain microRNA biogenesis contributes to phenotypic deficits in a 22q11-deletion mouse model. Nat. Genet., 40, 751–760.

Stark E, Roux L, Eichler R, Senzai Y, Royer S, Buzsáki G (2014). Pyramidal cell-interneuron interactions underlie hippocampal ripple oscillations. Neuron., 83(2):467-80.

Sternson, S.M., and Roth, B.L. (2014). Chemogenetic tools to interrogate brain functions. Ann. Rev. Neurosci. *37*, 387-407.

Uhlhaas PJ, Singer W (2010). Abnormal neural oscillations and synchrony in schizophrenia. Nat Rev Neurosci., 11(2):100-13.

Wen, L. et al. (2010). Neuregulin 1 regulates pyramidal neuron activity via ErbB4 in parvalbumin-positive interneurons. Proc. Natl. Acad. Sci. USA 107, 1211–1216.

Woodin M, Wang PP, Aleman D, McDonald-McGinn D, Zackai E, Moss E. (2001). Neuropsychological profile of children and adolescents with the 22q11.2 microdeletion. Genet Med., 3:34–39.

Xu, B., Roos, J.L., Levy, S., van Rensburg, E.J., Gogos, J.A., Karayiorgou, M., (2008). Strong association of de novo copy number mutations with sporadic schizophrenia. Nat. Genet. 40, 880–885.

3. General Discussion

The primary focus of my PhD thesis work was on identifying the circuit level mechanisms, which operate within the prefrontal cortex to mediate higher order cognitive functions like decision-making. Subsequently I also investigated circuit level dysfunctions in a mouse model of Schizophrenia, a disorder that affects prefrontal cortical function. Here I will briefly summarize the key results of this thesis and then discuss the general relevance of the data and outline future studies that may follow up from this thesis.

In the first part of the thesis I investigated how two distinct but functionally related prefrontal cortical areas, Prelimbic and Infralimbic, exert complimentary as well as opposite roles to support new learning. I have shown that in new learning PreL is required for perseverance of previously learnt associations while the IL is required to learn new alternative associations. I also provide evidence of direct, layer 5/6 derived, reciprocal connectivity between the PreL and IL which is required for the IL to learn alternative associations than those supported by the PreL.

Interestingly only the IL→PreL projections are specifically required during IL-dependent alternative learning. This data matches well with recent findings, which showed that activation of deep layer pyramidal neurons in the IL suppressed activity of pyramidal neurons in the PreL while local interneuron firing in the IL remain unaffected (Ji and Neugebauer, 2012). This suggests that the pyramidal neuronal component of the IL→PreL projections mediate feedforward inhibition onto PreL neurons. Indeed, my data shows that silencing the IL→PreL projection neurons during extinction leads to increased cFos expression in the PreL and behavioral perseverance. Thus, it is likely that learning alternative choices and strategies first require an IL driven inhibition of PreL activity to prevent perseverance to the current rule. I have also shown that PreL→IL connectivity is required during a specific time window +12-14 hours post the initial learning to setup the role of IL for subsequent alternative learning. Unlike, the IL→PreL projection neurons silencing the PreL→IL projection neurons at +12-14h prevents cFos induction in IL in this window and a subsequent failure to extinguish the fear memory. This would suggest that these projections are excitatory in nature. However, the exact nature of information conveyed by these neurons from the PreL to the IL remains to be determined. Interestingly activity of the IL→PreL projections are also necessary in this +12-14h

window for successful extinction later on. One exciting possibility is that fear memory is initially learnt by the PreL which is then transferred to the IL by the PreL→IL projections at +12-14h. Following this IL→PreL neurons are also activated, in the +12-14h window, to balance PreL driven perseverance to previously learnt associations in favor of alternative strategies. Whether such a sequential activation of the PreL→IL and IL→PreL projections is indeed required could be an exciting avenue of future research.

The PreL↔IL projection neurons, while originating in the deep layers, terminate in all layers of the PreL and IL. The mPFC acts as a site of convergence integrating inputs from various brain structures including hippocampal inputs conveying contextual information relevant for the expression of extinction memories (Sotres-Bayon et al., 2012; Hobin et al., 2006). Recent reports also show that the various mPFC projections to subcortical structures originate at different cortical layers. For example, dmPAG targeting neurons originate from layer 5 only while nucleus accumbens targeting neurons originate in layer 2/3 of the PreL (Franklin et al., 2017). Thus, it is probable that the PreL↔IL projection neurons are comprised of intermingled subpopulations, which differentially target the cortical layers in IL and PreL, giving specificity to PreL/IL driven modulation of subcortical structures.

Furthermore, the PreL↔IL projection neurons are not comprised of pyramidal neurons alone. Roughly, 5-10% of these neurons are GABAergic in nature. There has been a general consensus that inhibitory GABAergic neurons in the cortex participate mainly in local microcircuits. However, long-range GABAergic interneurons have remained poorly understood. A recent study showed that long-range GABAergic interneurons originating in the mPFC target the Nucleus accumbens shell and their stimulation results in avoidance in a real time place preference task (Lee et al., 2014). Thus, the pyramidal and GABAergic components of the PreL↔IL projection neurons might have different functional roles. Taken together one can strongly argue that further dissection of the composition of these projection neurons and their targets will give us an integrated understanding of functional circuit organization at both the local and global scale and how complex behavior emerge through them.

A further key result is that the role of IL in promoting learning of alternative associations is setup in a window 12-14h post the acquisition of the initial association and requires direct PreL↔IL communication. Such late windows are thought to be important for long-term memory consolidation events between distributed networks (Girardeau et al., 2009; Carr et al., 2011). The late time frame for setting up systems balances that define subsequent learning suggests a hierarchical systems logic between PreL and IL, where relevant information obtained before or after the initial acquisition can be included into an updated representation of learned rules and their values. Recent studies have uncovered network mechanisms of formation and retrieval of single trial memories, involving populations of memory neurons sometimes referred to as 'engrams'. Such engrams are selected through new learning, and can again be recruited in memory recall through partial cue-mediated reactivation (Liu et al., 2012, Kim et al., 2014; Reijmers et al., 2007, Tayler et al., 2013, Zelikowsky et al., 2014). By taking a similar approach network mechanisms involved in encoding and retrieval of memories formed through learning events spread over separate days can give us a better understanding of the role of the +12-14h window.

In the second part of the thesis, I explored the dysfunction in the Parvalbumin interneuronal network state and behavioral deficits in the prefrontal cortex and hippocampus of a genetic model of Schizophrenia in mice – LgDel+/-. My results show a dramatic shift towards low fractions of PV/GAD67 neurons and an associated aberrant power of baseline gamma oscillations in the mPFC of these animals without any changes in the density of the PV neurons themselves. Interestingly the increased low PV fraction has a neurodevelopmental origin where the PV neurons fail to increase their PV content with maturation. These animals also show strong deficits in prefrontal and hippocampal dependent cognitive tasks.

The deficits seen in LgDel+/- mice closely resemble those seen in human schizophrenic patients. For example, a decreased expression of PV mRNA and protein but not the number of interneurons themselves have been observed in the dorsolateral prefrontal cortex of human schizophrenic patients (Lewis et al., 2012; Hashimoto et al., 2003). Moreover, schizophrenic patients exhibit altered activation of

the dlPFC (Minzenberg et al., 2009) and lower power of gamma oscillations (Cho et al., 2006; Minzenberg et al., 2010) during tasks that require cognitive control. Also, animal models with targeted disruption of genes that play a crucial role in circuit integration and functioning of PV neurons in rodents, lead to cognitive symptoms and PV network deficits similar to those seen in schizophrenia (Fazzari et al., 2010; Hikida et al., 2007; Marin 2012; Wen et al., 2010; Cho et al., 2015). A study by Cho et al. (2015) showed that in an animal model of impaired PV neuron maturation (Dlx5/6+/- mice) deficits in intrinsic firing properties of fast spiking interneurons only appear in early adulthood (P63-82) while they are comparable to WT neurons at earlier ages. Moreover, these animals show rule shift deficits, along with aberrant base line gamma power, only at early adulthood (10 weeks) and not earlier (7 weeks). Recent studies have also shown that there is a selective increase in excitatory inputs onto prefrontal PV positive fast-spiking basket cells during adolescence (Caballero et al., 2014a). Moreover, PFC LTP, following hippocampal stimulation, does not emerge until P50 although the amygdala can trigger PFC LTP from P30 itself, suggesting a delayed strengthening of the hippocampus-PFC projections (Caballero et. al., 2014b; Flores-Barrera et. al., 2014). Thus the PFC PV network as well as the vH-PFC axis completes its maturation around late adolescence/early adulthood. Taken together one reasonable hypothesis could be that with maturation of the vH-mPFC axis around early adulthood there is a shift in dependence of rule learning and other cognitive processes onto the vH-mPFC axis. Thus, the emergence of deficits in PV neuronal network and cognitive tasks in Dlx5/6+/- as well as LgDel+/- mice appears around this age. Indeed evidence for this hypothesis is found in a recent paper which showed that in human subject's transition from childhood to adolescence was marked by a ventral-to-dorsal shift in medial prefrontal responses to aversive, but not neutral, stimuli, suggesting that adolescence is characterized by a shift towards representing emotional events in increasingly PFC driven cognitive terms (Silvers et al., 2017). Moreover, in human Schizophrenia patients, the first episode of psychosis and diagnosis of Schizophrenia usually happens around early adulthood (Millan et al., 2016).

Taken together, my data suggests that impaired functioning PV interneurons in the vH-mPFC axis may form a convergent endpoint of genetic and environmental insults in schizophrenia. This finding is especially relevant to understanding the etiology of the disorder and designing of novel therapeutics for the treatment of Schizophrenia as

it provides a common target for drug development notwithstanding the multitude of genetic and environmental factors that contribute to the etiology of the disorder.

In an attempt to target the PV network for designing a rescue strategy, I found a late window maturation of the PreL PV network in wild type mice. Interestingly LgDel+/- mice fail to show an increase in PV expression, unlike wild type animals, as they transition from adolescence to adulthood. Remarkably targeting the PreL PV network in this sensitive period for direct and chronic chemogenetic stimulation led to a long-term rescue of the PV network, gamma power and cognitive deficits in LgDel+/- mice. I further showed that this rescue strategy works via the vH-PreL axis as selective rescue of the PV network in either of the structures rescues the network in the other structure while preventing the rescue in either of the structures failed to mediate a functional rescue. Considering that in human schizophrenic patients, the first episode of psychosis usually manifests around early adulthood this therapeutic strategy has an exciting potential for translation to human patients with either using non-invasive procedures like transcranial magnetic stimulation (TMS) (George and Post, 2011) or more conventional drug based approaches. One interesting question arises from the data, which shows that rescue can only be mediated in a very specific time window in early adulthood. It remains to be elucidated what sets up this sensitive period and whether it can be reopened in later life. Recent studies have shown that HDAC inhibitors like Valproate can reopen critical period of learning in adult humans (Gervain et al., 2013). It remains to be seen if similar strategy will work in mediating a rescue in older LgDel+/- animals. If yes then the therapeutic strategy described here could be extended to older patients beyond the first episode of psychosis thus providing us with a therapy for Schizophrenia irrespective of age.

4. Bibliography

Adhikari, A, Topiwala, MA, and Gordon, JA (2010). Synchronized activity between the ventral hippocampus and the medial prefrontal cortex during anxiety. Neuron 65, 257–269.

Ahn K, et al (2011). Probing GABA receptor function in schizophrenia with iomazenil. Neuropsychopharm., 36:677–683.

Baeg EH, Kim YB, Huh K, Mook-Jung I, Kim HT, Jung MW (2003). Dynamics of population code for working memory in the prefrontal cortex. Neuron., 25;40(1):177-88

Balleine BW, O'Doherty JP (2010). Human and rodent homologies in action control: corticostriatal determinants of goal-directed and habitual action. Neuropsychopharmacology, 35:48–69.

Barbas H, Pandya DN (1989). Architecture and intrinsic connections of the prefrontal cortex in the rhesus monkey. J Comp Neurol., 286:353–75.

Barker JM, Taylor JR, Chandler LJ (2014). A unifying model of the role of the infralimbic cortex in extinction and habits. Learn. Mem., 21:441–448.

Barthas F, Sellmeijer J, Hugel S, Waltisperger E, Barrot M, Yalcin I (2015). The anterior cingulate cortex is a critical hub for pain-induced depression. Biol. Psychiatry 77, 236–245.

Bartos M, Vida I, Frotscher M, Meyer A, Monyer H, Geiger JR, Jonas P (2002). Fast synaptic inhibition promotes synchronized γ oscillations in hippocampal interneuron networks. Proc Natl Acad Sci U S A 99:13222– 13227.

Bedwell SA, Billett EE, Crofts JJ, Tinsley CJ (2014). The topology of connections between rat prefrontal, motor and sensory cortices. Front Syst Neurosci., 8:177.

Bekinschtein, P. et al. Persistence of long-term memory storage requires a late protein synthesis- and BDNF- dependent phase in the hippocampus. Neuron 53, 261–277 (2007).

Birrell, J.M., and Brown, V.J. (2000). Medial frontal cortex mediates perceptual attentional set shifting in the rat. J. Neurosci. *20*, 4320-4324.

Bliss, TV, and Lomo, T (1973). Long-lasting potentiation of synaptic transmission in the dentate area of the anaesthetized rabbit following stimulation of the performant path. J. Physiol. 232, 331–356.

Bliss TV, Collingridge GL, Kaang BK, Zhuo M. (2016). Synaptic plasticity in the anterior cingulate cortex in acute and chronic pain. Nat Rev Neurosci., 17(8):485-96.

Bloss, EB, Janssen, WG, McEwen, BS, and Morrison, JH (2010). Interactive effects of stress and aging on structural plasticity in the prefrontal cortex. J. Neurosci. 30, 6726–6731.

Bloss, EB, Janssen, WG, Ohm, DT, Yuk, FJ, Wadsworth,S, Saardi, KM, et al. (2011). Evidence for reduced experience-dependent dendritic spine plasticity in the aging prefrontal lcortex. J. Neurosci., 31, 7831–7839.

Boix-Trelis N, Vale-Martinez A, Guillazo-Blanch G, Marti-Nicolovius M (2007). Muscarinic cholinergic receptor blockade in the rat prelimbic cortex impairs the social transmission of food preference. Neurobiol Learn Mem., 87:659–668.

Bonelli RM, Cummings JL (2007). Frontal-subcortical circuitry and behavior. Dialogues Clin Neurosci.;9(2):141-51.

Bragin EO, Yeliseeva ZV, Vasilenko GF, Meizerov EE, Chuvin BT, Durinyan RA (1984). Cortical projections to the periaqueductal grey in the cat: a retrograde horseradish peroxidase study. Neurosci. Lett., 51, 271–275.

Bremner J. D., Staib L. H., Kaloupek D., Southwick S. M., Soufer R., Charney D. S. (1999). Neural correlates of exposure to traumatic pictures and sound in vietnam combat veterans with and without posttraumatic stress disorder: a positron emission tomography study. Biol. Psychiatry 45, 806–816.

Bronstein YL, Cummings JL (2001). Neurochemistry of frontal-subcortical circuits. In: Lichter DG, Cummings JL, eds. Frontal-Subcortical Circuits in Psychiatric and Neurological Disorders. New York, NY: Guilford Press, 59-91.

Buchanan, SL, Thompson, RH, Maxwell, BL, Powell, DA (1994). Efferent connections of the medial prefrontal cortex in the rabbit. Exp. Brain Res. 100, 469–483.

Buzsáki, G (2002). Theta oscillations in the hippocampus. Neuron 33, 325–340.

Caballero, A, Flores-Barrera, E, Cass, DK, Tseng, KY, (2014a). Differential regulation of parvalbumin and calretinin interneurons in the prefrontal cortex during adolescence. Brain Struct. Funct., 219, 395–406.

Caballero, A, Thomases, DR, Flores-Barrera, E, Cass, DK, Tseng, KY, (2014b). Emergence of GABAergic-dependent regulation of input-specific plasticity in the adult rat prefrontal cortex during adolescence. Psychopharmacology (Berl.) 231, 1789–1796.

Caballero A, Granberg R, Tseng KY (2016). Mechanisms contributing to prefrontal cortex maturation during adolescence. Neurosci Biobehav Rev., 70:4-12.

Cardinal RN, Parkinson JA, Marbini HD, Toner AJ, Bussey TJ, Robbins TW, Everitt BJ (2003). Role of the anterior cingulate cortex in the control over behavior by Pavlovian conditioned stimuli in rats. Behav Neurosci., 117(3):566-87.

Caroni, P, Chowdhury, A, Lahr, M (2014). Synapse rearrangements upon learning: from divergent-sparse connectivity to dedicated sub-circuits. Trends Neurosci. 37, 604-14

Caroni, P, Donato, F, and Muller, D (2012). Structural plasticity upon learning: regulation and functions. Nat. Rev. Neurosci. 13, 478–490 (2012).

Carr, M.F., Jadhav, S.P., and Frank, L.M. (2011). Hippocampal replay in the awake state: a potential substrate for memory consolidation and retrieval. Nat. Neurosci. 14, 147-153.

Cassell, MD & Wright, DJ (1986). Topography of projections from the medial prefrontal cortex to the amygdala in the rat. Brain Res. Bull. 17, 321–333.

Cass, DK, Flores-Barrera, E, Thomases, DR, Vital, WF, Caballero, A, Tseng, KY (2014). CB1 cannabinoid receptor stimulation during adolescence impairs the maturation of GABA function in the adult rat prefrontal cortex. Mol. Psychiatry19, 536–543.

Cassel, JC, Pereirade Vasconcelos, A, Loureiro, M, Cholvin, T, Dalrymple-Alford, JC, and Vertes, RP (2013). The reuniens and rhomboid nuclei: neuroanatomy, electrophysiological characteristics and behavioral implications. Prog. Neurobiol. 111, 34–52.

Caviness VS Jr. (1975). Architectonic map of neocortex of the normal mouse. J Comp Neurol., 164(2):247-63.

Cho RY, et al (2006). Impairments in frontal cortical gamma synchrony and cognitive control in schizophrenia. Proc Natl Acad Sci U S A., 103:19878–19883.

Cho KK, Hoch R, Lee AT, Patel T, Rubenstein JL, Sohal VS (2015) γ rhythms link prefrontal interneuron dysfunction with cognitive inflexibility in Dlx5/6(+/-) mice. Neuron 85:1332–1343.

Chudasama, Y, and Robbins, TW (2003). Dissociable contributions of the orbitofrontal and Infralimbic cortex to pavlovian autoshaping and discrimination reversal learning: further evidence for the functional heterogeneity of the rodent frontal cortex. J. Neurosci., 23, 8771–8780.

Churchwell JC, Morris AM, Musso ND, Kesner RP (2010). Prefrontal and hippocampal contributions to encoding and retrieval of spatial memory. Neurobiol Learn Mem., 93:415–421.

Churchwell J. C., Kesner R. P. (2011). Hippocampal-prefrontal dynamics in spatial working memory: interactions and independent parallel processing. Behav. Brain Res. 225, 389–395.

Colgin, L.L., Denninger, T., Fyhn, M., Hafting, T., Bonnevie, T., Jensen, O., Moser, M.B., and Moser, E.I. (2009). Frequency of gamma oscillations routes flow of information in the hippocampus. Nature 462, 353–357.

Comeau, W, McDonald, R, and Kolb, B (2010). Learning-induced structural changes in the prefrontal cortex. Behav.BrainRes. 214, 91–101.

Condé, F., Maire-lepoivre, E, Audinat, E, and Crépel, F (1995). Afferent connections of the medial frontal cortex of the rat. II.Cortica land subcortical afferents. J. Comp.Neurol. 352, 567–593.

Cook, SC, and Wellman, CL (2004). Chronic stress alters dendritic morphology in rat medial prefrontal cortex. J. Neurobiol., 60, 236–248.

Corcoran KA, Quirk GJ (2007). Activity in the prelimbic cortex is necessary for the expression of learned, but not innate, fears. J. Neurosci., 37:840–844.

Crombag, HS, Gorny, G, Li, Y, Kolb, B, and Robinson,TE (2005). Opposite effects of amphetamine self-administration experience on dendritic spines in the medial and orbital prefrontal cortex. Cereb.Cortex 15, 341–348.

Cuppini, C, Ambrogini, P, Lattanzi, D, Ciuffoli, S, and Cuppini,R (2009). FGF2 modulates the voltage dependent K+ curren tand changes excitability of rat Dentate gyrus granule cells. Neurosci.Lett., 462, 203–206.

Curley AA, et al (2011). Cortical deficits of glutamic acid decarboxylase 67 expression in schizophrenia: clinical, protein, and cell type-specific features. Am J Psychiatry, 168:921–929.

Dawirs, R.R, Teuchert-Noodt, G, and Nossoll, M (1997). Pharmacologically induced neural plasticity in the prefrontal cortex of adult gerbils (Meriones unguiculatus). Eur. J. Pharmacol., 327, 117–123.

Delevich K, Tucciarone J, Huang ZJ, Li B. (2015). The mediodorsal thalamus drives feedforward inhibition in the anterior cingulate cortex via parvalbumin interneurons. J Neurosci., 35(14):5743-53.

De Roo, M. et al (2008). LTP promotes a selective long-term stabilization and clustering of dendritic spines. PLoS Biol. 6, e219.

Devinsky, O., Morrell, MJ & Vogt, BA (1995). Contributions of anterior cingulate cortex to behavior. Brain, 118, 279–306.

Ding HK, Teixeira CM, Frankland PW (2008). Inactivation of the anterior cingulate cortex blocks expression of remote, but not recent, conditioned taste aversion memory. Learn Mem., 15:290–293.

Do-Monte FH, Manzano-Nieves G, Quinones-Laracuente K, Ramos-Medina L, Quirk GJ (2015). Revisiting the role of infralimbic cortex in fear extinction with optogenetics. J. Neurosci., 35:3607–3615.

Dudchenko PA (2004). An overview of the tasks used to test working memory in rodents. Neurosci. Biobehav. Rev. 28, 699–709.

Elvevåg B, Goldberg TE (2000). Cognitive impairment in schizophrenia is the core of the disorder. Crit Rev Neurobiol., 14(1):1-21.

Etkin A, Egner T, Kalisch R (2011). Emotional processing in anterior cingulate and medial prefrontal cortex. Trends Cogn Sci., 15(2):85-93.

Euston DR, Gruber AJ, McNaughton BL (2012). The role of medial prefrontal cortex in memory and decision-making. Neuron., 76(6):1057-70.

Fazzari P, Paternain AV, Valiente M, Pla R, Luján R, Lloyd K, Lerma J, Marín O, Rico B (2010). Control of cortical GABA circuitry development by Nrg1 and ErbB4 signaling. Nature., 464(7293):1376-80.

Flores-Barrera, E, Thomases, DR, Heng, LJ, Cass, DK, Caballero, A. Tseng, KY (2014). Late adolescent expression of GluN2 B transmission in the prefrontal cortex is input-specific and requires postsynaptic protein kinase A and D1dopamine receptor signaling. Biol. Psychiatry 75, 508–516.

Floyd, NS, Price JL, Ferry AT, Keay KA, Bandler R. (2000). Orbitomedial prefrontal cortical projections to hypothalamus in the rat. J. Comp. Neurol., 432: 307–328.

Frankland PW, Bontempi B, Talton LE, Kaczmarek L, Silva AJ (2004). The involvement of the anterior cingulate cortex in remote contextual fear memory. Science., 304:881–883.

Franklin TB, Silva BA, Perova Z, Marrone L, Masferrer ME, Zhan Y, Kaplan A, Greetham L, Verrechia V, Halman A, Pagella S, Vyssotski AL, Illarionova A, Grinevich V, Branco T, Gross CT (2017). Prefrontal cortical control of a brainstem social behavior circuit. Nat Neurosci., 20(2):260-270.

Fries P, Nikolic´ D, Singer W (2007) The γ cycle. Trends Neurosci 30:309–316.

Fuster, JM, and Jervey, JP (1981). Inferotemporal neurons distinguish and retain behaviorally relevant features of visual stimuli. Science, 212, 952–955.

Funahashi S (2006). Prefrontal cortex and working memory processes. Neuroscience., 139:251–261.

Gabbott, P. L., Warner, T. A., Jays, P. R., Salway, P, and Busby, SJ (2005). Prefrontal cortex in the rat: projections to subcortical autonomic, motor, and limbic centers. J. Comp. Neurol., 492, 145–177.

Gabbott, PLA, Warner, TA, and Busby, SJ (2006). Amygdala input monosynaptically innervates Parvalbumin immunoreactive local circuit neurons in rat medial prefrontal cortex. Neuroscience 139, 1039–1048.

Galarreta M, Hestrin S (1999) A network of fast-spiking cells in the neocortex connected by electrical synapses. Nature 402:72–75.

Gallagher, M, McMahan, RW, and Schoenbaum, G (1999). Orbitofrontal cortex and representation of incentive value in associative learning. J. Neurosci., 19, 6610–6614.

Garfinkel S. N., Abelson J. L., King A. P., Sripada R. K., Wang X., Gaines L. M., et al.. (2014). Impaired contextual modulation of memories in PTSD: an fMRI and psychophysiological study of extinction retention and fear renewal. J. Neurosci. 34, 13435–13443.

George, MS; Post, RM (2011). "Daily Left Prefrontal Repetitive Transcranial Magnetic Stimulation for Acute Treatment of Medication-Resistant Depression". American Journal of Psychiatry. 168 (4): 356–364.

Gervain J, Vines BW, Chen LM, Seo RJ, Hensch TK, Werker JF, Young AH (2013). . Valproate reopens critical-period learning of absolute pitch. Front Syst Neurosci., 7:102.

Gibson JR, Beierlein M, Connors BW (1999). Two networks of electrically coupled inhibitory neurons in neocortex. Nature 402:75–79.

Gilboa A., Shalev A. Y., Laor L., Lester H., Louzoun Y., Chisin R., et al. . (2004). Functional connectivity of the prefrontal cortex and the amygdala in posttraumatic stress disorder. Biol. Psychiatry 55, 263–272.

Gilmartin, M.R., Miyawaki, H., Helmstetter, F.J. and Diba, K. (2013). Prefrontal activity links non-overlapping events in memory. J. Neurosci. *33*, 10910-10914.

Girardeau, G, Benchenane, K, Wiener, SI, Buzsáki, G, Zugaro, MB (2009). Selective suppression of hippocampal ripples impairs spatial memory. Nat Neurosci. 12, 1222-3.

Giustino, T.F. and Maren, S. (2015). The role of the medial prefrontal cortex in the conditioning and extinction of fear. Front. Behav. Neurosci. *9*, 298.

Godsil, B.P., Kiss, J.P., Spedding, M., and Jay, T.M. (2013). The hippocampal-prefrontal pathway: the weak link in psychiatric disorders? Eur. Neuropsychopharmacol. 23, 1165–1181.

Goldwater, DS, Pavlides, C, Hunter, RG, Bloss, EB, Hof, PR, McEwen, BS, et al. (2009). Structural and functional alterations to rat medial prefrontal cortex following chronic restraint stress and recovery. Neuroscience 164, 798–808.

Gonzalez, M.C. Kramar, C.P., Tomaiuolo, M., Katche, C., Weisstaub, N., Cammarota, M., and Medina, J.H. (2014). Medial prefrontal cortex dopamine controls the persistent storage of aversive memories. Front. Behav. Neurosci. *8*, 408.

Gorelova, N, Seamans, JK, Yang, CR (2002). Mechanisms of dopamine activation offast-spiking interneurons that exert inhibition in rat prefrontal cortex. J.Neurophysiol. 88, 3150–3166.

Gothelf D, Presburger G, Zohar AH, Burg M, Nahmani A, Frydman M, Shohat M, Inbar D, Aviram-Goldring A, Yeshaya J, et al. (2004). Obsessive-compulsive disorder in patients with velocardiofacial (22q11 deletion) syndrome. Am J Med Genet B Neuropsychiatr Genet. 126B:99–105.

Green T, Gothelf D, Glaser B, Debbane M, Frisch A, Kotler M, Weizman A, Eliez S. (2009). Psychiatric disorders and intellectual functioning throughout development in velocardiofacial (22q11.2 deletion) syndrome. J Am Acad Child Psy. 48:1060–1068.

Groenewegen, HJ (1988). Organization of the afferent connections of the mediodorsal thalamic nucleus in the rat, related to the mediodorsal-prefrontal topography. Neuroscience 24: 379–431.

Groenewegen HJ, Uylings HB (2000). The prefrontal cortex and the integration of sensory, limbic and autonomic information. Prog Brain Res., 126:3–28.

Guidotti A, et al (2000). Decrease in reelin and glutamic acid decarboxylase67 (GAD67) expression in schizophrenia and bipolar disorder. Arch Gen Psychiatry., 57:1061–1069.

Han, JH, Kushner, SA, Yiu, AP, Cole, CJ, Matynia, A, Brown, RA, Neve, RL, Guzowski, JF, Silva, AJ, and Josselyn, SA (2007). Neuronal competition and selection during memory formation. Science 316, 457–460.

Han, JH, Kushner, SA, Yiu, AP, Hsiang, HLL, Buch, T, Waisman, A, Bontempi, B, Neve, RL, Frankland, PW, and Josselyn, SA (2009). Selective erasure of a fear memory. Science 323, 1492–1496.

Han, S, Soleiman, MT, Soden, ME, Zweifel, LS, Palmiter, RD (2015). Elucidating an affective pain circuit that creates a threat memory. Cell, 162, 363–374.

Harris AZ, Gordon JA (2015). Long-range neural synchrony in behavior. Annu Rev Neurosci., 38:171-94.

Hashimoto T, et al (2003). Gene expression deficits in a subclass of GABA neurons in the prefrontal cortex of subjects with schizophrenia. J Neurosci., 23:6315–6326.

Hebb, D.O (1949). The Organization of Behavior: A Neuropsychological Approach John Wiley & Sons, New York.

Herry, C., and Johansen, J.P. (2014). Encoding of fear learning and memory in distributed neuronal circuits. Nat. Neurosci. 17, 1644-1654.

Hikida T, Jaaro-Peled H, Seshadri S, Oishi K, Hookway C, Kong S, Wu D, Xue R, Andradé M, Tankou S, Mori S, Gallagher M, Ishizuka K, Pletnikov M, Kida S, Sawa A (2007). Dominant-negative DISC1 transgenic mice display schizophrenia-associated phenotypes detected by measures translatable to humans. Proc Natl Acad Sci U S A., 104(36):14501-6.

Hobin, J.A., Ji, J., Maren, S. (2006). Ventral hippocampal muscimol disrupts context-specific fear memory retrieval after extinction in rats. Hippocampus, 16, pp. 174-182.

Holtmaat, A. & Caroni, P (2016). Functional and structural underpinnings of neuronal assembly formation in learning. Nat Neurosci.

Holtmaat, A & Svoboda, K (2009). Experience-dependent structural synaptic plasticity in the mammalian brain. Nat. Rev. Neurosci. 10, 647-658.

Holroyd CB, Coles MGH (2002). The neural basis of human error processing: reinforcement learning, dopamine, and the error-related negativity. Psychol Rev., 109(4):679-709.

Hoover WB, Vertes RP (2007). Anatomical analysis of afferent projections to the medial prefrontal cortex in the rat. Brain Struct Funct., 212(2):149-79.

Hoover WB, Vertes RP (2011). Projections of the medial orbital and ventral orbital cortex in the rat. J Comp Neurol., 519(18):3766-801.

Horst NK, Laubach M (2009). The role of rat dorsomedial prefrontal cortex in spatial working memory. Neuroscience., 1;164(2):444-56.

Houk JC (2001). Neurophysiology of frontal-subcortical circuits. In: Lichter DG, Cummings JL, eds. Frontal-Subcortical Circuits in Psychiatric and Neurological Disorders. New York, NY: Guilford Press, 92-113.

Howard, M.W. et al. (2003). Gamma oscillations correlate with working memory load in humans. Cereb. Cortex 13, 1369–1374.

Hugues S., Chessel A., Lena I., Marsault R., Garcia R. (2006). Prefrontal infusion of PD098059 immediately after fear extinction training blocks extinction-associated prefrontal synaptic plasticity and decreases prefrontal ERK2 phosphorylation. Synapse 60, 280–287.

Hutcheson, DM, and Everitt, BJ (2003). The effects of selective orbitofrontal cortex lesions on the acquisition and performance of cue‐controlled cocaine seeking in rats. Ann. NY Acad. Sci. 1003, 410–411.

Jankowski MM, Ronnqvist KC, Tsanov M, Vann SD, Wright NF, Erichsen JT, Aggleton JP, O'Mara SM (2013). The anterior thalamus provides a subcortical circuit supporting memory and spatial navigation. Front Syst Neurosci., 7:45.

Jacobsen CF (1936) Studies on cerebral function in primates: 1. The function of the frontal association areas in monkeys. Comp Psychol Monog 13:1-60.

Jones M. W., Wilson M. A. (2005). Theta rhythms coordinate hippocampal-prefrontal interactions in a spatial memory task. PLoS Biol. 3:e402.

Kalsbeek, A., Voorn, P., Buijs, R.M., Pool, C.W., Uylings, H.B., (1988). Development of the dopaminergic innervation in the prefrontal cortex of the rat. J. Comp.Neurol. 269, 58–72.

Kandel, ER, Dudai, Y, Mayford, MR (2014). The molecular and systems biology of memory. Cell 157,163–186.

Karunakaran, S, Chowdhury, A, Donato, F, Quairiaux, C, Michel, CM, Caroni, P (2016). PV plasticity sustained through D1/5 dopamine signaling required for long-term memory consolidation. Nat. Neurosci. 19, 454–464.

Katche, C. et al (2010). Delayed wave of c-Fos expression in the dorsal hippocampus involved specifically in persistence of long-term memory storage. Proc. Natl. Acad. Sci. USA 107, 349–354.

Katche, C., Cammarota, M. & Medina, J.H (2013). Molecular signatures and mechanisms of long-lasting memory consolidation and storage. Neurobiol. Learn. Mem. 106, 40–47.

Kessels, HW, and Malinow, R (2009). Synaptic AMPA receptor plasticity and behavior. Neuron 61, 340–350.

Kim, J, Kwon, JT, Kim, HS, Josselyn, SA, and Han, JH (2014). Memory recall and modifications by activating neurons with elevated CREB. Nat. Neurosci. 17, 65–72.

Kim H, Ahrlund-Richter S, Wang X, Deisseroth K, Carlen M (2016) Prefrontal parvalbumin neurons in control of attention. Cell 164:208 –218.

Kolb B, Gibb R, Gorny G (2003). Experience-dependent changes in dendritic arbor and spine density in neocortex vary qualitatively with age and sex. Neurobiol Learn Mem., 79(1):1–10.

Kolb, B, Muhammad, A, Ilnytskyy, S, and Mychasiuk, R (2014). Chronic stress induces epigenetic modification to the mPFC, OFC and HPC of adult rats. Soc. Neurosci.Abst.

Kondo H, Witter MP (2014).Topographic organization of orbitofrontal projections to the parahippocampal region in rats. J Comp Neurol., 522(4):772-93.

Laurent V, Westbrook RF (2009). Inactivation of the infralimbic but not the prelimbic cortex impairs consolidation and retrieval of fear extinction. Learn. Mem., 16:520–529.

LaLumiere RT, Smith KC, Kalivas PW (2012). Neural circuit competition in cocaine-seeking: roles of the infralimbic cortex and nucleus accumbens shell. Eur. J. Neurosci., 35:14–622.

LeDoux, JE (2000). Emotion circuits in the brain. Annu. Rev. Neurosci., 23, 155–184.

Lee I, Solivan F (2008). The roles of the medial prefrontal cortex and hippocampus in a spatial paired association task. Learn Mem., 15:357–367.

Lewis DA, et al (2008). Subunit-selective modulation of GABA type A receptor neurotransmission and cognition in schizophrenia. Am J Psychiatry., 165:1585–1593.

Liu, X, Ramirez, S, Pang, PT, Puryear, CB, Govindarajan, A, Deisseroth, K, and Tonegawa, S (2012). Optogenetic stimulation of a hippocampal engram activates fear memory recall. Nature 484, 381–385.

Machado, CJ, and Bachevalier, J (2007). The effects of selective amygdala, orbital frontal cortex or hippocampal formation lesions on reward assessment in nonhuman primates. Eur. J. Neurosci., 25, 2885–2904.

Marín O (2012). Brain development: The neuron family tree remodelled. Nature., 490(7419):185-6.

Medalla, M. & Barbas, H. (2012). The anterior cingulate cortex may enhance inhibition of lateral prefrontal cortex via m2 cholinergic receptors at dual synaptic sites. J. Neurosci. 32, 15611–15625

McDonald, AJ, Mascagni, F, and Guo, L. (1996). Projections of the medial and lateral prefrontal cortices to the amygdala: aphaseolus vulgaris leucoagglutinin study in the rat. Neuroscience 71, 55–75.

Meechan DW, Rutz HLH, Fralish MS, Maynard TM, Rothblat LA, LaMantia AS. (2015). Cognitive ability is associated with altered medial frontal cortical circuits in the LgDel mouse model of 22q11.2DS. Cereb Cortex. 25:1143–1151.

Milad M. R., Quirk G. J., Pitman R. K., Orr S. P., Fischl B., Rauch S. L. (2007). A role for the human dorsal anterior cingulate cortex in fear expression. Biol. Psychiatry 62, 1191–1194.

Milad M. R., Pitman R. K., Ellis C. B., Gold A. L., Shin L. M., Lasko N. B., et al. (2009). Neurobiological basis of failure to recall extinction memory in posttraumatic stress disorder. Biol. Psychiatry 66, 1075–1082.

Minzenberg, M.J. et al. (2009) Meta-analysis of 41 functional neuroimaging studies of executive function in schizophrenia. Arch. Gen. Psychiatry 66, 811–822.

Minzenberg MJ, et al (2010). Gamma oscillatory power is impaired during cognitive control independent of medication status in first-episode schizophrenia. Neuropsychopharm., 35:2590–2599.

Mobini S, Body S, Ho MY, Bradshaw CM, Szabadi E, Deakin JF, Anderson IM (2002). Effects of lesions of the orbitofrontal cortex on sensitivity to delayed and probabilistic reinforcement. Psychopharmacology, 160, 290–298.

Moorman DE, James MH, McGlinchey EM, Aston-Jones G (2014). Differential roles of medial prefrontal subregions in the regulation of drug seeking. Brain Res.

Moser, EI, Witter, MP, and Moser, MB (2010). ‘‘Entorhinal cortex,’’ in Handbook of Brain Microcircuits, eds G.M. Shepherd and S. Grillner (Oxford: Oxford University Press),175–190.

Motzkin J. C., Philippi C. L., Wolf R. C., Baskaya M. K., Koenigs M. (2015). Ventromedial prefrontal cortex is critical for the regulation of amygdala activity in humans. Biol. Psychiatry 77, 276–284.

Muhammad, A, Carroll, C, and Kolb, B (2012). Stress during development alters dendritic morphology in the nucleus accumbens and prefrontal cortex. Neuroscience, 216, 103–109.

Mueller D, Porter JT, Quirk GJ (2008). Noradrenergic signaling in infralimbic cortex increases cell excitability and strengthens memory for fear extinction. J. Neurosci., 28:369–375.

Nakayama, D. et al (2015). Long-delayed expression of the immediate early gene Arc/Arg3.1 refines neuronal circuits to perpetuate fear memory. J. Neurosci. 35, 819–830.

Narayanan NS, Laubach M (2006). Top-down control of motor cortex ensembles by dorsomedial prefrontal cortex. Neuron. 52:921–931.

Niv, Y, and Schoenbaum, G (2008). Dialogues on prediction errors. Trends Cogn. Sci., 12, 265–272.

Nabavi, S. et al (2014). Engineering a memory with LTD and LTP. Nature 511, 348–352.

O'Donnell, P, (2010). Adolescent maturation of cortical dopamine. Neurotox. Res.18, 306–312.

Ongur D, Price JL (2000). The organization of networks within the orbital and medial prefrontal cortex of rats, monkeys and humans. Cereb Cortex, 10: 206–219.

Petanjek Z, Judaš M, Šimic G, Rasin MR, Uylings HB, Rakic P, Kostovic I (2011). Extraordinary neoteny of synaptic spines in the human prefrontal cortex. Proc Natl Acad Sci USA., 108:13281–13286.

Peters J., Dieppa-Perea L. M., Melendez L. M., Quirk G. J. (2010). Induction of fear extinction with hippocampal-infralimbic BDNF. Science 328, 1288–1290.

Peyrache A., Khamassi M., Benchenane K., Wiener S. I., Battaglia F. P. (2009). Replay of rule-learning related neural patterns in the prefrontal cortex during sleep. Nat. Neurosci. 12, 919–926.

Pickens, CL, Saddoris, MP, Gallagher, M, and Holland, PC (2005). Orbitofrontal lesions impair use of cue-outcome associations in a devaluation task. Behav. Neurosci., 119, 317–322

Pickens CL, Saddoris MP, Setlow B, Gallagher M, Holland PC, Schoenbaum G (2003). Different roles for orbitofrontal cortex and basolateral amygdala in a reinforce devaluation task. J. Neurosci., 23, 11078–11084.

Radley, JJ, Arias, CM, and Sawchenko, PE (2006). Regional differentiation of the medial prefrontal cortex in regulating adaptive responses to acute emotional stress. J. Neurosci., 26, 12967–12976.

Radley, JJ, Rocher, AB, Rodriguez, A, Ehlenberger, DB, Dammann, M, McEwen, BS,et al., (2008). Repeated stress alters dendritic spine morphology in the rat medial prefrontal cortex. J. Comp. Neurol., 507, 1141–1150.

Rajasethupathy, P, Sankaran, S, Marshel, JH, Kim, CK, Ferenczi, E, Lee, SY, etal. (2015). Projections from neocortex mediate top-down control of memory retrieval. Nature 526, 653–659.

Ramon y Cajal, S (1893). Neue Darstellung vom histologischen Bau des Central nerven systems. Arch. Anat. Physiol. 17, 9–428.

Ramirez-Amaya, V., Vazdarjanova, A., Mikhael, D., Rosi, S., Worley, P. F., & Barnes, C. A. (2005). Spatial exploration-induced Arc mRNA and protein expression: Evidence for selective, network-specific reactivation. Journal of Neuroscience, 25(7), 1761–1768.

Ray, JP and Price JL (1992). The organization of the thalamocortical connections of the mediodorsal thalamic nucleus in the rat, related to the ventral forebrainprefrontal cortex topography. J. Comp. Neurol., 323: 167–197.

Reijmers, LG, Perkins, BL, Matsuo, N, and Mayford, M (2007). Localization of a stable neural correlate of associative memory. Science 317, 1230–1233.

Rempel-Clower NL (2007a). Role of orbitofrontal cortex connections in emotion. Ann N Y Acad Sci., 1121:72-86

Rempel-Clower, NL (2007b). Pattern of projections from orbitofrontal cortex to the amygdala in the rat. Soc. Neurosci. Abstr.

Robbins, M., DeBerry, J, and Ness, T (2007). Chronic psychological stress enhances nociceptive processing in the urinary bladder in high-anxiety rats. Physiol. Behav., 91, 544–550.

Richards, S, Mychasiuk, R, Kolb, B, and Gibb, R (2012).Tactile stimulation during development alters behavior and neuroanatomical organization of normal rats. Behav.Brain Res., 231, 86–91.

Robinson, TE, and Kolb, B (1999a). Alterations in the morphology of dendrites and dendritic spines in the nucleus accumbens and prefrontal cortex following repeated treatment with amphetamine or cocaine. Eur.J.Neurosci. 11, 1598–1604.

Robinson, TE, and Kolb, B (1999b). Morphine alters the structure of neurons in nucleus accumbens and neocortex. Synapse 33, 160–162.

Robinson, TE, and Kolb, B (2004).Structural plasticity associated with drugs of abuse. Neuropharmacology, 47,33–46.

Rolls E, Critchley H, Mason R, Wakeman E (1996). Orbitofrontal cortex neurons: role in olfactory and visual association learning. J Neurophysiol., 75:1970–1981.

Ross DA, Arbuckle MR, Travis MJ, Dwyer JB, van Schalkwyk GI, Ressler KJ (2017). An Integrated Neuroscience Perspective on Formulation and Treatment Planning for Posttraumatic Stress Disorder: An Educational Review. JAMA Psychiatry., 74(4):407-415.

Rossato JI, Bevilaqua LR, Izquierdo I, Medina JH, Cammarota M (2009). Dopamine controls persistence of long-term memory storage. Science., 325(5943):1017-20.

Roux F, Wibral M, Mohr HM, Singer W, Uhlhaas PJ (2012) γ-band activity in human prefrontal cortex codes for the number of relevant items maintained in working memory. J Neurosci 32:12411–12420.

Ruediger, S, Spirig, D., Donato, , Caroni, P (2012). Goal-oriented searching mediated by ventral hippocampus early in trial-and-error learning. Nature Neuroscience 15, 1563-1571.

Rushworth MF, Walton ME, Kennerley SW, Bannerman DM (2004). Action sets and decisions in the medial frontal cortex. Trends Cogn Sci., 8(9):410-7.

Rushworth MF, Noonan MP, Boorman ED, Walton ME, Behrens TE (2011). Frontal cortex and reward-guided learning and decision-making. Neuron, 23;70(6):1054-69.

Sangha S, Robinson PD, Greba Q, Davies DA, Howland JG (2014). Alterations in reward, fear and safety cue discrimination after inactivation of the rat prelimbic and infralimbic cortices. Neuropsychopharmacology., 39:2405–2413.

Santini E, Ge H, Ren K, Pena de Ortiz S, Quirk GJ (2004). Consolidation of fear extinction requires protein synthesis in the medial prefrontal cortex. J. Neurosci., 24:5704–5710.

Semple, WE, Goyer, PF, McCormick, R, Compton-Toth, B, Morris, E, Donovan, B.,et al.(1996). Attention and regional cerebral blood flow in post-traumatic stress disorder patients with substance abuse histories. Psychiatry Res. 67, 17–28.

Schacter, DL, Eich, JE, and Tulvlng, E (1978). Richard Semon' s Theory of Memory. J. Verbal Learn. Verbal Behav. 17, 721–743.

Schneider M, Debbane M, Bassett AS, Chow EWC, Fung WLA, Van den Bree M, Owen M, Murphy KC, Niarchou M, Kates WR, et al. International Consortium on Brain and Behavior in 22q11.2 Deletion Syndrome. (2014). Psychiatric disorders from childhood to adulthood in 22q11.2 deletion syndrome: results from the International

Consortium on Brain and Behavior in 22q11.2 Deletion Syndrome. Am J Psychiatry. 171:627–639.

Schoenbaum, G, Chiba, AA, and Gallagher, M (1998). Orbitofrontal cortex and basolateral amygdala encode expected outcomes during learning. Nature Neurosci., 1, 155–159.

Schoenbaum, G, Setlow, B, Saddoris, MP, and Gallagher, M (2003). Encoding predicted outcome and acquired value in orbitofrontal cortex during cue sampling depends upon input from basolateral amygdala. Neuron, 39, 855–867.

Schubert D, Martens G.J., Kolk SM (2015). Molecular underpinnings of prefrontal cortex development in rodents provide insights into the etiology of neurodevelopmental disorders. Mol Psychiatry, 20(7):795-809.

Seamans JK, Floresco SB, Phillips AG (1995). Functional differences between the prelimbic and anterior cingulate regions of the rat prefrontal cortex. Behav Neurosci., 109:1063–1073.

Semon, R. (1904). Die Mneme als erhaltendes Prinzip im Wechsel des organischen Geschehens (Leipzig: Wilhelm Engelmann).

Semon, R. (1909). Die nmemischen Empfindungen (Leipzig: Wilhelm Engelmann).

Senn V, Wolff SB, Herry C, Grenier F, Ehrlich I, Gründemann J, Fadok JP, Müller C, Letzkus JJ, Lüthi A (2014). Long-range connectivity defines behavioral specificity of amygdala neurons. Neuron, 81(2):428-37.

Shyu, BC & Vogt, BA (2009). Short-term synaptic plasticity in the nociceptive thalamic-anterior cingulate pathway. Mol. Pain 5, 51.

Siapas, AG, Lubenov, EV, and Wilson, MA. (2005). Prefrontal phase locking to hippocampal theta oscillations. Neuron 46, 141–151.

Sierra-Mercado D, Padillo-Coreano N, Quirk GJ (2011). Dissociable roles of prelimbic and infralimbic cortices, ventral hippocampus, and basolateral amygdala in the expression and extinction of conditioned fear. Neuropsychopharmacology., 36:529–538.

Sigurdsson, T, Stark, KL, Karayiorgou, M, Gogos, JA, and Gordon, JA (2010). Impaired hippocampal-prefrontal synchrony in a genetic mouse model of schizophrenia. Nature 464, 763–767.

Sigurdsson T, and Duvarci, S (2016). Hippocampal-Prefrontal Interactions in Cognition, Behavior and Psychiatric Disease. Front Syst Neurosci., 9: 190.

Silvers JA, Insel C, Powers A, Franz P, Helion C, Martin R, Weber J, Mischel W, Casey BJ, Ochsner KN (2017). The transition from childhood to adolescence is marked by a general decrease in amygdala reactivity and an affect-specific ventral-to-dorsal shift in medial prefrontal recruitment. Dev Cogn Neurosci., 25:128-137.

Singer W (1993) Synchronization of cortical activity and its putative role in information processing and learning. Annu Rev Physiol 55:349 –374.

Sohal VS (2016). How Close Are We to Understanding What (if Anything) γ Oscillations Do in Cortical Circuits? J Neurosci., 36(41):10489-10495

Sotres-Bayon, F., Sierra-Mercado, D., Pardilla-Delgado, E., Quirk, G.J. (2012). Gating of fear in prelimbic cortex by hippocampal and amygdala inputs. Neuron, 76, pp. 804-812.

Spellman T, Rigotti M, Ahmari SE, Fusi S, Gogos JA, Gordon JA (2015) Hippocampal-prefrontal input supports spatial encoding in working memory. Nature 522:309 –314.

Stark KL, Xu B, Bagchi A, Lai W-S, Liu H, Hsu R, Wan X, Pavlidis P, Mills AA, Karayiorgou M, et al. (2008). Altered brain microRNA biogenesis contributes to phenotypic deficits in a 22q11-deletion mouse model. Nat Genet. 40:751–760.

Swanson, LW (1981). A direct projection from ammon's horn to prefrontal cortex in the rat. Brain Res. 217, 150–154.

Takahashi YK, Roesch MR, Stalnaker TA, Haney RZ, Calu DJ, Taylor AR, Burke KA, Schoenbaum G (2009). The orbitofrontal cortex and ventral tegmental area are necessary for learning from unexpected outcomes. Neuron, 62, 269–280.

Takeuchi, T. et al (2013). The synaptic plasticity and memory hypothesis: encoding, storage and persistence. Philos. Trans. R. Soc. Lond. B: Biol. Sci. 369.

Tamura M, Mukai J, Gordon JA, Gogos JA (2016) Developmental inhibition of Gsk3 rescues behavioral and neurophysiological deficits in a mouse model of schizophrenia predisposition. Neuron 89:1100 –1109.

Tang J, Ko S, Ding HK, Qiu CS, Calejesan AA, Zhuo M (2005). Pavlovian fear memory induced by activation in the anterior cingulate cortex. Mol. Pain, 1, 6.

Tayler, KK, Tanaka, KZ, Reijmers, LG, and Wiltgen, BJ (2013). Reactivation of neural ensembles during the retrieval of recent and remote memory. Curr. Biol. 23, 99–106.

Teixeira CM, Pomedli SR, Maei HR, Kee N, Frankland PW (2006). Involvement of the anterior cingulate cortex in the expression of remote spatial memory. J Neurosci., 26:7555–7564.

Thierry, AM, Gioanni, Y, Dégénétais, E, and Glowinski, J (2000). Hippocampo-prefrontal cortex pathway: anatomical and electrophysiological characteristics. Hippocampus 10, 411–419.

Tovote, P, Fadok, JP, Luthi, A (2015). Neuronal circuits for fear and anxiety. Nat. Rev. Neurosci., 16, 317–331.

Trifilieff, P, Herry, C, Vanhoutte, P, Caboche, J, Desmedt, A, Riedel, G, Mons, N, Micheau, J (2006). Foreground contextual fear memory consolidation requires two independent phases of hippocampal ERK/CREB activation. Learning & Memory 13,

349-358.

Tseng, KY, O'Donnell, P, (2005). Post-pubertal emergence of prefrontal cortical upstates induced by D1-NMDA co-activation. Cereb. Cortex 15, 49–57.

Tseng, KY, O'Donnell, P, (2007). Dopamine modulation of prefrontal corticalinterneurons changes during adolescence. Cereb. Cortex 17, 1235–1240.

Tseng, KY, Mallet, N, Toreson, KL, Le Moine, C, Gonon, F, O'Donnell, P, (2006). Excitatory response of prefrontal cortical fast-spiking interneurons to ventral tegmental area stimulation in vivo. Synapse 59, 412–417.

Tseng, K.Y., Chambers, R.A., Lipska, B.K., (2009). The neonatal ventral hippocampal lesion as a heuristic neurodevelopmental model of schizophrenia. Behav. Brain Res. 204, 295–305.

Uylings HB, Groenewegen HJ, Kolb B (2003). Do rats have a prefrontal cortex? Behav Brain Res., 146(1-2):3-17.

Uylings, HB, and van Eden, CG. (1990). Qualitative and quantitative comparison of the prefrontal cortex in rat and in primates, including humans. Prog. BrainRes., 85, 31–62.

van Aerde, KI, Heistek, TS, and Mansvelder, HD (2008). Prelimbic and infralimbic prefrontal cortex interact during fast network oscillations. PLoS One 3:e2725.

Van den Oever MC, Rotaru DC, Heinsbroek JA, Gouwenberg Y, Deisseroth K, Stuber GD, Mansvelder HD, Smit AB (2013). Ventromedial prefrontal cortex pyramidal cells have a temporal dynamic role in recall and extinction of cocaine-associated memory. J. Neurosci., 33:18225–1833.

van De Werd HJ, Rajkowska G, Evers P, Uylings HB (2010). Cytoarchitectonic and chemoarchitectonic characterization of the prefrontal cortical areas in the mouse. Brain Struct Funct., 214(4):339-53.

van Eden CG, Kros JM, Uylings HBM (1990). The development of the rat prefrontal cortex. Its size and development of connections with thalamus, spinal cord and other cortical areas. Prog Brain Res., 85:169–183.

Vertes RP (2004). Differential projections of the infralimbic and prelimbic cortex in the rat. Synapse, 51(1):32-58.

Vertes, RP (2006). Interactions among the medial prefrontal cortex, hippocampus and midline thalamus in emotional and cognitive processing in the rat. Neuroscience 142, 1–20.

Vianna, DML, and Brandão, ML (2003). Anatomical connections of the periaqueductal gray: specific neural substrates for different kinds of fear. Braz. J. Med.Biol.Res. 36, 557–566.

Vicini, S, Wang, JF, Li, JH, Zhu, WJ, Wang, YH, Luo, JH, Wolfe, BB, Grayson, DR (1998). Functional and pharmacological differences between recombinant N-methyl-D-aspartate receptors. J. Neurophysiol. 79, 555–566.

Volk DW, Lewis DA (2010). Prefrontal cortical circuits in schizophrenia. Curr Top Behav Neurosci., 4:485-508.

Wallis JD (2011). Cross-species studies of orbitofrontal cortex and value-based decision-making. Nat Neurosci., 15(1):13-9.

Walton ME, Bannerman DM, Alterescu K, Rushworth MF (2003). Functional specialization within medial frontal cortex of the anterior cingulate for evaluating effort-related decisions. J Neurosci., 23(16):6475-9.

Wang GW, Cai JX (2006). Disconnection of the hippocampal-prefrontal cortical circuits impairs spatial working memory performance in rats. Behav. Brain Res. 175, 329–336.

Wen L, Lu YS, Zhu XH, Li XM, Woo RS, Chen YJ, Yin DM, Lai C, Terry AV Jr, Vazdarjanova A, Xiong WC, Mei L (2010). Neuregulin 1 regulates pyramidal neuron

activity via ErbB4 in parvalbumin-positive interneurons. Proc Natl Acad Sci U S A., 107(3):1211-6.

Wierzynski, CM, Lubenov, EV, Gu, M, and Siapas, AG (2009). State-dependent spike-timing relationships between hippocampal and prefrontal circuits during sleep. Neuron 61, 587–596.

Womelsdorf, T, Schoffelen, JM, Oostenveld, R, Singer, W, Desimone, R, Engel, AK, and Fries, P (2007). Modulation of neuronal interactions through neuronal synchronization. Science, 316, 1609–1612.

Wu, L. J, Li, X, Chen, T, Ren, M. & Zhuo, M (2009). Characterization of intracortical synaptic connections in the mouse anterior cingulate cortex using dual patch clamp recording. Mol. Brain 2, 32.

Yang CR, Seamans JK, Gorelova N (1996). Electrophysiological and morphological properties of layers V-VI principal pyramidal cells in rat prefrontal cortex in vitro. J Neurosci., 16(5):1904-21.

Yang, JW, Shih, HC & Shyu, BC (2006). Intracortical circuits in rat anterior cingulate cortex are activated by nociceptive inputs mediated by medial thalamus. J. Neurophysiol., 96, 3409–3422.

Yiu, AP, Mercaldo, V, Yan, C, Richards, B, Rashid, AJ, Hsiang, HL, Pressey, J, Mahadevan, V, Tran, MM, Kushner, SA, et al. (2014). Neurons are recruited to a memory trace based on relative neuronal excitability immediately before training. Neuron 83, 722–735.

Yoon T, Okada J, Jung MW, Kim JJ (2008). Prefrontal cortex and hippocampus subserve different components of working memory in rats. Learn. Mem. 15, 97–105.

Zelikowsky, M, Hersman, S, Chawla, MK, Barnes, CA, and Fanselow, MS (2014). Neuronal ensembles in amygdala, hippocampus, and prefrontal cortex track differential components of contextual fear. J. Neurosci., 34, 8462–8466.

Zhou, Y, Won, J, Karlsson, MG, Zhou, M, Rogerson, T, Balaji, J, Neve, R, Poirazi, P, and Silva, AJ (2009). CREB regulates excitability and the allocation of memory to subsets of neurons in the amygdala. Nat. Neurosci., 12, 1438–1443.

Zhu, JJ (2000). Maturation of layer 5 neocortical pyramidal neurons: amplifying salient layer 1 and layer 4 inputs by Ca2+ action potentials in adult rat tuft dendrites. J. Physiol. 526 (Pt. 3), 571–587.

5. Acknowledgements

First, I would like to thank Pico Caroni for giving me this wonderful opportunity to work with him. Thank you for your mentorship in not only the doctoral thesis but also in life in general. Working with you has taught me how to ask interesting questions and what a rewarding experience scientific research can be. Finally, thank you for your enthusiasm for my ideas, even the crazy ones, and your support for my abnormal working hours.

I thank my thesis committee members, Andreas Luthi and Georg Keller for their guidance and inputs to give direction to my doctoral work. A special thanks goes to Silvia Arber for sharing innumerable viruses and mice which made this thesis possible!

I would like to thank the former lab members Flavio, Mike, Francesco and Smitha, who helped me and gave me advice while I started at the deep end of the pool. Thank you very much for all your help. Also thanks to Maria Lahr and Annapoorani for being great friends and for all the discussions about everything in the universe and more importantly, for tolerating my tasteless jokes.

I would like to thank Komal, Melissa, Kerstin, Matteo, Maria Spolidoro, Ananya, Olga, Sebastian, Lisa, Giulia, Ange, Lara and all other members of the Caroni lab for creating a nice scientific environment in the laboratory and for all the help.

I would like to thank the members of the FAIM facility and the animal house facility for their support.

Special thanks to my parents, for their love and support and for introducing me to the wonderful world of Biology. To my little brother Atreyo, for being my constant partner in all my crazy adventures and business schemes. Last but not the least, a big thank you to Shalaka for being there through the thick and thin, for pushing me when the goals seemed too far and cheering me through success and failure. Your exceptional mind and brilliant suggestions, made many of my experiments possible. Thank you, Shark!